
Computación Avanzada, Energía y Plasmas

# Estudio experimental sobre la exposición de personas a contaminantes exhalados en habitaciones de hospital

-

# Experimental study of personal exposure to exhaled contaminants in hospital rooms

Directores: Manuel Ruíz de Adana Santiago e Inés Olmedo Cortés

Autor: Félix Antonio Berlanga Cañete

Depósito de la tesis 19 de octubre de 2018

TITULO: *Experimental study of personal exposure to exhaled contaminants in hospital rooms*

AUTOR: *Félix Antonio Berlanga Cañete*


Campus de Rabanales
Ctra. Nacional IV, Km. 396 A
14071 Córdoba

https://www.uco.es/ucopress/index.php/es/
ucopress@uco.es

**TÍTULO DE LA TESIS: Estudio experimental sobre la exposición de personas a contaminantes exhalados en habitaciones de hospital**

**DOCTORANDO: Félix Antonio Berlanga Cañete**

## INFORME RAZONADO DEL/DE LOS DIRECTOR/ES DE LA TESIS

(se hará mención a la evolución y desarrollo de la tesis, así como a trabajos y publicaciones derivados de la misma).

El doctorando Félix Antonio Berlanga Cañete ha realizado bajo nuestra dirección la tesis doctoral titulada "*Estudio experimental sobre la exposición de personas a contaminantes exhalados en habitaciones de hospital*".

Félix Antonio Berlanga Cañete presentó sus primeros resultados en esta línea de investigación con su incorporación al Proyecto del Plan Nacional DPI2014-55357-C2-2-R *Influencia del sistema de ventilación en la dispersión aérea de bioaerosoles exhalados por personas. Evaluación del riesgo de infección cruzada*. El Doctorando se incorporó al proyecto en 01/02/2016 y es investigador del proyecto hasta el 31/12/2018.

Félix Antonio Berlanga Cañete ha realizado la mayor parte del trabajo de investigación de su tesis doctoral en el Laboratorio de Investigación en Climatización de la Universidad de Córdoba. Esta instalación experimental ha permitido alcanzar resultados de investigación significativos en el estudio y caracterización de la exposición de personas a contaminantes exhalados en habitaciones de hospital.

El avance en esta línea de trabajo propició una estancia de investigación de 3 meses en el Departamento de Ingeniería Civil de la Universidad de Aalborg (Dinamarca), bajo la supervisión del Profesor Li Liu. La estancia se realizó en el periodo comprendido entre el 01/08/2017 y el 01/11/2017. Durante esta estancia se realizó el estudio y caracterización experimental del jet de una exhalación en un modelo 3D semejante a la anatomía humana con resultados muy satisfactorios.

Una vez concluida su estancia de investigación, Félix Antonio Berlanga Cañete ha desarrollado la última etapa de la tesis consistente en la realización de ensayos experimentales de dispersión de contaminantes exhalados en habitaciones de hospital equipadas con distintos sistemas de ventilación. Esta fase se ha desarrollado en el Laboratorio de Investigación en Climatización de la Universidad de Córdoba.

El trabajo de investigación de Félix Antonio Berlanga Cañete ha requerido el desarrollo de numerosos estudios experimentales. Los resultados de estos trabajos de investigación han dado lugar a distintas publicaciones entre las que cabe destacar:

tres artículos publicados en revistas internacionales de impacto (Q1), así como distintas comunicaciones en cuatro congresos de carácter internacional y tres congresos de carácter nacional.

Del doctorando, aparte de su excelente calidad humana, me gustaría destacar, entre otras cualidades, su extraordinaria capacidad de trabajo, así como su constancia, tesón y disciplina, valores que han soportado todo el trabajo de investigación desarrollado y que han contribuido a resolver las numerosas dificultades inherentes al trabajo de investigación experimental desarrollado. Los Directores de esta tesis consideran que este periodo ha permitido que el doctorando desarrolle las cualidades propias de un excelente investigador.

Concluyendo, la metodología, calidad científica y resultados de investigación de esta tesis se valoran de forma MUY FAVORABLE.

Por todo ello, SE AUTORIZA LA PRESENTACIÓN DE LA TESIS DOCTORAL.

Córdoba, 17 de octubre de 2018

Firma de los directores

Fdo.: Manuel Ruiz de Adana Santiago

Fdo.: Inés Olmedo Cortés

I would like to dedicate this thesis to my partner Carmen.
Thank you for your unconditional love and support.

# Declaration

I hereby declare that except where specific reference is made to the work of others, the contents of this dissertation are original and have not been submitted in whole or in part for consideration for any other degree or qualification in this, or any other University. This dissertation is the result of my own work and includes nothing which is the outcome of work done in collaboration, except where specifically indicated in the text.

Autor: Félix Antonio Berlanga Cañete

19 de octubre de 2018

# Acknowledgements

The author acknowledge the financial support received from the Ministerio de Economia y Competitividad, Secretaría de Estado de Investigación, Desarrollo e Innovación, Spain, to the National R&D project TRACER with reference DPI2014-55357-C2-2-R, entitled “Ventilation system influence on airborne transmission of human exhaled bioaerosols. Cross infection risk evaluation”. This project is cofinanced by the European Regional Development Fund (ERDF).

# Preface

This thesis was written as a part of a PhD study carried out during the past four years in the Department of Chemical Physics and Applied Thermodynamics of the University of Cordoba, Spain. The thesis is presented as a collection of ten peer-reviewed articles. Three of which are published in journals indexed in JCR index. This thesis also presents four different peer reviewed international and three national conference proceedings. The document is composed as compendium of articles, meeting the requirements under Regulatory Guidelines for PhD Studies of the University of Córdoba (May, 2013). This option requires that, at least three of the collected articles are published or accepted for publication in JCR indexed journals. The three articles that meet these requirements are marked in bold in the list below.

Paper I Berlanga, F.A., Ruiz de Adana, M., and Olmedo, I. 2015. "Diseño y construcción de maniquíes térmicos para la realización de ensayos experimentales de sistemas de climatización." In *Proceedings of 9th National Thermodynamics Engineering Conference, 1–8 June., 1–8 June. Cartagena, (Spain)*.

Paper II Berlanga, F.A., Ruiz de Adana, M., and Olmedo, I. 2015. "Diseño y construcción de un sistema de emulación de la respiración para maniquíes térmicos para la realización de ensayos experimentales de sistemas de climatización." In *Proceedings of 9th National Thermodynamics Engineering Conference, 1–8 June. Cartagena, (Spain)*.

Paper III Berlanga, F.A., Olmedo, I., Ruiz de Adana, M. and Peci, F. 2016. "Influence of the air renovation rate on the risk of cross infections in a hospital room

with a combined radiant and mixing ventilation system." In *CLIMA 2016 - Proceedings of the 12th REHVA World Congress. Aalborg (Denmark).*

**Paper IV** **Berlanga, F.A., Olmedo, I. and Ruiz de Adana, M. 2016. "Experimental Analysis of the Air Velocity and Contaminant Dispersion of Human Exhalation Flows" *Indoor Air*. https://doi.org/10.1111/ina.12357.**

Paper V Berlanga F.A. Olmedo I. Rúiz de Adana M., 2017, "Evaluation of the thermal comfort in a hospital room considering different air ventilation rates" *Proceedings of the 10th National Thermodynamics Engineering Conference. Lleida (Spain).*

Paper VI Berlanga, F.A., Ruiz de Adana, M., and Olmedo, I. 2017. "Influence of the breathing function on the airborne cross-infection risk in a hospital environment." In *IFHE-EU 2017European Conference for Hospital Engineering, 29–31 May. Bologna, (Italy)*.

Paper VII Berlanga, F.A., and Ruiz de Adana, M. 2017. "Can contaminant air quality indices be used to analyze the risk of airborne cross infections in hospital environments?" In *AIVC 2017 Workshop on IAQ Metrics, 14–15 May. Brussels, (Belgium)*.

Paper VIII Berlanga, F.A., Olmedo, I., and Ruiz de Adana, M. 2018. "Experimental measurements of the exposure to exhaled contaminants from different breathing modes." In *Roomvent and Ventilation, 2-5 June*. Helsinki (Finland).

**Paper IX** **Berlanga, F.A., Ruiz de Adana, M., Olmedo, I., Villafruela, J.M., San José, J.F. and Castro, F. 2017. "Experimental evaluation of thermal comfort, ventilation performance indices and exposure to airborne contaminant in an airborne infection isolation room equipped with a displacement air distribution system" *Energy and Buildings*. https://doi.org/10.1016/J.ENBUILD.2017.09.100.**

**Paper X** **Berlanga, F.A., Olmedo, I., Ruiz de Adana, M., Villafruela, J.M., San José, J.F. and Castro, F. 2018. "Experimental Assessment of Different Mixing Air Ventilation Systems on Ventilation Performance and Exposure to Exhaled Contaminants in Hospital Rooms"** ***Energy and Buildings*****. https://doi.org/10.1016/j.enbuild.2018.07.053.**

# Abstract

Human beings need breathing to survive. The air emitted over the course of respiratory events such as breathing, sneezing and coughing is seeded with small particles known as droplets. These droplets can contain pathogens, which can be a source of airborne cross infections.

People spend an increasing amount of time in indoor environments. In such spaces the probability of inhaling droplets emitted by other person increases. Hence, the probability of the occurrence of a cross infection also increases.

From all the indoor spaces, hospital environments are perhaps the most enabling for cross infections. In these spaces coexist in close contact health workers, patients and familiars. The infection of a health worker is a major concern issue hence, because of his activity, is in contact with dozens of patients and familiars, becoming an infected vector.

A correct design of the ventilation facility of the indoor space together with other individual protective measures helps to avoid airborne cross infections. Ventilation flows can remove the emitted droplets or maintain them far from the other occupant's inhalation zone.

The use of the ventilation is also crucial to maintain the thermal comfort of the occupants. Supplying fresh air, the ventilation facility compensates the present heat gains and removes the pollutants emitted inside. An incorrect ventilation facility design could lead to weaken thermal comfort conditions of the occupants so, this issue must be evaluated commissioning it .

The dispersion of the emitted droplets through respiratory events depends on the interaction between the ventilation flows and the exhalation flow. Different previous studies on the matter

reveal that the changes in both flows can modify the final distribution of the exhaled droplets. Since the droplets are seeded through the exhalation flow, its development must be studied in detail in order to gain knowledge on how and where are contaminants transported depending on the breathing function performed.

This thesis aims to gain knowledge on the distribution of the exhaled droplets in hospital environments. It permits the evaluation of the exposure of the rest of the occupants to these contaminants and hence estimate their cross infection risk. To reach this milestone, it is necessary to characterize the exhalation flow from simplified airways as a source of contaminants and hence evaluate its resemblance with real exhalation flows.

Different breathing exhalation flows are characterized. The flow is studied by using particle image velocimetry technique while the droplet distribution has been analysed using tracer gas as a surrogate. After that, different ventilation configurations are tested on a typical individual room setup considering a lying patient, as a source of contaminants and a standing health worker close to it, as a target or susceptible person.

The occupants, represented by thermal breathing manikins, are equipped with the simplified airways considered for the study. Tracer gas technique is used to evaluate health worker exposure to patient exhaled contaminants. It is possible to measure health worker's exposure by measuring the contaminants amount present in its inhalation from the exhaled by the patient. This way it is possible to determine the optimum ventilation configuration for the setup in terms of reducing health worker's exposure.

During these experiments thermal comfort for both, the patient and the health worker, is evaluated in order to assure that the ventilation configuration guarantee the required thermal comfort indices by international standards.

The results obtained in this thesis permit obtain valuable conclusions. The exposure of a health worker to the patient's exhaled contaminants is evaluated considering different parameters. The influence of the patient' breathing function and exhalation mode is addressed concluding

that it has a non-despicable influence on the flow and exhaled contaminants diffusion. Different ventilation strategies are tested, considering mixing, displacement ventilation configurations, and several air ventilation rates. Results show that is feasible to reduce health worker exposure by a selecting proper design of the ventilation facility. Occupant's thermal comfort turn out to be a major issue in such scenario, being a challenge obtain a reasonable comfort indices for the two occupants due to their different activities performed.

# Resumen

Los seres humanos necesitan respirar para sobrevivir. El aire emitido a través de procesos respiratorios tales como la respiración, la tos y los estornudos contiene pequeñas partículas conocidas como “droplets” (gotitas). Estas gotitas pueden contener patógenos, que pueden ser una fuente de infecciones de transmisión por vía aérea.

Pasamos cada vez más tiempo en ambientes interiores. Dentro de estos espacios aumenta la probabilidad de inhalar partículas emitidas por otra persona. Por lo tanto, la probabilidad de que ocurra una transmisión de una enfermedad también aumenta.

De todos los ambientes interiores, los espacios sanitarios son quizá, los más propensos para las infecciones cruzadas. En estos espacios coexisten en contacto estrecho, trabajadores sanitarios, pacientes y familiares. El contagio de un trabajador sanitario es un hecho especialmente preocupante porque, debido a su actividad, se encuentra en contacto con docenas de pacientes y familiares, convirtiéndose en un vector de enfermedad.

Un diseño correcto de la instalación de ventilación de un ambiente interior ayuda a evitar las infecciones cruzadas por vía aérea. Los flujos de ventilación pueden eliminar las gotitas emitidas o mantenerlas lejos de la zona de inhalación de otros ocupantes.

El uso de la ventilación es también crucial para mantener el confort térmico de los ocupantes. Proporcionando aire fresco y limpio, la instalación de ventilación compensa las cargas térmicas y elimina los contaminantes producidos en su interior. Un diseño incorrecto de la instalación de ventilación puede conducir a un deterioro de las condiciones de confort de los ocupantes, de modo que este hecho ha de ser evaluado antes de dar por buena la instalación.

La distribución de las partículas emitidas a través de procesos respiratorios depende de la interacción entre los flujos de ventilación y el de exhalación. Diferentes estudios previos revelan que los cambios en estos dos flujos derivan en una diferente distribución final de las partículas emitidas. Ya que las gotitas son emitidas a través del flujo de exhalación, su desarrollo ha de ser estudiado en detalle para incrementar el conocimiento sobre cómo y dónde son transportadas las partículas dependiendo de la función respiratoria realizadas.

Esta tesis tiene como objeto profundizar en el conocimiento de la distribución de los contaminantes exhalados en ambientes hospitalarios. Esto permite evaluar la exposición del resto de ocupantes y de este modo estimar su riesgo de infección cruzada. Para lograr este objetivo es necesario caracterizar el flujo de exhalación emitido a través de las vías respiratorias simplificadas como fuente de contaminantes y evaluar su parecido con flujos exhalados reales.

Se caracterizan diferentes exhalaciones respiratorias. Utilizando la técnica de velocímetría de imagen de partícula se estudia su flujo mientras que la distribución de las partículas emitidas se ha estudiado sustituyéndolas por un gas trazador. Una vez concluido este estudio, se prueban diferentes sistemas de ventilación utilizando una configuración típica para habitaciones de hospital individuales, considerando un paciente tumbado, como fuente de contaminantes, y un trabajador sanitario erguido situado cerca del mismo, como objetivo de los mismos.

Los ocupantes, representados por maniquíes térmicos, están equipados con las vías aéreas simplificadas consideradas en este estudio. La técnica de gases trazadores se utiliza para evaluar la exposición del trabajador sanitario a los contaminantes exhalados por el paciente. Es posible estimar la exposición del trabajador sanitario midiendo la cantidad de contaminantes presente in su área de inhalación frente a los emitidos por el paciente. De este modo es posible determinar la configuración de ventilación optima en términos de reducción de la exposición del trabajador sanitario.

Durante el transcurso de los experimentos se evalúa el confort térmico de los ocupantes con objeto de comprobar que la configuración de ventilación probada asegura los valores exigidos por las normas internacionales.

Los resultados obtenidos en esta tesis permiten obtener valiosas conclusiones. La exposición del trabajador sanitario a los contaminantes exhalados se evalúa considerando diferentes parámetros. La influencia de la función respiratoria del paciente y del modo de respiración es abordada concluyéndose que tiene una influencia no despreciable en la difusión de los contaminantes exhalados. Se prueban diferentes estrategias de ventilación, considerando ventilación por mezcla y por desplazamiento, y diferentes tasas de renovación de aire. Los resultados muestran que es posible reducir la exposición del trabajador sanitario a través de una selección de un diseño apropiado de la instalación de ventilación. El confort térmico de los ocupantes resulta ser un problema importante en este escenario, siendo un reto obtener resultados de confort razonables para los dos ocupantes debido a las diferentes actividades desarrolladas por los mismos

# Contents

# List of Figures

# Nomenclature

| | |
|---|---|
| CDC | Centers for Disease Control and Prevention |
| DV | Displacement ventilation strategy. |
| GD | Upper wall supply grilles, lower wall exhaust grilles ventilation configuration. |
| GU | Upper wall supply grilles, upper wall exhaust grilles ventilation configuration. |
| HVAC | Heating, ventilation and air conditioning. |
| $f_{125\%}$ | Contaminant concentration peak frequency (1/h) |
| HN | High male breathing function, exhalation through the nose. |
| HM | High male breathing function, exhalation through the mouth |
| $IF$ | Intake fraction. |
| $IF_{125\%}$ | Peak average intake fraction. |
| $IF_{max}$ | Maximum concentration intake fraction. |
| LAVEC | Laboratory of Ventilation and Climatization of the University of Córdoba |
| LN | Low female breathing function, exhalation through the nose |
| LM | Low female breathing function, exhalation through the mouth |
| SD | Ceiling supply swirl diffusers, lower West wall exhaust grilles configuration |
| SU | Ceiling supply swirl diffusers, upper West wall exhaust grilles configuration |

# Introduction

Recent research studies have proved that different diseases are airborne transmitted [1,2]. Pathogens present in the environment can be inhaled by a person or reach its mucosa transmitting a disease [3]. As a response, different international standards provide recommendations to avoid this issue in healthcare environments [3–5].

These pathogens can be emitted though respiratory events such as breathing, coughing or sneezing [6–8]. The flow produced during these events contains different matter, among which water based drops are found [9–11]. Pathogens can survive inside these particles even when they lose mass because of evaporation and become in droplets nuclei [12]. In this form, pathogens can travel long distances driven by indoor airflows [13].

Indoor spaces are conducive spaces for airborne cross infections. This is because, in these spaces, people share long periods of time in close contact with other occupants in the same environment increasing the possibilities of disease transmission. One of the tools to remove the pollutants generated inside an indoor space is the use of a proper ventilation strategy. Indoor occupied environments dispose of a ventilation facility that supply fresh air strategically to displace or dilute the undesirable matter and this way avoid the exposure of the occupants [14,15].

The effectivity in removing the pollutants of the ventilation facility depends on the specific characteristics of the ventilated space and on the ventilation configuration chosen. Parameters such as the position of the occupants and the situation and the amount of the heat gains affect the effectivity of the ventilation system [16]. Therefore, a correct design of a ventilation facility needs to take into account these parameters.

The effectiveness of the ventilation is evaluated by using different indices. On one side, there are indices used to quantify the ability to remove the contaminants globally and locally, such as the air change efficiency, the local air change index, the contaminant removal effectiveness and the local air quality index [17]. On the other side, indices such as the contaminants exposure [18–20] or the intake fraction[21–23], value the effective amount of contaminants that reach the inhalation of the occupants.

The evaluation of the effect of different ventilation configurations on an indoor environment is carried out through experimental and numerical studies. Experimental studies use techniques such as tracer gases or tracer particles to surrogate the contaminants released in the indoor space [14,24–28]. The surrogating element is seeded into the contamination source flow, being its concentration registered in different places inside the indoor space in order to evaluate its concentration. Different gases and particles of different size can be used to surrogate the exhaled droplets. Different authors have studied the convenience of the use particles and tracer gases for exhaled contaminants surrogate [29–31].

One of the most sensible environments to airborne cross infections are healthcare facilities. Although, not all the spaces inside healthcare centres require the same attention. International standards fix different ventilation requirements based on the use of the spaces.

One of the main requisites imposed is the air ventilation rate. Based on the criteria fixed by CDC [5], the most ventilation demanding spaces are operation theatres, where the minimum air changes per hour (ACH) value is fixed to 15. Other spaces with a high demand of ventilation are patient rooms, which requires a minimum ventilation rate of 6 ACH and a maximum of 12 ACH if the room is catalogued as an airborne infection isolation room (AIIR). The rest of the spaces require lower ventilation rates.

Different studies have investigated the role of the ventilation flows in the contaminant removal and contaminant exposure occupants' reduction in such environments. The performance of different ventilation configurations in operating theatres was studied by Chow [32] finding

important differences between them. The risk of cross infection in an operating room equipped with a ultraclean ventilation system was numerically evaluated [33] concluding that even using this equipment, the cross infection is possible [34]. The impact of surgical lamps and the pursuit of a more effective design in terms of ventilation performance is also challenge regarding these spaces [35] so the pursuit of new designs that don't obstruct ventilation flows is contingent.

The study of the ventilation of hospital rooms can be classified in the study of multiple wards and individual rooms. Multiple patients hospital wards are still common in healthcare facilities [36,37]. Due to the cohabitation of patients with different diseases in different immune system conditions, it presents an interesting scenario in the struggle to reduce cross infection risk by means of ventilation. The distribution of exhaled droplets in these scenarios has been studied revealing that the ventilation plays a significant role on it [38,39]. The distribution of the exhaled contaminants has been also studied for two bed hospital rooms under different ventilation configurations [12,40] obtaining that the ventilation system is crucial in the reduction of the occupants exposure to the exhaled contaminants.

Nowadays, new hospitals tend to provide individual rooms for the patients. The study of the individual hospital rooms is faced from different perspectives. Some authors studied the distribution of the exhaled contaminants inside the indoor space [41–43]. This topic was simulated numerically considering a typical individual hospital room setup [44] underscoring the importance of understanding the mean and turbulent airflow patterns in order to improve the performance of the ventilation facility. Also using numerical methods, a mathematical model that allows the prediction of the environmental contamination caused by airborne particles was developed for single and multiple hospital rooms [36]. More specific numerical studies have focused their attention in the influence of very specific parameters, such as the study carried out by Wang. J. et al [45], who focus their attention on the influence of the human walking on exhaled contaminants distribution. The distribution of the contaminants and its relation with the exposure of other occupants is analysed numerically. Memarzadeh L. et al. studied numerically the ventilation performance and thermal comfort of the patients considering different ventilation configurations [46]. Using the same experimental conditions,

the authors also studied the airborne cross infection risk [47]. The author concluded that there is not a unique solution for such spaces and the results obtained are dependent on a number of parameters. Another systematic study considering different ventilation elements position was numerically conducted by Villafruela J.M. et al. [48] which conclusions reinforce the importance of the relative positions of the ventilation elements inside the experimental chamber in contaminants distribution and their removal.

The experimental research on the diffusion of exhaled contaminants in individual hospital rooms is scarce. An experimental study on the ventilation performance of an individual room was conducted using tracer gas technique considering a fixed ventilation elements configuration and testing different ventilation rates [49]. The study revealed that the increase of the air ventilation rate reduces the amount of contaminants present in the indoor space. The study is carried out without considering the presence of a health worker and using a very simplified thermal manikin. Novel personalized ventilation systems have been tested in individual hospital rooms in order to determine their performance in avoid cross infection risk [50,51]. The effect of the differential pressure between the indoor space and the effect of the door opening has also been studied in individual hospital rooms [52]. Different ventilation flow and pressure control systems have been also experienced [53] highlighting the importance of maintaining the door of the room closed as much as possible. However, scantly experimental systematic research to determine the exposure of a health worker to patient exhaled contaminants considering different ventilation configurations has been carried out so far.

Several studies have focused their attention in the characterization of the mechanisms of the distribution of the contaminants emitted by different respiratory processes [54–57]. Valuable information such as the maximum propagation distance of the particles [58] or their size distribution [10,59] are obtained from these studies. Sneeze is a violent respiratory event that emit a considerable amount of contaminants in form of bio-aerosols. Different authors have performed the study of the propagation of the particles that contains its flow. These studies use different techniques. Some of them are numerical studies [60,61] while other use experimental

techniques such as particle image velocimetry (PIV) [54,62]. All these studies add knowledge about how the flow spread the contaminants in the environment. Cough is also a violent respiratory event associated with different diseases. The study of the mechanic of the release of the particles has been developed recently [62,63] presenting a different contaminants emitting pattern that the sneezing. The exposure of other people to the contaminants emitted in the cough flow has also attracted the attention of different researchers [64,65], who stand out the importance of the environmental parameters such as the ventilation flows and the distance between the source of contaminants and the target person. Breathing is the most common respiratory event since it is a basic and necessary process for human life. Exhalation releases the inhaled air loaded with the waste products of cellular respiration, in addition, the exhaled air can contain different organic compounds and pathogens. Different studies have approached exhalation in order to describe its dynamics [58,66] and determine the way the exhaled matter distributes [67]. Different experimental techniques are used to characterize exhalation flow. Gupta et al. [68] uses a basic spirometer in a numerous population to determinate the most influencing parameters in exhalation flow and obtain correlations based on these parameters to obtain realistic breathing functions. Other authors analysed the transient jet created by the exhalation flow by describing the velocity decay along the centreline using hot wire anemometers [42,69,70]. Particle image velocimetry is also used to describe the field of velocities created by the exhalation flow [58,66]. The studies analysing the exhalation flow were performed with standing persons or thermal manikins. Standing and lying persons exhalation has been also studied by using Schlieren visualization technique [71] standing out the differences in terms of propagation through time of different exhalations.

The ventilation facility is not only important to remove the indoor emitted contaminants; it also must provide the necessary environmental conditions to achieve thermal comfort for the occupants. Hence, an incorrect design of a ventilation facility could deteriorate the thermal comfort conditions of the occupants, being possible falling out of the international standards fixed thermal comfort ranges. There are several reasons related to ventilation that could deteriorate thermal comfort such as a high velocity air currents or a high temperature stratification in the occupied area. Thermal comfort is a crucial issue to consider in indoor

space ventilation system designs as it evidences the international standards regarding this topic [72]. A high number of studies focus their attention in this issue. Occupants thermal comfort considering different ventilation configurations have been studied systematically [26]. Focusing the attention on healthcare environments, different studies evaluate thermal comfort in different locations in the pursuit of improving it for all the occupants. The achievement of this goal require reaching specific environmental conditions [73]. The comfort of the occupants of an operating room is studied in detail concluding that achieve an acceptable values for all the of them is difficult due to the diverse activities carried out [74], the high air ventilation rate required and the presence of important heat gains such as the lamps. The study of this issue in hospital individual rooms has been evaluated in different ways. General studies considering the thermal comfort of specific occupants in such spaces have been carried out [75]. The particularities sleeping patients have been studied by different authors [76,77] obtaining that the optimum comfort environmental temperature is higher than for standing persons. Other studies face the differences of thermal comfort conditions for people of different characteristics [78]. However, this issue has not been addressed systematically for confined patients and health workers inside hospital rooms.

Once the state of the art is analysed, the most relevant parameters that affect the health worker exposure to the patient exhaled contaminants in a hospital room are the following.

- Relative position of the patient and the health worker.
- Relative position of the ventilation supply and exhaust.
- Ventilation configuration and strategy.
- Air ventilation rate set.
- Breathing functions performed by the health worker and the patient.

- Exhalation route, nose or mouth, followed by the exhalation flow in its path to the external environment.
- Movement of the occupants of the space.
- Position and magnitude of the heat gains inside the indoor space.

This thesis is intended to evaluate the exposure of a health worker to the exhaled contaminants emitted by a lying confined patient in an individual hospital room considering some of the parameters listed above. This is conducted experimentally in the HVAC Laboratory of the University of Córdoba (LAVEC) using two breathing thermal manikins. Realistic ventilation and heat gains conditions can be reproduced in the laboratory facilities. Heat gains, apart from the recreated by the thermal manikins, can be simulated by the use of hydronic radiant panels, installed in the floor, ceiling and one of the walls. The radiant wall is used to reproduce the heat gain of an external wall in the summer for several experiments carried out in the frame of this thesis. Different ventilation configurations have been tested in order to determine their performance in reducing health worker exposure. Displacement (DV) and mixing (M) ventilation strategies are tested. Four mixing ventilation configurations are tested as a combination of two supply and two exhaust modes. The air can be supplied though swirl diffusers (S) or through grilles mounted in the upper part of a wall (G). While the exhaust can be performed though grilles mounted in the upper part of a wall (U) or in the lower part of the wall (D). Three different air ventilation rates 6, 9 and 12 ACH are tested for all the configurations. The influence of the source of contaminants, considering different breathing modes and exhalation functions, and the influence of the ventilation strategy chosen, considering different ventilation configurations and air ventilation rates, is seized in order to determine the conditions that permit reduce the exposure of the health worker to patient exhaled contaminants in hospital rooms.

# Hypothesis and Objectives

The main hypothesis on which this thesis is based is that a proper design of the ventilation facility of an indoor space can reduce the exposure of the occupants to the exhaled contaminants. In this case, the study focuses in an individual hospital room, being the source of contaminants the exhalation of a confined lying patient. The evaluation of the contaminants exposure and hence the cross infection risk between the patient and the health worker is done considering a health worker standing close to the patient. The design considers both the relative position of the supply and the exhaust respect to the occupants and the air ventilation rate performed. The ventilation facility design must provide also correct ventilation performance indices inside the indoor space and assure that the occupants benefit from a thermal comfort compatible with the standard requirements.

In view of the hypothesis developed, it is possible to define the main question to solve by the research carried out during this thesis: **Which is the most effective ventilation configuration to reduce the exposure of the health worker to the contaminants exhaled by a patient in a hospital room?**

Different objectives can be raised to completely answer the main question stated.

- The main objective of this thesis is determine the exposure of the health worker to the contaminants exhaled by a patient in hospital rooms. The gathering of the distribution of the exhaled contaminants near the inhalation point of the health worker is considered in order to determine how the contaminants reach the microenvironment of the target person.

As secondary objectives that permit understand the process as a whole can be stated the following:

- Characterize and evaluate the influence of the different exhalation modes and breathing functions of the patient's exhalation as contaminants source. Additionally, exhalation through nose or mouth must be tested.
- Evaluate the influence of different ventilation configurations in removing the indoor emitted contaminants, weighting their impact in health worker exposure to exhaled contaminants.

The pursuit of the different objectives stated requires the research to be developed in a controlled environment. For that purpose, the design and construction of the necessary apparatus to perform the required experimental is required. Likewise, the evaluation of the correct operation and design of the ventilation facility configuration is carried out by checking that the ventilation effectiveness indices and the global and local thermal comfort indices for both occupants are consistent with the international standards and recommendations stated [17,79]. In this way, it is possible to confirm that the ventilation configuration solutions tested assure the wellbeing of the occupants.

# Research Development

In order to assess these objectives, different actions are conducted to obtain the experimental results that answer the fixed objectives.

With the purpose of determine the exposure of the health worker to the contaminants exhaled by the patient, the laboratory must reproduce realistic conditions. For that purpose, it is equipped with the necessary apparatus to reproduce the conditions that can be found in an individual hospital room. The scenarios provide the possibility to test different ventilation configurations and simulate several indoor heat gains.

Thermal manikins that conduct breathing activities through simplified airways surrogate the presence of people. The breathings performed are controlled through independent artificial lungs that permit modify the flow at convenience. Papers I and II address the design of the thermal manikins and the artificial lungs respectively.

The manikins' position emulates a typical individual hospital room situation. One of the thermal manikins, performing as a health worker stands close to the other thermal manikin that lies on a bed performing as a confined patient. Considering this configuration, a preliminary test on the influence of the air ventilation rate on the health worker exposure to patients' released contaminants is addressed in Paper III.

The study of the exhalation flow of the lying patient requires a transient study of the dynamics of the flow and a specific research on the contaminants distribution around. The flow characterization requires the use of the particle image velocimetry (PIV) technique. While the characterization of the distribution of contaminants around the exhalation point is characterized by using tracer gas technique. The results obtained from this study were published in Paper IV.

Two different patient breathing functions were tested. The health worker contaminant exposure to the contaminants released by these exhalations was described in Paper VI

The methods stated in ISO EN 7730 [79] international standard provide global and local thermal comfort indices for the two occupants of the indoor space. Different environmental probes installed along two vertical poles close to the thermal manikins return the necessary data to obtain these indices. An approach to the influence of different air ventilation rates on the thermal comfort of the occupants is developed in Paper V.

Once it is checked that the health worker is exposed to the contaminants released by the patient, it is time to analyse the way the contaminants reach its inhalation area. For this purpose, the tracer gas registers are examined in detail over the whole experiment in pursuit of transient effects such as concentration peaks. In order to deal with the transient processes, different indices are defined to better compare and analyse the different cases tested. Results were published in Paper VII.

In order to address the influence of the different exhalation modes, the influence of the exhalation way that the patient uses to exhale is evaluated. Exhalation is performed through mouth and nose and the effects on health worker exposure are registered. Results resulted in Paper VIII.

Once the influence of the ventilation system on the indoor space was delimited, a systematic study considering a number of ventilation configurations and air ventilation rates was designed. The objective was the study of the exposure of the health worker to the patients' exhaled contaminants in each situation. Results became in the origin of papers IX and X.

Figure 1 presents a summary of the development of the experimental activities. The relation between the parameters tested in each set of experiments, the tasks carried out to meet the stated objectives and the publication obtained from the research experience.

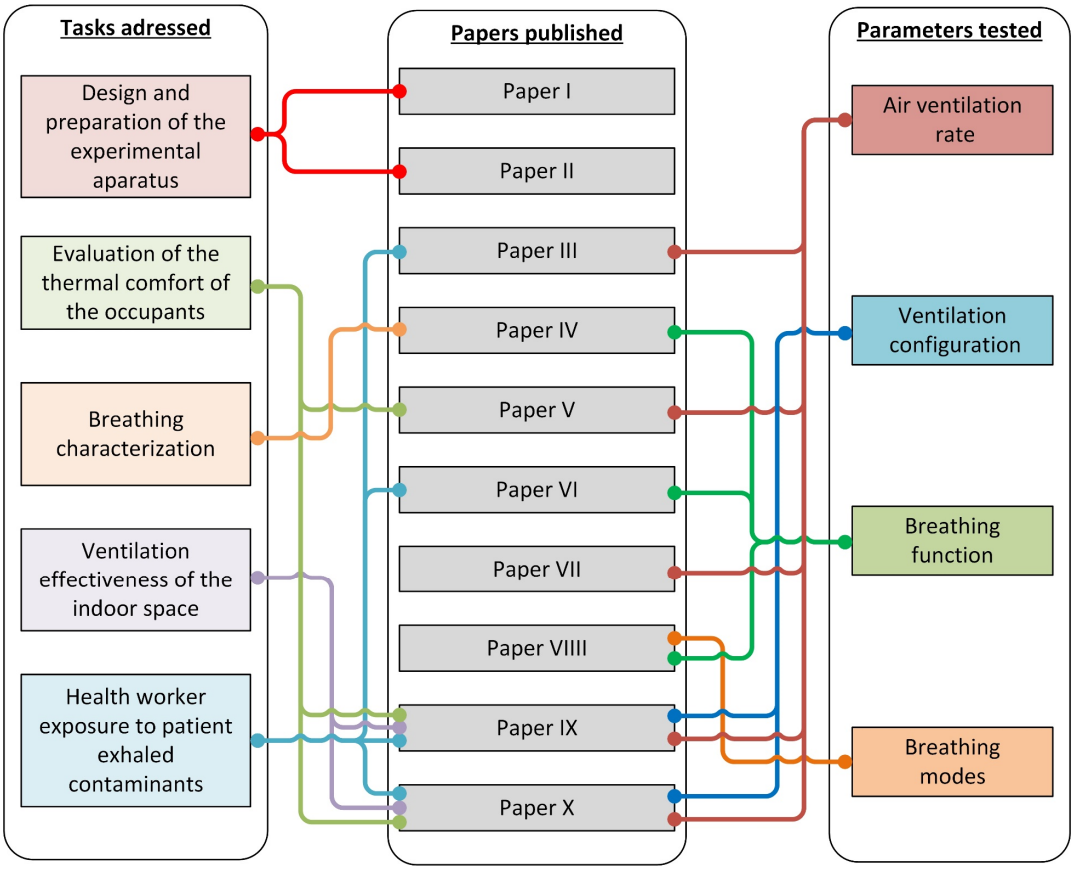


Figure 1. Relation between the parameters tested in each test batch, the tasks intended to address and the research production obtained in the frame of the development of the thesis.

# Paper I. Design and assembly of thermal manikins for HVAQ systems testing


*This paper was presented in* the *9th National Thermodynamics Engineering Conference, 1–8 June, 2015,. Cartagena, (Spain) and was published in the proceedings of the congress.*

This paper describes the geometry of the two identical thermal manikins designed for their use in HVAQ studies of indoor spaces. The document also contains a description of the heat emission system implemented. The manikins emit an adjustable amount of energy in four differentiated zones, the head, the arms, the trunk and the legs. The energy is released by means of Joule principle, being the body of the manikin coiled with nickel wire.

The control of the system is performed by using an Arduino microcontroller pate. The emission of the heat is carried out by using a pulse width modulation (PWM). The disposable energy is trimmed over time at high velocity to obtain the effective energy emission. This control method assures a very accurate energy emission as it has been checked using an independent energy measurement system.

# DISEÑO Y CONSTRUCCIÓN DE MANIQUÍES TÉRMICOS PARA LA REALIZACIÓN DE ENSAYOS EXPERIMENTALES DE SISTEMAS DE CLIMATIZACIÓN

**BERLANGA CAÑETE, FÉLIX A.** [1]**; RUIZ DE ADANA SANTIAGO, MANUEL** [1]

**OLMEDO, INÉS** [1]**;**

felix.berlanga@uco.es

[1]Universidad de Córdoba, Departamento de Química Física y Termodinámica Aplicada

## RESUMEN

Los maniquíes térmicos son dispositivos que simulan la presencia humana en una estancia de la manera más realista posible. Se establecen como una herramienta validada para la realización de ensayos experimentales de sistemas de climatización, permitiendo imponer cargas térmicas internas originadas por personas en locales [1], [2], [3].

En este trabajo se presenta el diseño y construcción de una serie de maniquíes térmicos para la realización de ensayos experimentales en el laboratorio de Ventilación y Climatización de la Universidad de Córdoba.

La geometría de los maniquís térmicos se corresponde de manera aproximada a la de una mujer de complexión media. Los maniquíes térmicos desarrollados tienen cuatro modos de funcionamiento: temperatura constante, calor constante, modo bienestar térmico y modo calibración. Cada maniquí térmico permite regular de forma independiente cuatro zonas: cabeza, brazos, tronco y piernas.

En modo de funcionamiento calor constante, la transferencia de calor sensible de los maniquíes pueden ajustarse a los valores recogidos en la norma UNE EN 13779 [4] relativa al calor emitido por personas con distintos grados de actividad.

Este equipamiento permite el desarrollo de ensayos experimentales de sistemas de climatización, sistemas de difusión de aire y estudios de contaminación cruzada entre personas.

**Palabras clave:** Maniquí térmico, Simulación de cargas térmicas, Confort

## 1. Introducción

La presencia de personas en estancias genera una carga térmica sensible y latente que deben compensar los sistemas de climatización y ventilación. Dichas cargas emitidas por una persona provienen de la piel y la respiración de la misma. Las cargas sensibles se originan por la diferencia de temperatura entre el ser humano y el ambiente. Las cargas latentes se originan al evaporarse cierto volumen de agua ya sea sobre la superficie de la piel o a través del aire emitido por la respiración. Los mecanismos de transporte principales son la convección, la radiación y la conducción.

El método más realista para realizar este tipo de estudios es el uso de personas para realizar ensayos en los locales bajo estudio. Esta manera de proceder es complicada, ya que las condiciones de las mismas son variables con el tiempo y el individuo. Para evitar la problemática asociada al uso de personas reales para este tipo de estudios, se utilizan instrumentos de simulación de cargas térmicas conocidos como maniquíes térmicos. Existen diferentes tipos de maniquíes térmicos en función de la verosimilitud de la simulación de las cargas conseguida [2], [5].

En este trabajo se presenta el desarrollo y construcción de un maniquí térmico que permita generar carga interna sensible y que sea capaz de estimar el confort térmico en el ambiente de ensayo de acuerdo con la norma UNE-EN ISO 7730 [6].

## 2. Objetivos

El objetivo de este trabajo es el desarrollo de un maniquí térmico para la realización de ensayos experimentales de sistemas de climatización.

El maniquí térmico debe reproducir la carga térmica equivalente de una persona, en distintos niveles de actividad y estimar el confort térmico del ambiente.

## 3. Métodos

Para obtener una herramienta que permita simular diferentes tipos de carga térmica emitida a través de la piel asociada a la presencia humana, el maniquí térmico debe proporcionar diferentes modos de funcionamiento. Se han implementado dos modos de funcionamiento del maniquí, modo de control de temperatura constante y en modo de control calor constante. En el modo de temperatura constante, el sistema permitirá mantener constante la temperatura superficial del maniquí manteniendo el valor previamente consignado. En el modo calor constante, se entregará una potencia térmica constante a cada zona del maniquí térmico. En cada modo de funcionamiento, se establecen cuatro zonas de control independientes correspondientes a cabeza, tronco, brazos y piernas. En cada zona, es posible establecer de forma independiente, consignas de temperatura cuando trabaja en modo temperatura constante o bien de potencia térmica cuando se trabaja en modo calor constante.

Para estimar el confort térmico del ambiente, se evalúa el voto medio previsto (PPD) así como el porcentaje de personas insatisfechas (PMV). A partir de estos dos valores se establece la clasificación del ambiente térmico de acuerdo a la norma UNE-EN ISO 7730 [6].

### Diseño del dispositivo físico

Para que la emisión de la carga térmica sea lo más verosímil posible, se ha de distribuir de manera uniforme por una superficie parecida a la del ser humano. Para ello se ha trabajado con un modelo de geometría muy cercana a la de un ser humano de complexión media, tomando como referente las medidas de una mujer. La altura del maniquí es de 1,70 metros y su superficie exterior es de 1,4395 $m^2$. En la Tabla 1 se pueden observar las superficies de cada una de las zonas en las que el maniquí se divide para su control.

Superficie de cada una de las zonas de control del maniquí.

| Zona | Superficie ($m^2$) |
|---|---|
| Cabeza | 0,1366 |
| Torso | 0,4171 |
| Brazos | 0,2538 |
| Piernas | 0,6320 |

Para la construcción del maniquí térmico se parte de un maniquí comercial de poliuretano. El maniquí tiene una estructura metálica con articulaciones flexibles, y un cuerpo formado por espuma de poliuretano de alta densidad. La estructura articulada metálica– permite que el maniquí varíe su postura, pudiendo mantener posiciones de persona sentada o de persona de pie.

En la Figura 1 se puede observar uno de los maniquíes construidos con las dimensiones básicas del mismo.

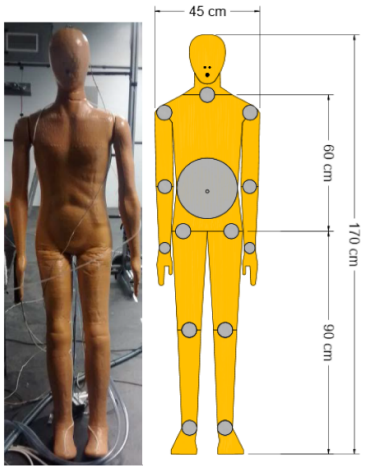


Figura 1. Dimensiones geométricas del maniquí.

Se han previsto los orificios corporales, nasales y boca, necesarios para la implementación de un sistema de respiración independiente. Este sistema permite imponer las cargas debidas a la respiración del individuo, no incluidas en el presente estudio y presentadas en otro trabajo [7]

El calor generado en cada una de las cuatro zonas de los maniquíes se basa en el efecto Joule. La resistencia empleada es un hilo de níquel de 0,3 mm de diámetro enrollado entorno a las diferentes zonas del maniquí. El calor generado en cada zona es proporcional a la corriente circulante por las resistencias arrolladas en cada una de las zonas.

El control térmico se realiza variando la tensión eléctrica de cada resistencia. Las zonas de control implementadas para cada uno de los maniquíes térmicos son cabeza, tronco, brazos y piernas. El control de cada zona se realiza de forma independiente, manteniendo la entrega de calor constante independientemente de las condiciones ambientales.

El sistema de control lo constituyen dos circuitos electrónicos independientes, uno de mando y otro de potencia. Estos circuitos se comunican mediante una tarjeta PCB diseñada específicamente para esta aplicación. La tarjeta de control integra la regulación de las cuatro zonas del maniquí. El esquema del se observa en la Figura 2.

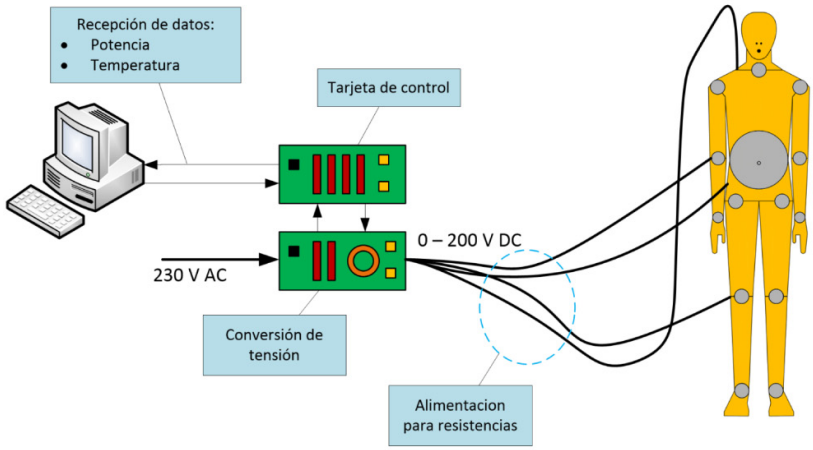


Figura 2. Esquema de control de carg en el maniquí.

El sistema de control se gestiona a través de un equipo informático, PC, mediante el puerto USB. El PC establece una comunicación tipo serie con un microprocesador dentro de la tarjeta de control. El microprocesador gestiona las órdenes que se envían al circuito de potencia y recoge datos del mismo que constituyen la retroalimentación del sistema. El circuito de potencia entrega tensión en intervalos de tiempo de entre 0 y 500 ms a cada una de las zonas de control del maniquí.

Para la configuración, y la visualización en tiempo real de las variables de control del maniquí, se ha generado una interfaz gráfica para para PC. Desde esta interfaz se puede seleccionar el modo de trabajo, temperatura constante, calor constante o modo confort y ajustar las variables en cada caso.

En la Figura 3 se puede observar la interfaz de usuario del programa de control. Se muestra la información de la temperatura y potencia emitida en cada una de las zonas. En función del modo de funcionamiento seleccionado se muestran diferentes campos de introducción de información adicional necesaria para la configuración del modo.

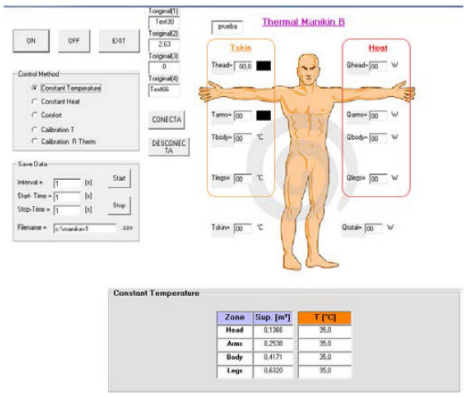


Figura 3. Interfaz gráfica de usuario.

## Control de la carga térmica en cada uno de los modos de funcionamiento

### *Modo temperatura constante*

En este modo el usuario fija a través de la interfaz del programa de control, la temperatura deseada para cada una de las zonas del maniquí. En este modo el objetivo principal es mantener la temperatura superficial de cada una de las zonas en un valor consignado seleccionable por el usuario. La acción de control se realiza utilizando la lectura de la temperatura proporcionada por la resistencia del hilo de níquel de cada zona. El sistema registra la temperatura actual representativa de la zona a controlar, y en función de la misma realiza una acción correctora en la potencia emitida.

### *Modo calor constante*

En este caso el usuario fija una potencia a entregar por cada zona del maniquí controlado, en función del grado de actividad. El sistema de control se limita a corregir las posibles derivas de la resistencia en función de su temperatura a través del tiempo. En este caso el valor de la lectura de temperatura es sólo informativo.

### *Modo confort*

En este modo de trabajo se realiza una estimación del confort térmico existente en el ambiente de estudio. Para lograr esta estimación se utiliza una modificación del método desarrollado en la norma UNE-EN ISO 7730 [6]. En la citada norma se desarrolla el cálculo de los valores de voto medio previsto y porcentaje de personas insatisfechas para obtener finalmente una clasificación de confort térmico.

Para conseguir estos valores se precisa conocer ciertos valores ambientales, temperatura ambiente ($T_a$), la presión de vapor ambiental ($P_v$), así como datos de la persona, actividad metabólica (M), el índice de vestimenta ($I_{clo}$) y el trabajo adicional llevado a cabo (W). Los datos sobre la persona se introducirán a través de la interfaz del programa mientras que los datos.

Con todos estos valores se obtiene el calor emitido al ambiente por el individuo por diferentes factores, entre los que se encuentra el calor latente emitido a través de la piel. Como los maniquíes térmicos diseñados no tienen la capacidad de generar carga latente, se compensa la carga térmica latente que no se puede emitir, a través de la carga sensible. Para ello, se asume una presión de vapor típica para experimentos sobre climatización en interiores, considerando unas condiciones de temperatura seca de 24ºC y un 50% de humedad relativa [8].

El proceso es semejante al llevado a cabo en la citada norma [9]. Se añade un proceso iterativo para obtener la temperatura superficial de la ropa ($T_{cl}$) a partir de la temperatura de la superficie medida ($T_s$) y el calor emitido ($Q_t$).

Para establecer la clasificación de confort térmico de cada situación experimental se utiliza la normativa UNE-EN 15251 [8]. En esta norma se establecen diferentes niveles de confort térmico en función de los valores calor emitido por una persona situada en dicho ambiente. Para obtener este valor se necesita obtener con anterioridad el porcentaje estimado de insatisfechos (PPD), que a su vez exige el cálculo del valor del porcentaje de voto estimado (PPV). Estos valores se obtienen según los procedimientos descritos en la norma UNE-EN ISO 7730 [6]. El procedimiento de cálculo secuencial se muestra en la figura 4.

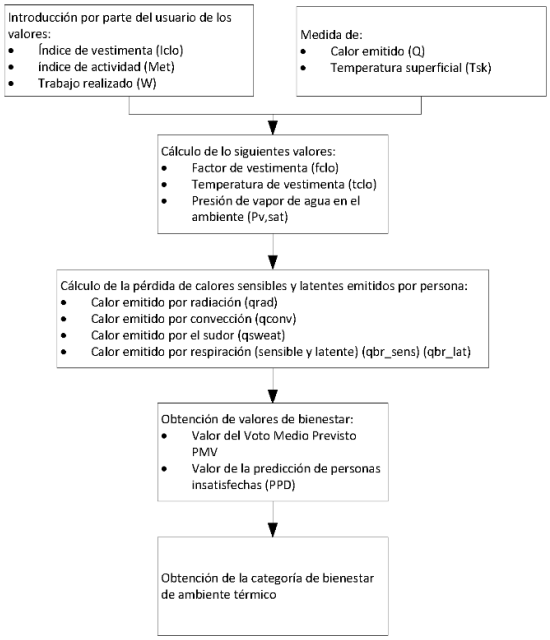


Figura 4. Proceso secuencial de control dentro del modo confort.

El control del sistema registra la temperatura actual de cada zona del maniquí, así como la potencia térmica emitida. El usuario debe introducir a través de la interfaz del sistema de control, el valor de la actividad metabólica, el índice de vestimenta y el trabajo directo que el individuo está realizando en el caso que existiese. Con estos datos, el programa obtiene los valores de factor de vestimenta, la temperatura de la ropa así como la presión de vapor de agua en el ambiente. Estos valores se utilizan para calcular el Voto Medio Estimado (PMV).

$$\mathrm{PMV} = \left(0.303 \cdot e^{-0.36 \cdot \dot{Q}_{met} - \dot{Q}_T} + 0.028\right) \cdot \left(\dot{Q}_{met} - \dot{Q}_T\right)$$

Finalmente se obtiene el valor del Porcentaje Previsto de Personas Insatisfechas (PPD) a través de la expresión

$$\mathrm{PPD} = 100 - 95 \cdot e^{-\left(0.03353 \cdot \mathrm{PMV}^4 + 0.2179 \cdot \mathrm{PMV}^2\right)}$$

Utilizando el valor del porcentaje previsto de personas insatisfechas se obtiene la categoría de bienestar según norma UNE-EN ISO 15251 [8].

*Modo calibración*

Este modo se utiliza para calibrar la medida de las sondas de temperatura. Para calibrar dichas sondas, el sistema obtiene las diferencias entre la temperatura ambiental y la registrada por las sondas y corrige su medida mediante un ajuste lineal. Para poder llevar a cabo la calibración hay que situar el maniquí en un ambiente de temperatura conocida e introducir dicho valor en la interfaz del programa. Se establece que se realicen al menos tres medidas. Los valores han de estar suficientemente separados para conseguir un buen ajuste de la deriva característica de cada sonda.

## 4. Resultados

El maniquí térmico desarrollado puede trabajar en distintos rangos de funcionamiento, tal y como se recoge en la tabla 2.

Tabla 2. Rangos de trabajo de cada uno de los modos.

| Modo de control | Rango de trabajo |
|---|---|
| Calor constante | 0 – 50 W/zona |
| Temperatura constante | 15 ºC – 40 ºC |
| Modo confort | 0 – 15 PPD / -0,7 – 0,7 PMV |

El calor generado en cada zona del maniquí térmico mantiene unas condiciones estables de temperatura, similar a la de la piel humana. Los resultados de inspecciones termográficas se muestran en la figura 5.

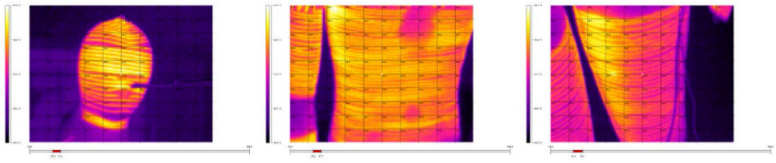

Figura 5. Resultados analizado con cámara termográfica

## 5. Conclusiones y consideraciones finales

Se ha desarrollado un maniquí térmico que permite simular la carga térmica de una persona, con diferentes grados de actividad metabólica. Por otro lado, el maniquí térmico desarrollado permite estimar el confort térmico en una situación concreta.

El maniquí térmico permite ajustar con detalle las cargas internas debidas a personas, en los ensayos experimentales realizados en el laboratorio de climatización y ventilación de la Universidad de Córdoba.

## 6. Referencias

[1] A. Melikov y J. Kaczmarczyk, *Measurement and prediction of indoor air quality using a breathing thermal manikin.*,Revista Indoor Air, 2007, vol. 17, pp. 50-9.

[2] A. Melikov, *Breathing thermal manikins for indoor environment assessment: Important characteristics and requirements*, Revista Eur. J. Appl. Physiol., 2004, vol. 92, pp. 710-713.

[3] E. Bjørn y P. V Nielsen, *Dispersal of exhaled air and personal exposure in displacement ventilated rooms.*,Revista Indoor Air, 2002, vol. 12, pp. 147-64.

[4] Comité: AEN/CTN 100 - CLIMATIZACIÓN, *UNE-EN 13779. Ventilación de edificios residenciales. Requisitos de prestaciones de los sistemas de ventilación y acondicionamiento de recintos.*, AENOR, Madrid, 2005.

[5] E. Bjørn, "Simulation of human respiration with breathing thermal manikin"., En *Proceedings of Third International Meeting on Thermal Manikin Testing*, Stockholm, 1999, pp. 78-81.

[6] Comité: AEN/CTN 81, *UNE-EN ISO 7730. Ergonomía en ambiente térmico. Determinación analítica e interpretación del bienestar térmico mediante el cálculo de los índices PMV y PPD y los criterios de bienestar térmico local*., AENOR, Madrid, 2006.

[7] F. A. Berlanga Cañete, M. R. de Adana, e I. Olmedo, "Diseño y construcción de un sistema de emulación de la respiración para maniquíes térmicos para la realización de ensayos experimentales de sistemas de climatización"., En *IX Congreso Nacional de Ingeniería Termodinámica (Cartagena, 3, 4 y 5 de junio de 2015)*, 2015, pp. 1-8.

[8] Comité: AEN/CTN 100 - CLIMATIZACIÓN, *UNE-EN 15251:2008. Parámetros del ambiente interior a considerar para el diseño y la evaluación de la eficiencia energética de edificios incluyendo la calidad del aire interior, condiciones térmicas, iluminación y ruido*. 2008.

# Paper II. Design and assembly of a breathing surrogating system for thermal manikins devoted to the HVAQ system testing


*This paper was presented in* the *9th National Thermodynamics Engineering Conference, 1–8 June, 2015. Cartagena, (Spain) and was published in the proceedings of the congress.*

This document describes the breathing system implemented for the thermal manikins assembled. Each manikin equips its own independent system. A linear actuator in combination with a double effect pneumatic cylinder performs as an artificial lung. A microcontroller (Arduino plate) operates the linear actuator controlling the position, acceleration, deceleration and maximum velocity of the piston inside the cylinder. This way the complete breathing function is reproduced. The accuracy of the system is evaluated by checking the position of the actuator over time.

# DISEÑO Y CONSTRUCCIÓN DE UN SISTEMA DE EMULACIÓN DE RESPIRACIÓN PARA MANIQUÍES TÉRMICOS PARA LA REALIZACIÓN DE ENSAYOS EXPERIMENTALES DE SISTEMAS DE CLIMATIZACIÓN

**BERLANGA CAÑETE, FÉLIX A. [(1)]; RUIZ DE ADANA SANTIAGO, MANUEL [(1)]**
**OLMEDO, INÉS [(1)];**
felix.berlanga@uco.es
[(1)]Universidad de Córdoba, Departamento de Química Física y Termodinámica Aplicada

## RESUMEN

La respiración de personas en locales influye en las cargas internas sensible y latente, y puede generar problemas de transmisión de contaminantes por vía aérea [1]–[3].
La realización de ensayos experimentales en condiciones controladas permite estudiar con detalle la influencia existente entre el sistema de difusión de aire y la transmisión de contaminantes.
En este trabajo se presenta el diseño y construcción un sistema de emulación de respiración para su implementación en maniquíes térmicos con el objetivo de poder realizar ensayos experimentales en condiciones controladas de distintos sistemas de difusión de aire y sistemas de climatización en el Laboratorio de Ventilación y Climatización de la Universidad de Córdoba.
El sistema de emulación de respiración consta de un subsistema mecánico, para desplazar el flujo de aire necesario, un subsistema térmico, para adecuar la temperatura del aire, un subsistema de dosificación de CO2, para obtener la concentración requerida y un subsistema de control que permite la integración de estos subsistemas para reproducir con precisión las características inherentes a las condiciones respiratorias requeridas.
El sistema de emulación de respiración se ha diseñado para conseguir reproducir un gran número de funciones respiratorias [4], en función del grado de actividad de la persona, su peso, altura, y sexo. El sistema se ha integrado con éxito en maniquíes térmicos para la realización de estudios de transmisión de contaminantes por vía aérea en el Laboratorio de Ventilación y Climatización de la Universidad de Córdoba.

**Palabras clave:** cargas térmicas, respiración.

## 1. Introducción

Para poder realizar un estudio pormenorizado de climatización en ambientes ocupados por personas, es preciso que, entre las cargas totales del mismo, se contemplen las cargas térmicas originadas por los ocupantes del mismo. Un ser humano situado en una estancia genera una carga térmica sensible y latente que ha de ser compensada por los sistemas de climatización y ventilación existentes. Dichas cargas provienen de la piel y la respiración de dicha persona [5].
En este documento se pretende simular las cargas térmicas emitidas por una persona a través de la respiración. En el proceso respiratorio, la carga sensible emitida se produce por la diferencia de temperaturas entre la masa de aire inspirado y el espirado por la persona. La carga latente se origina por la evaporación de cierto volumen de agua, emitida en la masa de aire exhalado.
Los medios utilizados en el presente estudio para simular la carga térmica de una respiración, permiten solo la emisión de calor sensible. Para compensar la ausencia de calor latente, se modifica la cuantía del calor sensible emitido. Para ello se utilizan compensaciones desarrolladas en otros trabajos de investigación[6]
Publicaciones recientes sobre confort térmico [5],[7]cuantifican la carga térmica originada por un individuo desglosada entre sus diversos orígenes, entre los que se encuentra la producida por la respiración.

## 2. Objetivos

Se pretende reproducirla carga térmica sensible generada a través de la respiración humana de la manera más realista posible. Para ello se diseña y desarrolla un sistema que permite reproducir ~~los~~ el caudal, la temperatura y la concentración de $CO_2$ del aire de respiración.
El sistema respiratorio permite reproducir distintas funciones respiratorias, en función del tipo de persona, peso, altura y grado de actividad, y se integra~~do~~ en los maniquíes térmicos existentes en el laboratorio de ventilación y climatización de la Universidad de Córdoba[8].

## 3. Métodos de trabajo

En la Figura 1 se puede observar un diagrama del sistema de simulación construido para satisfacer los objetivos planteados. Este sistema permite el control del flujo de aire inspirado y espirado así como la temperatura del aire durante la espiración.

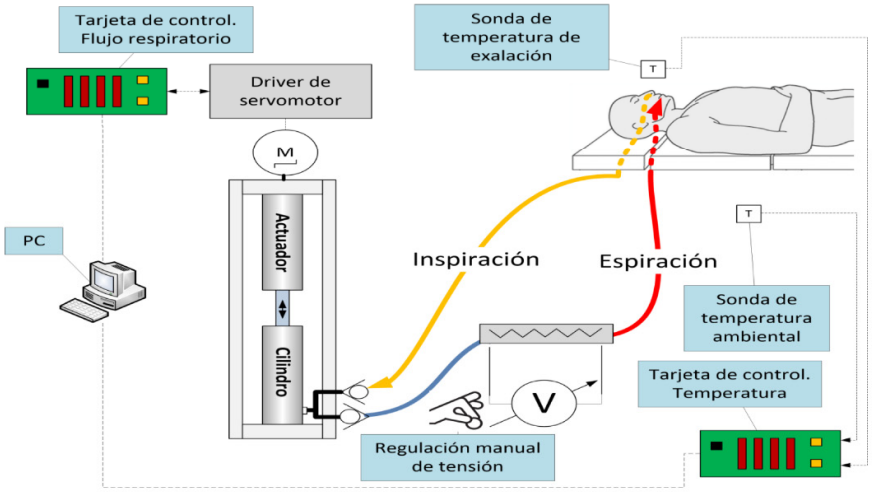


Figura 1. Esquema del sistema de emulación de respiración para maniquíes térmicos.

**Obtención del flujo respiratorio a reproducir y la temperatura de emisión del aire**

La carga térmica del aire respirado que una persona evacúa al ambiente en forma de carga sensible ($C_{res}$) y latente ($E_{res}$), depende de la temperatura seca, la humedad relativa del aire ambiente y de la actividad metabólica del individuo [5]:

$$C_{res} = 0.0014M(34 - t_a)$$
$$E_{res} = 0.0173M(5{,}87 - p_v)$$

Siendo M la tasa metabólica del individuo ($W/m^2$), $t_a$ la temperatura ambiental (ºC) y $p_v$ la presión de vapor de agua ambiental (kPa).

Para evitar la variación de la potencia latente con la humedad ambiental, se fija un valor de presión parcial de vapor de 1,5 kPa, correspondiente a unas condiciones típicas de ensayo de climatización en ambientes interiores (24ºC y 50% HR).Esta hipótesisha sido empleada en trabajos anteriores [6].

El aire se espira a una temperatura ($t_{ex}$) dependiente de la temperatura seca ($t_a$) y humedad relativa (HR) ambientales.

$$t_{ex} = 32.6 + 0.066 \cdot t_a + 32 \cdot HR$$

Al carecer de los medios necesarios para emitir calor latente, se va a compensar su ausencia a través de la corrección de los valores sensibles. Se considera como en el caso anterior una humedad relativa ambiental del 50 % para los cálculos de temperatura del flujo espirado.

La carga térmica se produce de manera cíclica asociada a los flujos respiratorios de la persona. El flujo de aire inspirado y espirado no es estacionario. Para modelar dicho flujo se consideran aproximaciones desarrolladas a partir de estudios experimentales sobre la respiración en diferentes tipos de persona [4]. Se concluye que el flujo respiratorio es dependiente de un número concreto de parámetros de la persona, género, peso, altura y actividad metabólica. Cada fase de la respiración, espiración e inspiración, se puede ajustar a través de una función senoidal de la forma:

$$Flow\ rate\ = a \cdot \sin(\beta t)$$

En función de si nos encontramos en una inspiración o una espiración los parámetros a y $\beta$ varían. Esta variación se traduce en que, tanto la duración como el flujo máximo de cada fase respiratoria, son diferentes.

**Control del flujo respiratorio**

El flujo de aire respirado se genera en un cilindro neumático. Durante la inspiración el émbolo del cilindro se mueve en una dirección introduciendo aire en la cámara del cilindro, mientras que, en la espiración, el émbolo se mueve en sentido contrario, evacuando el aire introducido previamente.

El aire recorre dos conductos diferentes durante la inspiración y la espiración. Para asegurar que en cada fase de la respiración el aire circula por el conducto adecuado, se han instalado sendas válvulas antirretorno en cada uno de los conductos.

El movimiento del émbolo del cilindro es solidario al de un actuador lineal. El actuador posee un sistema electrónico de control al que se le pueden programar diferentes movimientos. Los parámetros configurables para cada movimiento son posición final alcanzada, aceleración, velocidad máxima y deceleración del actuador.

Se utiliza una tarjeta de control para indicar, a través de un puerto de comunicación paralelo, el movimiento que ha de ejecutar el actuador de entre los programados en su sistema de control.

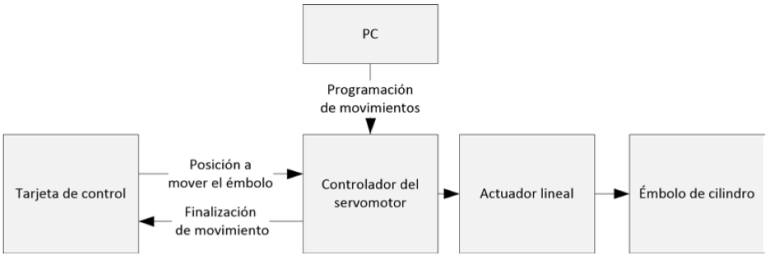


Figura 2. Esquema del proceso de control del flujo de aire emitido.

Se programan dos movimientos en el controlador del servomotor, uno para ejecutar la inspiración y otro para la espiración. El primero parte de la posición con la cámara del cilindro vacía, fin de la espiración, y mueve el pistón hasta el punto en el que el volumen de aire almacenado en el cilindro coincide con el volumen máximo inspirado, conocido como volumen tidal (TV). Se ajustan los valores de aceleración, deceleración y velocidad máxima del émbolo durante cada movimiento para que, tanto en la inspiración como en la espiración el flujo evacuado se ajuste a lo calculado analíticamente. En la Figura 3 se puede observar un ciclo completo de movimiento de pistón, se enfrentan las posiciones teóricamente desarrolladas frente a las obtenidas finalmente.

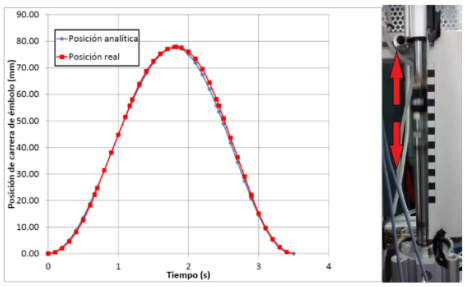


Figura 3. Posiciones analíticas y registradas por el émbolo dentro del cilindro.

**Control del flujo de calor**

El calor a transmitir al aire espirado se genera a través del efecto Joule. Para ello se utiliza una resistencia instaladaen el conducto que lleva el aire del sistema de simulación de la respiración al punto de emisión, ya en el cuerpo del maniquí.

La potencia térmica emitida se controla a través de un variador de tensión conectado a la resistencia instalada. El calor emitido por la resistencia será directamente proporcional a la tensión existente entre sus extremos. El variador se regula manualmente utilizando la temperatura del aire en el punto de emisión para retroalimentar el ajuste.

Para evitar que el flujo se perturbe en el punto de inserción de la resistencia se ha aumentado el diámetro del conducto y se han situado las resistencias sobre la superficie del mismo. Para evitar la pérdida de calor a través de las paredes del tubo, se ha aislado en todos los puntos en los que se ha detectado una posible pérdida de calor al ambiente.

Para hacer más sencillo el proceso de ajuste manual del regulador de tensión, se ha generado un programa de PC con una interfaz gráfica y un sistema de adquisición de temperaturas. El sistema de adquisición de temperaturas utiliza dos sondas PT100 para recoger tanto la temperatura ambiental como la del aire espirado. El programa utiliza el valor de la temperatura ambiental para calcular la temperatura a la que se ha de emitir el aire en la espiración. En una ventana de la interfaz gráfica del programa, se muestran, en tiempo real y de manera continua, el valor de temperatura de espiración calculado junto con la banda admisible en la que se puede

encontrar dicha temperatura sin incurrir en un error excesivo. Al tiempo, en dicha ventana, se grafica el valor de la temperatura de aire espirado recogida por la sonda situada en el punto de descarga de la respiración al ambiente. Utilizando este sistema es sencillo regular el variador de tensión hasta que la temperatura emitida se encuentre dentro de la banda de admisible mostrada. En la Figura 4 se muestra un diagrama en el que se muestra el proceso secuencial de toma de datos y regulación de la temperatura.

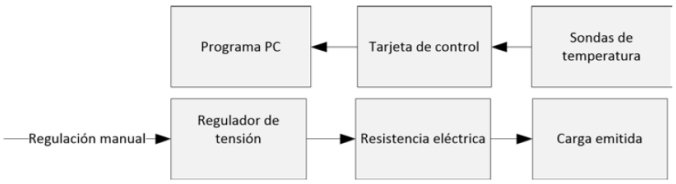


Figura 4. Esquema del proceso de control del flujo de calor emitido.

## 4. Resultados

Se han llevado a cabo diferentes pruebas para comprobar que el sistema posee la estabilidad y precisión deseadas, contabilizando los errores incurridos tanto en la temperatura como en el flujo de aire espirado.

Para estudiar el grado de desviación del flujo respiratorio simulado respecto al calculado, se ha medido la velocidad del aire en la descarga del conducto de espiración. Se ha utilizado una sonda de velocidad de esfera caliente para llevar a cabo la medida. Las desviaciones temporales máximas registradas entre los ciclos de respiración teóricos y los medidos experimentalmente han sido 0,05 s. Este error supone, considerando un ciclo típico de respiración de 4 segundos, un error inferior al 2 %.

En cuanto a la temperatura del aire emitida, la desviación máxima observada respecto al valor teórico calculado, una vez se ha estabilizado el sistema, es de 0,5 K. Esto supone, considerando una temperatura típica de espiración de 35º C, un error inferior al 1,5%.

Para ilustrar los resultados obtenidos, se muestran medidas de temperatura y velocidad a la descarga del sistema para un caso concreto de respiración simulada. Se ha obtenido el patrón de respiración y cargas térmicas para un hombre de 1,73 m de altura, un peso de 70 kg y una actividad metabólica correspondiente a un estado de reposo.

En la Figura 5 se puede observar una comparativa entre la velocidad teórica esperada y la velocidad real medida. Los valores de velocidad se han representado en forma proporcional, siendo 0 el valor de la velocidad teórica mínima alcanzada y 1 el valor de la velocidad teórica máxima medida.

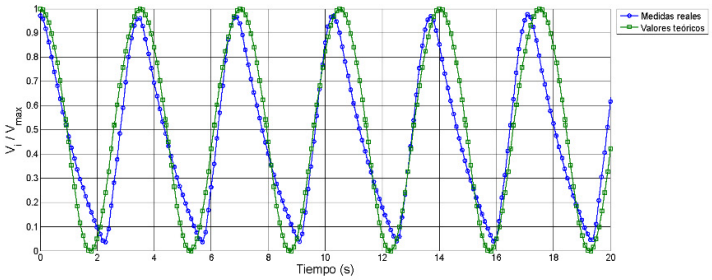


Figura 5. Velocidad teórica calculada frente a la velocidad finalmente registrada.

En la figura 6 se puede observar el registro de la temperatura a la descarga de la respiración del maniquí. Se trata del valor registrado por un sensor de temperatura PT100 instalado en el punto de exhalación de la respiración.
En la figura se muestran tres valores de temperatura calculada y uno medido. El sistema calcula en tiempo real la temperatura que se debe alcanzar en la expiración en función de las condiciones ambientales [5]. Se establecen dos límites, uno de temperatura superior y otro de temperatura inferior admisibles para el ensayo.

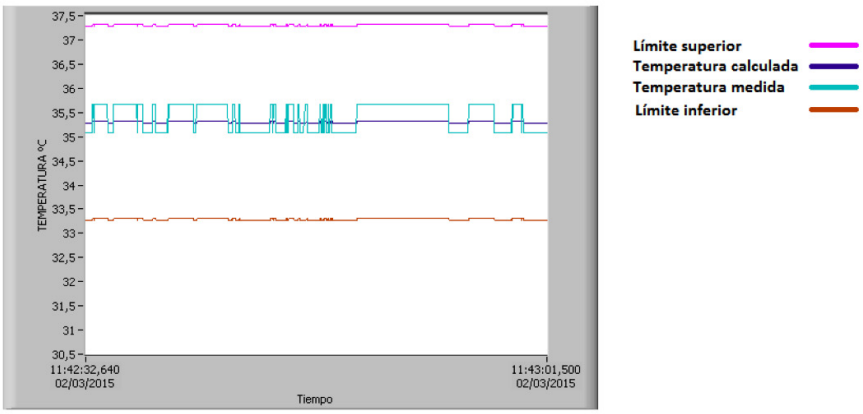


Figura 6. Estabilidad en la temperatura de aire exhalado.

## 5. Conclusiones

Se ha desarrollado un sistema de respiración artificial que permite emitir la carga térmica sensible originada por la respiración de una persona. Se puede modificar el valor de la carga emitida para simular la respiración de diferentes tipos de persona con diferentes actividades metabólicas.
El sistema se ha diseñado para poder ser integrado en los maniquíes térmicos desarrollados por el Laboratorio de Ventilación y Climatización de la Universidad de Córdoba[8]. De esta manera se mejora la capacidad de simulación de la carga térmica emitida por personas.

## 6. Referencias

[1] A. Melikov y J. Kaczmarczyk, *Measurement and prediction of indoor air quality using a breathing thermal manikin.*,RevistaIndoor Air,2007, vol. 17, pp. 50-9.

[2] J. Laverge, M. Spilak, y A. Novoselac, *Experimental assessment of the inhalation zone of standing, sitting and sleeping persons*,RevistaBuild. Environ., 2014, vol. 82, pp. 258-266.

[3] C. Xu, P. V Nielsen, G. Gong, L. Liu, y R. L. Jensen, *Measuring the exhaled breath of a manikin and human subjects*.,RevistaIndoor Air,2014, pp. 1-10.

[4] J. K. Gupta, C.-H. Lin, y Q. Chen, *Characterizing exhaled airflow from breathing and talking.*,RevistaIndoor Air, 2010, vol. 20, pp. 31-9.

[5] ASHRAE, *F09 SI: Thermal Comfort*, *ASHRAE Handb. Fundam.*, pp. 9.1-9.30, 2009.

[6] S. Tanabe, E. A. Arens, F. Bauman, H. Zang, y T. . Madsen, *Evaluating thermal environments by using a thermal manikin with controlled skin surface temperature*, Revista Ashrae Trans., 1994, vol. 100, pp. 39-47.

[7] Comité: AEN/CTN 81, *UNE-EN ISO 7730. Ergonomía en ambiente térmico. Determinación analítica e interpretación del bienestar térmico mediante el cálculo de los índices PMV y PPD y los criterios de bienestar térmico local*. AENOR, Madrid, 2006, p. 1-60.

[8] F. A. Berlanga Cañete, M. R. de Adana, e I. Olmedo, "Diseño y construcción de maniquíes térmicos para la realización de ensayos experimentales de sistemas de climatización.", En *IX Congreso Nacional de Ingeniería Termodinámica (Cartagena, 3, 4 y 5 de junio de 2015)*, 2015, pp. 1-8.

# Paper III. Influence of the air renovation rate on the risk of cross infections in a hospital room with a combined radiant and mixing ventilation system


*This paper was presented in the 12th REHVA World Congress held in Aalborg (Denmark), from 22nd to 25th of May 2016. The document was published in the congress proceedings.*

This study is meant to test the hypothesis of the influence of the ventilation flow on the exposure of the health worker to patient exhaled contaminants.

Thermal manikins distribute in a typical hospital room position with the health worker standing close a lying patient. This position remains constant in all the tests performed in this thesis.

Results show that the contaminants released by patient's exhalation depends on the ventilation configuration set. Hence, it is possible to look for the optimum ventilation strategy to reduce the health worker exposure to patient's exhaled contaminants.

# Influence of the air renovation rate on the risk of cross infections in a hospital room with a combined radiant and mixing ventilation system

F. A. Berlanga[#1], I. Olmedo[#2], M. Ruiz de Adana[#3], F. Peci[#4]

[#]*Department of Physical Chemistry and Applied Thermodynamics University of Cordoba*
*Medina Azahara 5.1407 Cordoba, Spain*

[1]felix.berlanga@uco.es
[2]ines.olmedo@uco.es
[3]manuel.ruiz@uco.es
[4]fernando.peci@uco.es

**Abstract**
*This study aims to test how mixing ventilation combined with a hydronic radiant floor system performs removing airborne exhaled contaminants using two different air renovation rates. The two selected renovation rates are 2 ACH and 7.5 ACH. Temperature and velocity probes are used to evaluate temperature and velocity profiles in the room. A tracer gas ($CO_2$) is used to measure the risk of cross infection between two breathing thermal manikins. One of the manikins (P) represents a lying person over a horizontal surface and its breathing represents the only source of contaminants into the chamber. The other one (HW) represents a standing person near P. The concentration of exhaled contaminants reaching its breathing zone is studied.*
*Temperature and air velocity profiles show that a nearly completely air stability situation is reached at the occupied zone. This stability is influenced by the air renovation rate performed. Tracer gas measurement results show a similar distribution of exhaled contaminants but with some discrepancies for both tests conducted. A higher tracer gas concentration reaches the nearby zone of HW manikin when the air renovation rate is increased from 2 to 7.5 ACH. This can lead to a higher cross infection rate.*
*The obtained results suggest that that a higher ventilation rate not necessary leads to a decrease of the airborne cross infection risk for the occupants in an enclosed area.*

***Keywords - Airborne Cross Infection; Breathing; Hydronic Radiant Systems; Ventilation***

## 1. Introduction

A significant increase in the study of ventilation performance in indoor public places such hospitals is being takin place in recent times [1–3]. New ventilation methods have been tested to provide better ventilation and energy efficient systems [4–6]. Hospitals are potentially risky places for airborne cross infection between patients, health workers and visitants [7].

One of the major source of contaminants which can transmit pathogens is breathing. Breathing exhaled air contents droplets in which nuclei can content several pathogens. Cause of the small size of the droplets exhaled, tracer gases are a good tool to study the spreading of these contaminants [8,9]. Usually, mixing ventilation is used to remove airborne contaminants [10]. Energy efficient systems like hydronic radiant floors and ceilings may be an alternative to provide comfort conditions and reduce ventilation rates [11,12].

This study aims to test how mixing ventilation combined with hydronic radiant systems performs removing airborne exhaled contaminants using two different air renovation rates

## 2. Methods

The experiments have been taken place into an isolated experimental chamber. People at the chamber are represented by two breathing thermal manikins. One of them (P) aims to represent a lying person at supine position over a horizontal surface, such a patient in a hospital ward. The other one (HW) represents a standing person near the first one, such a health worker. P manikin represents the only contaminant source of the room while the presence of contaminants into the breathing zone of HW is studied. The two breathing manikins, inhaling through the mouth and exhaling through the nose, have their mouths aligned in a vertical plane. A complete description of the distribution of the chamber can be seen in Figure 1 and Figure 2.

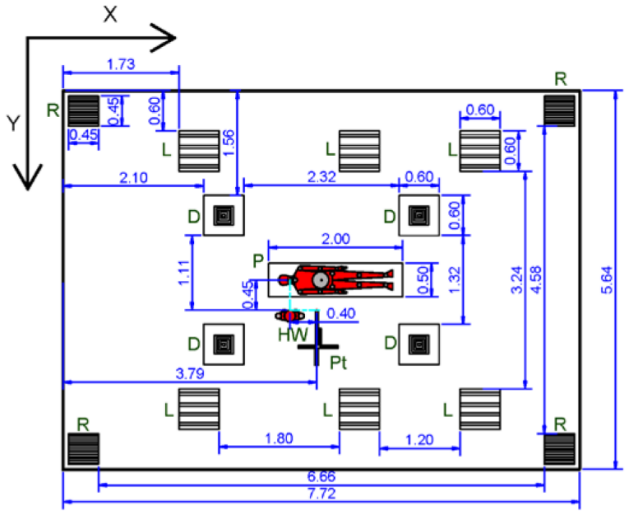


Fig. 1. Horizontal section of the experimental chamber. (D) Four-way mixing diffusers. (R) Exhaust grilles. (Pt) Vertical pole. (L) Lamps.

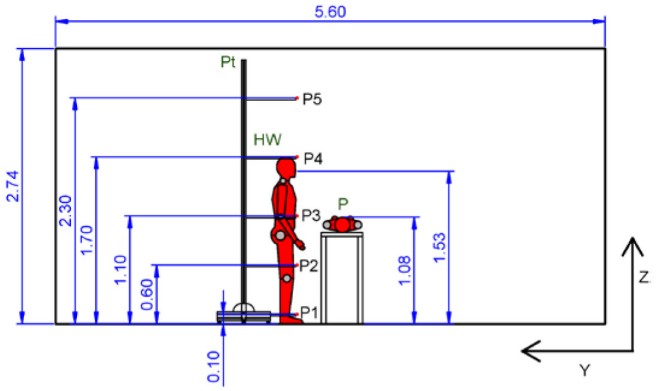


Fig. 2. Front view of the experimental chamber with the vertical pole (Pt). (P1 to P5) Probe positions.

Conditioned clean air at neutral conditions (24°C) is supplied to the room through four four-way mixing diffusers and extracted by four exhaust grills placed in the corners of the room. This study proposes two different experiments modifying the ventilation rate of the chamber. Test 1 is performed under a ventilation rate of 2 ACH (61.2 $m^3/h$) while Test 2 is performed under a ventilation rate of 7.5 ACH (229.5 $m^3/h$). During both tests the hydronic radiant system maintains a surface floor temperature of 17 °C.

Temperature of the two manikins is controlled to maintain it at 34 °C on their surface. Manikins' breathing corresponds with the one of a man of 1.70 m height and 70 kg weight using the expressions obtained from the research of Gupta [13]. Breathing orifices of the manikins corresponds with circles of 20 $mm^2$ for each nostril and 126 $mm^2$ for mouth. More information about the geometrical design and performance of the two breathing manikins can be found at [14,15].

Tests have been conducted once stationary conditions have been obtained inside the experimental chamber. Experimental chamber conditions are considered stationary when the temperature fluctuations inside the room remain under 0.5 °C. Each test has been performed during 2 hours.

Air velocity along the height of the room has been measured at five different points using a vertical pole (Pt) near the standing manikin, Figure 1 and Figure 2. The velocity probes, TSI 8475, have an accuracy of 1%.

Air temperature along the height of the room has also been measured at the same five points where the air velocity is registered. The exact heights of the temperature and velocity probes along the pole can be seen at Figure 2. Temperature has been registered using J type thermocouples with an

accuracy of 2%. Temperature measurement frequency is 1 Hz for each probe.

To measure contaminants propagation and evaluate HW cross infection risk, the breathing of P is seeded with 45000 ppm of $CO_2$ as tracer gas. This concentration is the one of a resting breathing [16]. Four CO2METER SprintIR 5% NDIR $CO_2$ probes with a 1% accuracy have been distributed around the experimental chamber to measure tracer gas concentration. Three of them have been placed near the breathing zone of the HW, as can be seen at Figure 3, the remaining one at the air exhaust of the room. Measurement frequency for each probe is 1 Hz.

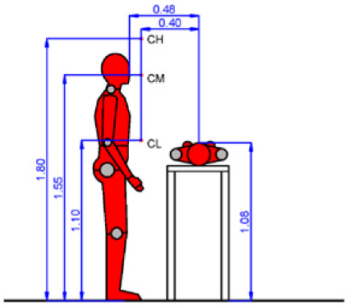


Fig. 3. $CO_2$ probe positions at the breathing area of HW.

## 3. Results and discussion

Absolute air velocity measurements along the vertical probe of the experimental chamber have been processed and their average value ($\overline{u}_i$) at each measurement point during each test have been obtained together with the standard deviation ($\sigma_i$). Results have been summarized in Table 1.

Table 1. Absolute average air velocity along the vertical pole (Pt) for the two tests performed. ($H_R$= z/H) represents the normalized height of each probe respect to the total height of the room.

| | | | Test 1 | | Test 2 | |
|---|---|---|---|---|---|---|
| Probe | *z*, (m) | $H_R$ | $\overline{u}_i$ ,(m/s) | $\sigma_i$ | $\overline{u}_i$ ,(m/s) | $\sigma_i$ |
| P1 | 0.1 | 0.04 | 0.00 | 0.00 | 0.06 | 0.02 |
| P2 | 0.6 | 0.22 | 0.00 | 0.00 | 0.04 | 0.03 |
| P3 | 1.1 | 0.40 | 0.01 | 0.02 | 0.06 | 0.02 |
| P4 | 1.7 | 0.62 | 0.03 | 0.02 | 0.10 | 0.03 |
| P5 | 2.3 | 0.84 | 0.08 | 0.02 | 0.30 | 0.05 |

Average air velocities along the height of the room for the two experiments performed are represented in Figure 4.

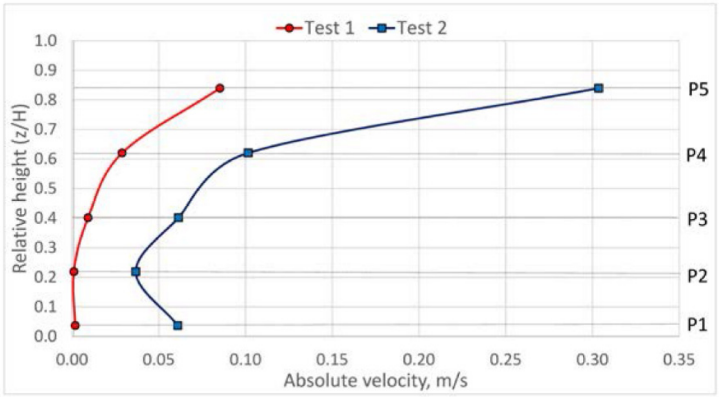


Fig. 4. Absolute average air velocity measurements along the vertical pole (Pt).

Results show that the air velocity values obtained at the occupied zone of the chamber, up to a normalized height of $H_R$=0.656, are relatively low in both cases. However, these velocity values are higher in the upper part of the room, close to the ceiling, for both cases. It seems clear the existence of an air stability region in the occupied zone that was also visualized in preliminary experiments using smoke. It is observed that the air velocity vertical profile is always higher in Test 2 than in Test 1.

Measurements obtained at the zone between the breathing points of the P and HW, placed at 0.394 and 0.558 in normalized height respectively, approximately at the interval between P3 and P4, shows that air velocity remains under 0.1 m/s at both experiments.

Temperature measurements conducted along the vertical pole have been obtained. Average temperature at each measurement point ( $\overline{T_i}$ ) and the exhaust air temperature ( $\overline{T_r}$ ) are used to obtain relative temperatures ($T_{Ri}$), using Equation 1.

$$T_{Ri} = \overline{T_i} / \overline{T_r} \quad (1)$$

Results for Test 1 and Test 2 are summarized at Table 2.

Table 2. Temperature measurements along the vertical pole.

| | | Test 1 | | | Test 2 | | |
|---|---|---|---|---|---|---|---|
| Probe | $H_R$ | $\overline{T_i}$ ,(ºC) | $T_{Ri}$ | σi | $\overline{T_i}$ ,(ºC) | $T_{Ri}$ | σi |
| P1 | 0.04 | 21.2 | 0.83 | 0.03 | 21.2 | 0.87 | 0.07 |
| P2 | 0.22 | 22.7 | 0.91 | 0.06 | 22.2 | 0.94 | 0.06 |
| P3 | 0.40 | 23.7 | 0.95 | 0.06 | 22.7 | 0.96 | 0.05 |
| P4 | 0.62 | 24.1 | 0.96 | 0.03 | 23.5 | 0.99 | 0.04 |
| P5 | 0.84 | 24.3 | 0.97 | 0.03 | 23.4 | 0.99 | 0.05 |
| Exhaust | 1.00 | 25.0 | - | 0.04 | 23.7 | - | 0.04 |

Average relative temperatures along with the relative height of the probes are represented in Figure 5 for the two experiments conducted.

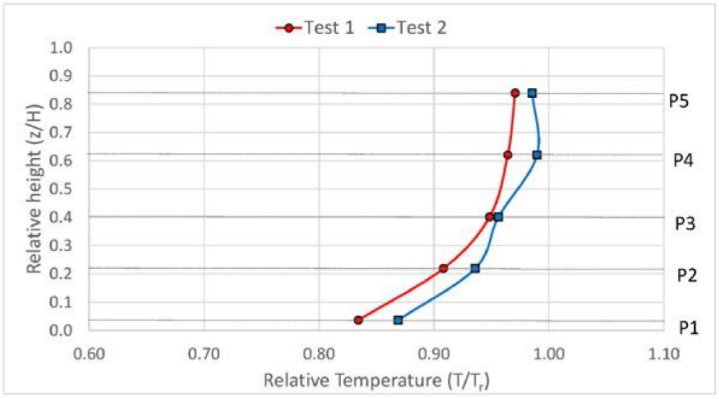


Fig. 5. Relative temperature distribution along the height of the experimental chamber.

Results show that the temperature profile along the height of the room is similar in both cases. The influence of the hydronic radiant floor is notable in the lower part of the room, where the minimum temperature value is registered. Test 2 provides a higher relative temperature values for all the points considered. This fact indicates that higher ventilation rates approximate temperature values registered along the vertical pole with the exhaust one, improving temperature homogeneity along the height of the room.

A vertical temperature gradient at the lower part of the room is present in both experiments. It shows a maximum value of 8.33 ºC/m in Test 1 and 5.51 ºC/m in Test 2 between probes positions P1 and P2. The slope of the gradient decreases with height being 1.81 ºC/m in Test 1 and 3.64 ºC/m in Test 2 between P3 and P4, which is the interval between the breathing

regions of the two manikins. Moderate positive temperature gradients such as the obtained at this research do not induce convective air flows [17].

Average concentration measurements of $CO_2$ ($\overline{c_i}$) as tracer gas at three different positions near the HW manikin are obtained together with the standard deviation ($\sigma_i$) of its values. Relative average tracer gas concentration ($c_{Ri}$) has been obtained against tracer gas concentration into the exhaust ($\overline{c_r}$) using Equation 2.

$$c_{Ri} = \overline{c_i} / \overline{c_r} \tag{2}$$

All these results together with the relative height of each $CO_2$ probe are summarized in Table 3 for Test 1 and Test 2.

Table 3. $CO_2$ concentration at three different heights close the HW manikin.

| | | Test 1 | | | Test 2 | | |
|---|---|---|---|---|---|---|---|
| Probe | $H_R$ | $\overline{c_i}$, (ppm) | $c_{Ri}$ | σi | $\overline{c_i}$, (ppm) | $c_{Ri}$ | σi |
| CL | 0.39 | 366.8 | 0.89 | 19.93 | 263.4 | 0.86 | 22.53 |
| CM | 0.55 | 359.5 | 0.87 | 29.98 | 290.1 | 0.94 | 34.72 |
| CH | 0.64 | 448.9 | 1.09 | 41.71 | 395.0 | 1.29 | 44.35 |
| Exhaust | 1.00 | 413.6 | - | 11.21 | 307.4 | - | 28.71 |

Relative $CO_2$ concentration against relative height is shown for both experiments in Figure 5.

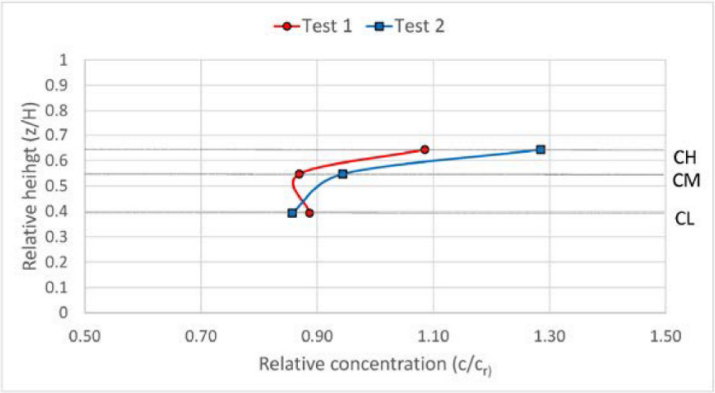


Fig. 5. Relative $CO_2$ concentration at the breathing zone of the standing manikin

Results show similar vertical concentration gradients for both tests but with some discrepancies. At the height of the chest of HW (CL), 0.02 m above the P´s mouth, the contaminant concentration is less than 1 for the two tests, which is considered lower than the value for a fully mixed air situation. There is an air stability of the air in the exhalation region of P generated by the temperature stratification provoked by the cool floor and the lack of air turbulence even when the airflow rate is high, corresponding to 7.5 ACH. This air stability makes the exhaled contaminants flow to the upper part of the room without mixing with the air surrounding HW. The clean air close to the floor is induced to the chest of HW by thermal stratification. This phenomenon also generates a low exposure level (CM) to the HW, below 1 for the two tests studied. The separation distance between the two manikins is enough to have no interference between the exhalation of P and the microenvironment around HW. However, at a higher position, above the head of HW manikin (CH), the contaminant concentration value is higher than 1, and the standard deviation increases especially for test 2. In that part of the room the air from the diffusers induces the exhaled contaminants, which are mixed with the clean air of the room, increasing the contaminant concentration above the head of HW (CH). The increase of the contaminant concentration for test 1 (2ACH) at this position is lower than for test 2 (7.5 ACH) due to the stronger influence of the air from the diffusers that induces more air from the stable region of the exhalation. The elevated flow rate of the air induces air from the lower part of the room driving it to the upper part and transporting the exhaled contaminants. The increasing of standard deviation with height also explains the distribution of exhaled contaminants in the upper part of the room, out of the stability region.

When using 2 ACH (test 1) the lack of air movement induced from the diffusers, produce a lock up phenomenon that maintains the contaminants above the patient. Many authors [18,19], for similar conditions of positive temperature gradient, have reported a lock-up phenomenon of the exhaled contaminants due to the air stability generated at the height of the exhalation of the source manikin. This makes the transport of contaminants in the air to other areas, such as to the microenvironment of HW difficult. For test 2 (7.5 ACH) there is a similar contaminant distribution, especially in the lower part of the room, due to the temperature gradient generated by the cool floor.

## 4. Conclusions

This study evaluates the influence of renovation rates in airborne contaminants removal when a mixing ventilation system is combined with a hydronic radiant floor system. Test 1 evaluates a very low ventilation rate, 2 ACH with the aim of comparing it with Test 2, which uses a common ventilation rate of 7.5 ACH.

Results obtained from measurements of absolute velocity and temperature along the height of the room show a positive vertical

temperature and velocity gradient generated by the cool hydronic floor and influenced by the ventilation rate used during each test. Higher ventilation rates lead to an increase of absolute air velocity and its variation with time inside the chamber, especially in the upper part.

$CO_2$ measurements show a similar distribution of exhaled contaminants but with some discrepancies. In both cases there is an air stability in the lower part of the room that generates low concentration values of contaminants in the region near the HW. However, the airflow generated by the diffusers in the upper part of the room induces a mixing flow that conduces to an increase value of the contaminant concentration above the head of the HW. This behavior is especially observed for test 2, using 7.5 ACH. While for test 1, 2 ACH, the concentration values above the head of the HW are still low. This study demonstrates that a higher ventilation rates does not necessarily lead to a better situation in terms of cross infection risk and contaminant exposition of people inside indoor places. Studying the dispersion of exhaled contaminants, special care should be taken on possible stability regions generated by the ventilation systems and on the temperature and velocity gradients that are generated in indoor environments.

**Acknowledgment**

The authors acknowledge the financial support received from the Ministerio de Economia y Competitividad, Secretaría de Estado de Investigación, Desarrollo e Innovación, Spain, to the National R&D project TRACER with reference DPI2014-55357-C2-2-R, entitled "Ventilation system influence on airborne transmission of human exhaled bioaerosols. Cross infection risk evaluation". This project is cofinanced by the European Regional Development Fund (ERDF).

**References**

[1] I. Eames, J.W. Tang, Y. Li, P. Wilson, Airborne transmission of disease in hospitals., J. R. Soc. Interface. 6 Suppl 6 (2009) S697–S702. doi:10.1098/rsif.2009.0407.focus.
[2] J.W. Tang, Investigating the airborne transmission pathway - different approaches with the same objectives, Indoor Air. 25 (2015) 119–124. doi:10.1111/ina.12175.
[3] J. Richmond-Bryant, Transport of exhaled particulate matter in airborne infection isolation rooms, Build. Environ. 44 (2009) 44–55. doi:10.1016/j.buildenv.2008.01.009.
[4] D. Licina, A.K. Melikov, C. Sekhar, K.W. Tham, Human convective boundary layer and its interaction with room ventilation flow., Indoor Air. (2014) 1–15. doi:10.1111/ina.12120.
[5] H. Qian, Y. Li, W.H. Seto, P. Ching, W.H. Ching, H.Q. Sun, Natural ventilation for reducing airborne infection in hospitals, Build. Environ. 45 (2010) 559–565. doi:10.1016/j.buildenv.2009.07.011.
[6] A.K. Melikov, Z.D. Bolashikov, E. Georgiev, Novel ventilation strategy for reducing the risk of airborne cross infection in hospital rooms, (2011) 1–6.
[7] C. Beggs, L.D. Knibbs, G.R. Johnson, L. Morawska, Environmental contamination and hospital-acquired infection: factors that are easily overlooked, Indoor Air. 25 (2015) 462–474. doi:10.1111/ina.12170.

[8] Y. Yin, J.K. Gupta, X. Zhang, J. Liu, Q. Chen, Distributions of respiratory contaminants from a patient with different postures and exhaling modes in a single-bed inpatient room, Build. Environ. 46 (2011) 75–81. doi:10.1016/j.buildenv.2010.07.003.
[9] C. a. Gilkeson, M. a. Camargo-Valero, L.E. Pickin, C.J. Noakes, Measurement of ventilation and airborne infection risk in large naturally ventilated hospital wards, Build. Environ. 65 (2013) 35–48. doi:10.1016/j.buildenv.2013.03.006.
[10] Y. Yin, W. Xu, J.K. Gupta, A. Guity, P. Marmion, A. Manning, et al., Experimental Study on Displacement and Mixing Ventilation Systems for a Patient Ward, HVAC&R Res. 15 (2009) 1175–1191. doi:10.1080/10789669.2009.10390885.
[11] N. Fonseca, Experimental study of thermal condition in a room with hydronic cooling radiant surfaces, Int. J. Refrig. 34 (2011) 686–695. doi:10.1016/j.ijrefrig.2010.12.019.
[12] M. De Carli, B.W. Olesen, Field measurements of operative temperatures in buildings heated or cooled by embedded water-based radiant systems, in: ASHRAE Trans., 2002: pp. 714–725. http://www.scopus.com/inward/record.url?eid=2-s2.0-0036459767&partnerID=tZOtx3y1.
[13] J.K. Gupta, C.-H. Lin, Q. Chen, Characterizing exhaled airflow from breathing and talking., Indoor Air. 20 (2010) 31–9. doi:10.1111/j.1600-0668.2009.00623.x.
[14] F.A. Berlanga Cañete, M.R. de Adana, I. Olmedo, Diseño y construcción de un sistema de emulación de la respiración para maniquíes térmicos para la realización de ensayos experimentales de sistemas de climatización (Thermal Manikin Breathing Systeem Design and Production Aimed to HVAQ Experimental Tests), in: IX Congr. Nac. Ing. Termodinámica, 2015: pp. 1–8.
[15] F.A. Berlanga Cañete, M.R. de Adana, I. Olmedo, Diseño y construcción de maniquíes térmicos para la realización de ensayos experimentales de sistemas de climatización (Thermal Manikin Design and Production Aimed to HVAQ Experimental Tests), in: IX Congr. Nac. Ing. Termodinámica, Cartagena, 2015: pp. 1–8. doi:978-84-606-8931-7.
[16] N.M. Tsoukias, Z. Tannous, a F. Wilson, S.C. George, Single-exhalation profiles of NO and CO2 in humans: effect of dynamically changing flow rate., J. Appl. Physiol. 85 (1998) 642–652.
[17] G. Gong, B. Han, H. Luo, C. Xu, K. Li, Research on the Air Stability of Limited Space, Int. J. Green Energy. 7 (2010) 43–64. doi:10.1080/15435070903501266.
[18] G. Cao, P. V. Nielsen, R.L. Jensen, P. Heiselberg, L. Liu, J. Heikkinen, Protected zone ventilation and reduced personal exposure to airborne cross-infection, Indoor Air. 25 (2015) 307–319. doi:10.1111/ina.12142.
[19] C. Xu, P. V. Nielsen, G. Gong, R.L. Jensen, L. Liu, Influence of air stability and metabolic rate on exhaled flow, Indoor Air. 25 (2015) 198–209. doi:10.1111/ina.12135.

# Paper IV. Experimental analysis of the air velocity and contaminant dispersion of human exhalation flows


*The paper has been published in Indoor Air journal (doi: 10.1111/ina.12357)*

Since the source of contaminants studied is patient's exhalation, the flow that projects the contaminants released must be studied in detail. This study considers two different exhalations in order to determine the influence of the exhalation mode in the distribution of the contaminants around the exhalation point.

Results show that the exhalation mode determines the resulting flow development over time and the distribution of the contaminants around the exhalation point. Through this study, it is possible to characterize the exhalation of a lying person, which permits gain knowledge on the flow that drives the contaminants out of the human body.

Received: 17 May 2016 | Accepted: 11 November 2016
DOI: 10.1111/ina.12357

ORIGINAL ARTICLE

WILEY

# Experimental analysis of the air velocity and contaminant dispersion of human exhalation flows

F. A. Berlanga | I. Olmedo | M. Ruiz de Adana

Department of Chemical Physics and Applied Thermodynamics, University of Córdoba, Córdoba, Spain

**Correspondence**
F. A. Berlanga, Department of Chemical Physics and Applied Thermodynamics, University of Córdoba, Córdoba, Spain.
Email: felix.berlanga@uco.es

**Funding Information**
European Regional Development Fund (ERDF)

## Abstract

Human exhalation flow is a potential source of pathogens that can constitute a cross-infection risk to people in indoor environments. Thus, it is important to investigate the characteristics of this flow, its development, area of influence, and the diffusion of the exhaled contaminants. This paper uses phase-averaged particle image velocimetry together with a tracer gas ($CO_2$) to study two different exhalation flows over time: the exhalation of an average male (test *M*) and an average female (test *F*), using a life-sized thermal manikin in a supine position. The exhalation jets generated for both tests are similar in terms of symmetrical geometry, vorticity values, jet opening angles, and velocity and concentration decays. However, there is a difference in the penetration length of the two flows throughout the whole exhalation process. There is also a time difference in reaching maximum velocity between the two tests. It is also possible to see that the tracer gas dispersion depends on the momentum of the jet so the test with the highest velocity decay shows the lowest concentration decay. All these results are of interest to better understand cross-infection risk.

**KEYWORDS**
contaminant dispersion, human exhalation flow, PIV, velocity and concentration decay

## 1 | INTRODUCTION

People spend much of their lifetime indoors where they are exposed to airborne pollution, such as VOCs (volatile organic contaminants), particles, or biological pathogens. These pathogens can be found inside small droplets or as particles emitted during normal human respiratory processes.[1]

Many researchers have found evidence of the airborne transmission routes of different diseases.[2–5] In indoor environments, there are many parameters that directly influence the dispersion of exhaled contaminants and therefore the airborne infection route. Some of these factors, such as ventilation mode,[6–9] air change rate (ACR),[10,11] or separation distance with respect to the source,[12] have been experimentally studied. Another key factor in the airborne transmission route of diseases is the different human breathing activities, such as exhalation, coughing, or sneezing, as they are considered the source of potential biological contaminants in indoor environments. In recent years, research has focused on increasing knowledge about these respiratory activities. Coughing, which is a quick process, has been studied using particle image velocimetry (PIV).[13–16] Sneezing, an even quicker expiration process, was studied using a shadowgraph imaging technique and a high velocity camera to measure the maximum distance reached by the puffs and the associated maximum velocities.[17] Airflow during speaking has been studied experimentally, using a spirometer to measure the resulting flow,[18] and also by PIV, obtaining the velocity field.[19]

Human exhalation is the most common breathing activity. Several studies have found viruses in human exhalation flows.[20–22] The particles sized ≤5 μm[23,24] that originated in a exhalation process are dispersed in the air and may potentially cause an airborne infection risk to a person inhaling them.[25–28]

Breathing has been considered as a source of contaminants in many airborne control infection studies.[6,12,29,30] However, its characteristics

  

such as frequency or tidal volume have not been considered in exactly the same measure in all of these studies. The breathing of a resting person was simulated by Bjørn and Nielsen[31] and Qian et al.,[30] considering a pulmonary ventilation flow of 6 L/min and a respiration frequency of 10 $min^{-1}$. Melikov and Kaczmarczyk[32] and Zhu et al.[33] considered the same pulmonary ventilation and breathing rate but included a short rest between inhalation and exhalation. Gao and Niu[34] assumed breathing to occur at a frequency of 17 times per minute with a pulmonary ventilation flow of 8.4 L/min, which represented a person undertaking light activity. Marr et al.[35] and Spitzer et al.[36] used a commercial simulator to execute average breathing, which performed a breathing waveform consisting of a breath volume of 1 L with a maximum flow rate of 0.6 L/s and 12.2 breaths per minute. Recently, Gupta et al.[18] undertook in-depth research on real human breathing flow, measuring the exhalation flow of people of different genders. As a result of that study, a series of equations were obtained by which the main properties of the flow, such as tidal volume or frequency, can be estimated from physical characteristics of the person (weight, gender, and height).

The aim of this study was to gain knowledge about the human exhalation flow and investigate its characteristics in detail. Two different cases, a standard man's and a standard woman's exhalation flows, have been recreated experimentally in the laboratory in order to analyze the influence of gender in the dynamic process of the exhalation flow. The characteristics of these two breathing functions are based on the study of Gupta et al.[18] Exhalation through the mouth has been selected for this study to analyze the more compromising situation for long-distance dispersion of exhaled contaminants and therefore an increased risk of potential cross-infection. Due to its perpendicular direction of the flow relative to the manikin's face, the contaminants may travel a larger distance from the manikin than when exhaling through the nose, especially with a supine position of the manikin. The exhaled flow is seeded with $CO_2$ tracer gas to measure the dispersion of possible exhaled contaminants. The velocity and concentration fields of the flows are thoroughly analyzed using different techniques.

First of all, both flows are visualized using smoke and a high-resolution camera to analyze its characteristics in terms of direction and penetration length of the exhalation flow. Secondly, as breathing is a transient process, a PIV system is used to measure the velocity field, penetration length, and vorticity at different instants of time during the exhalation process, providing transient results. The study reveals differences found in the exhalation jet characteristics over the time, which is a novel experimental result. The findings also allow for determining the jet opening angle of the two exhalation flows and improve the understanding of the human exhalation flow and therefore of the human microenvironment, taking gender influence into account. Finally, to analyze the dispersion of exhaled contaminants, the contaminant concentration is measured within the influence area of the exhalation flow. These results will help to understand airborne transmission route of diseases at short distances, where the contaminant dispersion is mainly influenced by the microenvironment between people.[26]

**Practical Implications**

- The experimental results of this study add further knowledge about the transient characteristics of male and female exhalation flows, quantifying their differences. These results are valuable for studying a long-distance dispersion of exhaled contaminants and therefore a possible cross-infection risk situation. The data may be used as boundary conditions or validation data for computational fluid dynamics simulations.

## 2 | METHODS

### 2.1 | Test room and thermal loads

This study was carried out at stable temperature and ventilation conditions within the HVAC (heating, ventilation and air-conditioning systems) laboratory at the University of Cordoba, which consists of a room 7.72 m length, 5.60 m width, and 2.74 m height (Figure 1). The ventilation system has been set at a constant air change rate of 7.5 per hour, supplying air at neutral conditions (24°C). The mean temperature in the occupied zone is maintained at 25±1°C. Clean air (917 $m^3$/h) is supplied through four four-way mixing diffusers, with a flow rate of 229 $m^3$/h each, and extracted by four exhaust grills placed at each corner of the room.

A hydronic floor radiant system maintains a homogeneous floor surface temperature of 17°C. Lighting is provided by six ceiling lamps, each one transmitting 174 W. The radiant wall of the room is provided with radiant panels that emit a heat flux of 63.8 W/$m^2$, simulating an external wall with a thermal load, which leads to a surface temperature of 35°C on the panel. The other walls are adiabatic. Tests are performed over 20 minutes after reaching stable conditions in the room.

A breathing thermal manikin (P) in a supine position on a horizontal surface simulates an infectious patient. The total thermal loads present in the room during the experiments, considering the thermal radiant panel (1350 W), the lighting of the room (1044 W), and the thermal manikin (128 W), reach 2520 W, which corresponds to 58.3 W/$m^2$.

### 2.2 | Thermal manikin and breathing simulation

The thermal breathing manikin is used to simulate an infectious patient placed horizontally on a bed. It is 1.70 m tall and has a surface of 1.6 $m^2$ (Figure 2(A)). The amount of heat supplied to the thermal manikin is controlled by a regulation system, which is set to maintain the surface temperature at 34°C. The manikin has four independent controlled heating zones: head (13 W), arms (30 W), torso (35 W), and legs (50 W). Other details about the design and performance of the thermal manikin can be found in Berlanga et al.[37]

The manikin has an independent breathing system that can simulate different breathing flows. The exhaled flow is emitted through the mouth of the manikin, which is a circular opening of 121 $mm^2$ placed in a horizontal plane. The exhalation flow is conducted to

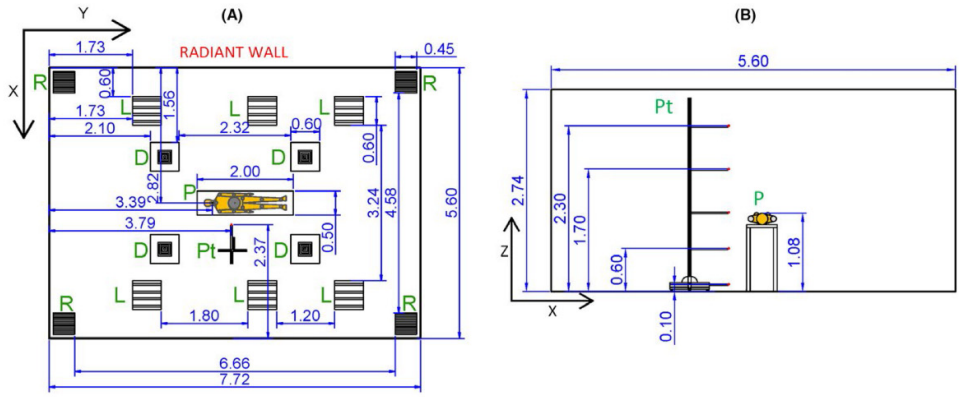


**FIGURE 1** (A) Plan view of the test chamber. Air diffusers (D); exhaust grilles (R); lamps (L); thermal manikin (P), vertical pole (Pt). (B) Profile view of the chamber. Air velocity and temperature probes (P1 to P5); vertical pole (Pt); thermal manikin (P). Dimensions in meters

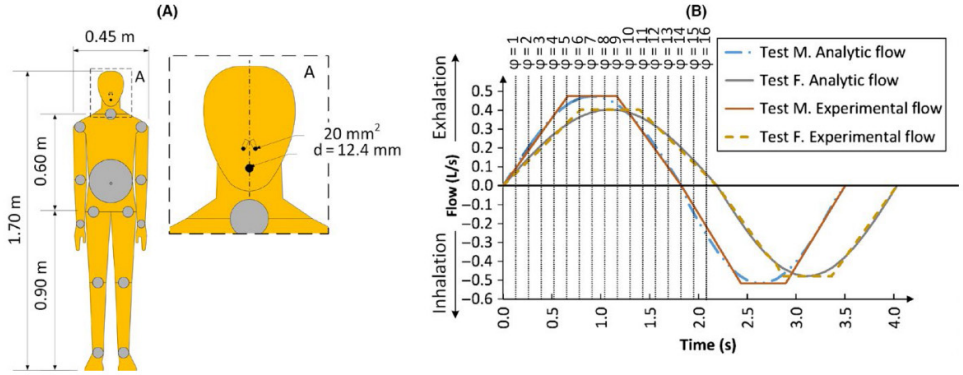


**FIGURE 2** (A) Geometry of the thermal manikin. (B) Breathing function for test *M* and test *F*

the mouth by a straight circular tube 100 mm length and 12.4 mm diameter. However, the inhalation is achieved through two nostrils (Figure 2(A)). The airflow rate and exhaled air temperature are controlled. The air exhalation flow is maintained at 34°C. Two different breathing types, which correspond to a standard male (test *M*) and a standard female (test *F*), are considered in this study. The characteristics of the two exhalation flows, test *M* and test *F*, are obtained using the expressions from Gupta et al.,[18] where it was found that they are mainly dependent on the gender, height, and weight of the person. The breathing function is obtained considering a standard male of 1.70 m height and 70 kg weight and a standard female of 1.60 m height and 60 kg weight. Table 1 shows a summary of the breathing characteristics introduced into the mechanical breathing system for each flow simulated.

Figure 2(B) presents a graphical comparison between the breathing modes described by the equations of Gupta et al. [18] and the

**TABLE 1** Characteristics of the two breathing functions, M and F

| Tests | Respiration frequency ($min^{-1}$) | | Minute volume (L/min) | Tidal volume (L) |
|---|---|---|---|---|
| | In | Out | | |
| test *M* | 17.90 | 16.43 | 9.46 | 0.55 |
| test *F* | 16.27 | 13.70 | 7.52 | 0.51 |

experimental functions obtained. In this figure, positive values represent exhalation, the negative ones represent the inhalation, and φ represents the instants of time that were considered to show results, which are spaced at intervals of 0.133 seconds, according to the frequency of the PIV laser system.

The exhalation flow is seeded with the same amount of $CO_2$ present in real human breath,[38] 45 000 ppm, using a $CO_2$ flow meter. $CO_2$ is used as tracer gas to track the contaminant distribution during

exhalation. The increase of $CO_2$ over the atmospheric concentration reveals the path of the exhaled contaminants.

## 2.3 | Measurement facilities

A particle image velocimetry system (PIV) has been used to measure and visualize the transient breathing flow. The exhalation flow is seeded with olive oil particles of around 1 μm diameter using an oil droplet generator (TSI 9307). A Nd: YAG laser (Solo 200XT, New Wave Research, California) has been used to illuminate a vertical symmetry plane that passes through the center point of the manikin's mouth. The plane is generated using a diverging lens ($f$=−15 mm) and a spherical lens ($f$=1000 mm). A digital camera (TSI Power Plus 4M) equipped with a photographic lens (NIKKOR 50 mm, NIKON, Japan) focuses on the plane of interest. The image acquisition process is controlled by a synchronizer (TSI Laser Pulse 610036, TSI, Minnesota). A scheme of the system configuration can be seen in Figure 3. The whole system is controlled by PC software (Insight 3G v9), which is also used as a post-processing tool for analyzing the results.

Measurement frame size for the PIV system is limited by the particle size, the velocity of the flow, and the image sensor resolution. In this study, a square frame of 160×160 mm was obtained. Previous smoke tests show that this frame size does not contain the complete development of the exhalation flow. To capture the whole exhalation velocity contours, three consecutive frames are used, as indicated in Figure 3. A summary of the parameters selected for the study is shown in Figure 3.

To obtain information regarding the whole exhalation process, sixteen different phases or instants of time ($\varphi$) are used. Phases are sequentially spaced at 133-ms intervals starting with the beginning of the exhalation process. The time spaced intervals are limited by the laser equipment response. An electronic system based on transistor–transistor logic communication was developed to synchronize the breathing control system and the PIV image acquisition.

Because exhalation flow is a transient process and turbulence is expected, a phase-averaged approximation to the study of velocity fields is selected. This method has already been used in different breathing studies.[35,39] Fifty exhalation processes (N=50) have been captured for test M and test F. All the PIV results are obtained considering the average value of the N measurements for each test. The final velocity vector field at each $\varphi$ is composed of the average of vectors obtained at each point using the valid measurements values in the following equation:

$$u = \frac{1}{N}\sum_{t=1}^{N} u_t \quad (1)$$

where $u_t$ is the instantaneous velocity of a phase in the $t$ breathing process, N is the total number of exhalation processes considered, and $u$ is the mean instantaneous velocity of a given phase at the point considered.

PIV measurements can be affected by different error sources which can be divided into systematic errors and statistical errors.[40] The systematic errors are mainly induced by problems in particle tracking, irregular particle seeding density, background noise, random displacement error, and so on.[40] The statistical error is mainly due to the random sampling error. A hot-wire anemometer (MiniCTA, Dantec, Denmark) utilized in combination with a sensor fiber-film probe (55R01, Dantec, Denmark) is used to measure the exhalation velocity at 50 mm from the manikin's mouth. These results are compared to the PIV measurements and are added as additional information in Supporting Information A.

To obtain vertical temperature and velocity profiles in the room, five temperature and five absolute velocity probes were positioned at different heights along a vertical pole placed in the occupied zone (Figure 1). Temperature probes consist of five J-type thermocouples, with an accuracy of 2% at the considered temperature range (15-45°C). Absolute air velocity has been measured using five hot-sphere anemometers (TSI Air Velocity Transducer 8475, TSI, Minnesota). These probes can measure an instantaneous velocity range from 0.02 to 2.5 m/s with a calibration accuracy of 3%.

A data logger (Cronos PL, IMC, Germany) equipped with specific electronic amplifiers for voltage measurements (IMC LV2-8, IMC, Germany) and precise temperature measurements (IMC C-8, IMC, Germany) is used to control, display, and analyze the data registered by temperature and velocity probes. The measurement frequency is set at 1 Hz.

A carbon dioxide ($CO_2$) tracer gas is used to simulate the pathogen released in the manikin exhalation. Laboratory based studies have shown that the residence time in air is comparable to small (~2 μm) bioaerosols.[41] Its suitability as an indoor air tracer gas has been demonstrated in different studies.[41–45] Tracer gas concentration is measured

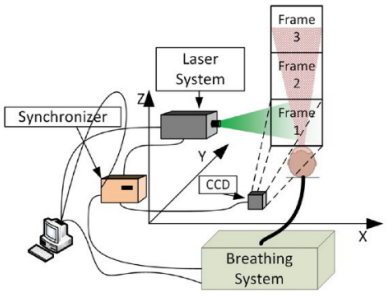


| Parameter | Value |
|---|---|
| Laser wavelenght | 532 nm |
| PIV exposure | 405 μs |
| Laser pulse delay | 400 μs |
| Pulse separation time | 100 μs |
| Repetition rate | 7.25 Hz |

**FIGURE 3** PIV system configuration

at different positions along the exhalation flow by five $CO_2$ sensors (SprintIR 5%, $CO_2$ Meter, Florida). This technology has been used in different fields like environmental gas monitoring[46,47] and medicine.[48] Each $CO_2$ sensor has been previously calibrated against three different $CO_2$-$N_2$ gas bottles of fixed concentration: 1000 ppm, 20 000 ppm, and 45 000 ppm of $CO_2$.

## 3 | RESULTS AND DISCUSSION

### 3.1 | Test room conditions

Absolute air velocity and temperature have been measured during the experiments along the vertical pole Pt (Figure 1).

Instantaneous absolute air velocity and temperature values have been processed to obtain their absolute air velocity average values ($\bar{u}$) and dimensionless temperature values ($\bar{T}_R$), respectively, and their standard deviation ($\sigma_u$) and ($\sigma_T$) at each measuring point along the vertical pole. The dimensionless value of the temperature ($\bar{T}_R$) has been obtained taking into account the average value of the temperature measurements ($\bar{T}$), the inward average air temperature ($\bar{T}_{in}$), and the exhaust average air temperature ($\bar{T}_{out}$).

$$\bar{T}_R = \frac{\bar{T} - \bar{T}_{in}}{\bar{T}_{out} - \bar{T}_{in}} \quad (2)$$

The results can be seen in Table 2. Figure 4 shows the velocity and temperature results against the normalized height, $H_R$, which is obtained by dividing z, the height of each probe, by the total height of the room.

Results show that the vertical dimensionless temperature and the average absolute air velocity profiles in the room are similar for the two tests. Standard deviation values ($\sigma_u$) and ($\sigma_T$) are low. It shows that the variation of the chamber conditions during the experiments is not significant. The influence of the hydronic radiant floor is evident in the lower part of the room, where the minimum dimensionless temperature value is registered. Dimensionless temperature measurements in the occupied zone of the chamber, up to a normalized height of $H_R$=0.656, show a moderate positive slope which does not induce convective flow. In the area where the exhalation flow is analyzed, which covers 0.11 $H_R$, starting from the height of 0.3 $H_R$, the temperature gradient of the room air is 0.7°C/m. It constitutes a relative low positive temperature gradient which leads to a stable region in terms of temperature distribution.[49,50] Average absolute air velocity values obtained in the occupied zone of the chamber are relatively low in both cases, under 0.15 m/s. However, these velocity values are higher in the upper part of the room, close to the ceiling.

### 3.2 | Smoke visualization

Five different pictures (250×250 mm) are taken to visualize the resulting exhalation for test *M* and test *F*. Exhalation flow of the manikin has been seeded with oil droplets, sized 1 μm, and a laser plane is used to illuminate the XZ vertical plane centered on the mouth of the manikin. The centerline of the exhalation jet is found at this plane by measuring the velocity of the flow and selecting the points with maximum velocity values. Pictures have been taken for the first exhalation for each test, assuring that previous exhalation flows are not influencing the visualization. The smoke pictures along the exhalation XZ center plane allow a visual inspection of the development and penetration of the exhalation flow. Previous visualization and velocity measurements of the exhalation along the exhalation YZ center plane showed no significant differences with the data obtained for the XZ center plane. This results leads to a quasi-axisymmetric exhalation jet.

Figure 5 shows the flow obtained for the two exhalations, M and F, at different instants of time or phases (φ). It is possible to observe

**TABLE 2** Dimensionless temperature and air velocity conditions at the experimental chamber during the experiments

| | | test *M* | | | | test *F* | | | |
|---|---|---|---|---|---|---|---|---|---|
| Probe | $H_R$ | $\bar{u}$ (m/s) | $\sigma_u$ (m/s) | $\bar{T}_R$ | $\sigma_T$ (°C) | $\bar{u}$ (m/s) | σu (m/s) | $\bar{T}_R$ | $\sigma_T$ (°C) |
| P1 | 0.04 | 0.02 | 0.03 | −0.70 | 0.12 | 0.00 | 0.02 | −1.09 | 0.06 |
| P2 | 0.22 | 0.14 | 0.07 | −0.08 | 0.08 | 0.12 | 0.06 | −0.33 | 0.08 |
| P3 | 0.40 | 0.08 | 0.03 | 0.14 | 0.03 | 0.06 | 0.02 | −0.09 | 0.04 |
| P4 | 0.62 | 0.14 | 0.03 | 0.46 | 0.04 | 0.13 | 0.03 | 0.29 | 0.05 |
| P5 | 0.84 | 0.46 | 0.10 | 0.39 | 0.03 | 0.46 | 0.11 | 0.25 | 0.05 |

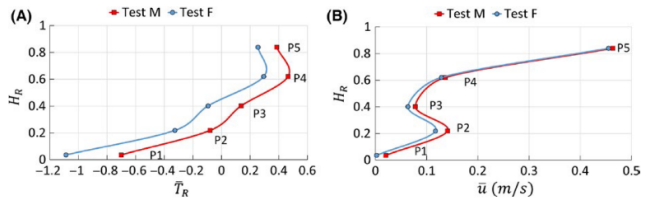


**FIGURE 4** (A) Dimensionless temperature at different heights. (P1 to P5) Probe positions. (B) Average absolute air velocity along the height of the chamber. Probe positions (P1 to P5)

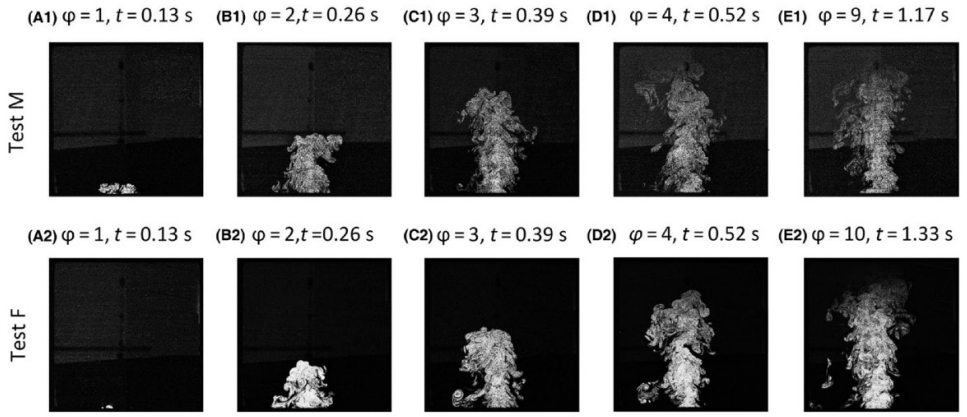


**FIGURE 5** Smoke test *F* or different phases for the two tests conducted

the transient development of the exhalation flow from the start of the process φ=1, to the instant of maximum velocity, φ=9 for test *M*, and φ=10 for test *F*. The main difference between the exhalation jets can be found in the distance reached by the particles, which is larger for test *M* during all phases. This is due to the higher flow rate of this breathing, 9.45 L/min of test *M* exhalation against 7.51 L/min of test *F*.

Over the first instants of time, φ=1 and φ=2, the flow develops in a subtle mushroom form, the typical form of non-developed jets caused by the resistance of the air in the outer section of the jets. This form is barely visible at φ=3 and φ=4 where jet structures and the transition zone are shown. Vortices are developed in the free shear region making the turbulence evident. The development of the exhalation jet is complete when the flow rate is maximum at φ=9 for test *M* and φ=10 for test *F*.

### 3.3 | PIV measurements

PIV is used to measure the whole exhalation jet velocity field in a vertical symmetry plane of the manikin's face, as shown in Figure 3. This is done using three measuring frames along the exhalation. Results are shown using dimensionless vertical ($z/d$) and horizontal ($x/d$) distances from the mouth, and dimensionless velocity ($u/u_0$), where $d$ is mouth diameter of the manikin, $u$ is the absolute velocity, and $u_0$ is the velocity at the origin of the jet.

Figure 6 shows the velocity results as the absolute air velocity contours of the exhalation for the same phases.

At φ=1, it is not possible to identify jet structures and the two tests show the initial mushroom structure of the exhalation. At φ=4, it is possible to observe an important difference with respect to φ=1: Due to the increase of the exhalation flow rate, the jet is developed and the typical jet core structure can be identified for test *M* and test *F*. The velocity registered near the mouth area has increased significantly. When the exhalation rate is at its maximum, which corresponds to φ=9 for test *M* and φ=10 for test *F*, the maximum penetration length of the exhalation flow is reached. The penetration length is defined as the vertical distance measured from the manikin's mouth, where the velocity value measured is 0.3 $u_0$. The results allow us to observe the delay of the instant of maximum penetration length of test *M* with respect to test *F*, which is in accordance with the different breathing functions. For φ=12, the velocity of the flow starts to decrease in both tests and that leads to a reduction of the penetration length and the influence area of the jet. It can be also noted that the jet becomes slightly wider due to the influence of turbulence.

A different penetration length of the transient jets can be observed for the two tests performed during the whole exhalation process, as can be seen at Figure 6. At φ=4, the penetration length of test *M* is about 20 $z/d$, while for test *F*, it is about 15 $z/d$. However, for the instants of maximum flow rate (φ=9 for test *M*, and φ=10 for test *F*), the penetration length differs by approximately 10 $z/d$. This means that the difference between the penetration length of the two exhalations increases with time. At φ=12, when the two jets are decreasing their velocities, the penetration length of test *M* is still higher than for test *F*. Exhalation velocity vector field for each phase considered at Figure 6 is added as additional information in Supporting Information B.

The jet opening angle is identified at the stages where the velocity is at its maximum. Jet influence area is determined by normalizing all velocities ($u/u_z$) at a distance of mouth plane using centerline velocity ($u_{cz}$). The limit of the jet diffusion area is usually considered at $u/u_{cz}$=0.05.[39,51] The results are shown in Figure 7.

Exhalation has a jet diffusion angle that varies from 20.5° for test *M* to 22.7° for test *F*, which means that the woman exhalation flow, test *F*, has a wider influence area.

Figure 8 shows the similarity of the mean velocity distribution at different distances from the mouth. All the velocities at each line have been normalized against the velocity at the centerline, while distance

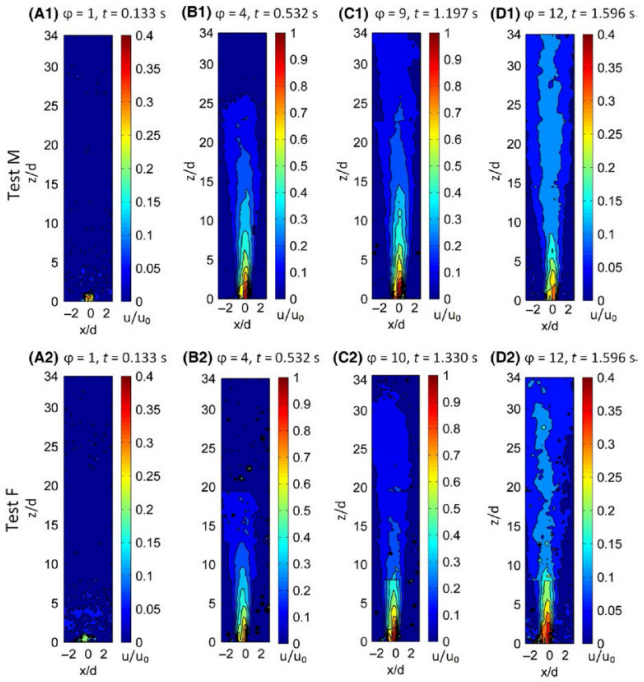


**FIGURE 6** Absolute air velocity development through time for test *M* and test *F*

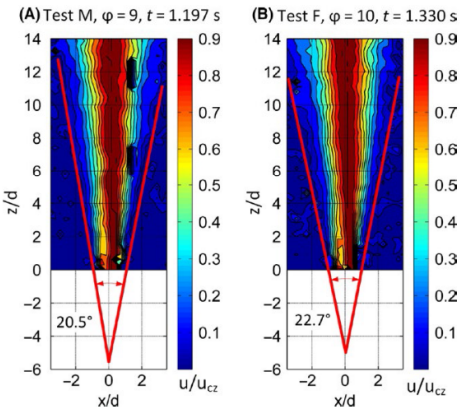


**FIGURE 7** Jet diffusion angle at stages of maximum exhalation flow. (A) test *M*. (B) test *F*

has been normalized using the perpendicular distance from the centerline where the registered velocity is half of the centerline velocity ($x_{1/2}$).

The velocity profiles are similar from $z/d>2.5$ and beyond for test *M* and test *F*. This corresponds to the beginning of the axisymmetric decay zone and the end of the potential core zone. For shorter distances, $z/d<2.5$, it is not possible to find the structure of the axisymmetric decay zone.

Finally, phase-averaged vorticity contours are obtained to investigate how vortices develop over the exhalation. The 2D vorticity is obtained by this equation:

$$\omega = \frac{\partial u_z}{\partial x} - \frac{\partial u_x}{\partial z} \tag{3}$$

Because of the discrete nature of the data obtained by the PIV system, a numeric differentiation scheme is used. In this case, a standard least squares method is used to obtain this expression:

$$\omega_{i,k} = \frac{1}{10\Delta X}\left(2u_{zi+2,k} + u_{zi+1k} - u_{zi-1,k} - 2u_{zi-2,k}\right) - \frac{1}{10\Delta Z}\left(2u_{xi,k+2} + u_{xi,k+1} - u_{xi,k-1} - u_{xi,k-2}\right) \tag{4}$$

The vorticity $\omega_{i,k}$ represents the value at the exact $(i,k)$ position, where $i$ represents the horizontal coordinate considered and $k$ the vertical one. With regard to the velocity vector components, $u_x$ represents the horizontal component of the velocity vector, while $u_z$ represents the vertical one. The increments $\Delta X$ and $\Delta Z$ are the horizontal and vertical distances between two considered points, respectively.

Figure 9 shows a graphical representation of the vorticity at four different phases.

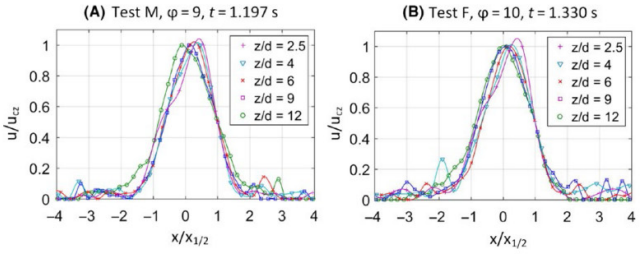


**FIGURE 8** Similarity of mean velocity. (A) test *M*, φ=9. (B) test *F*, φ=10

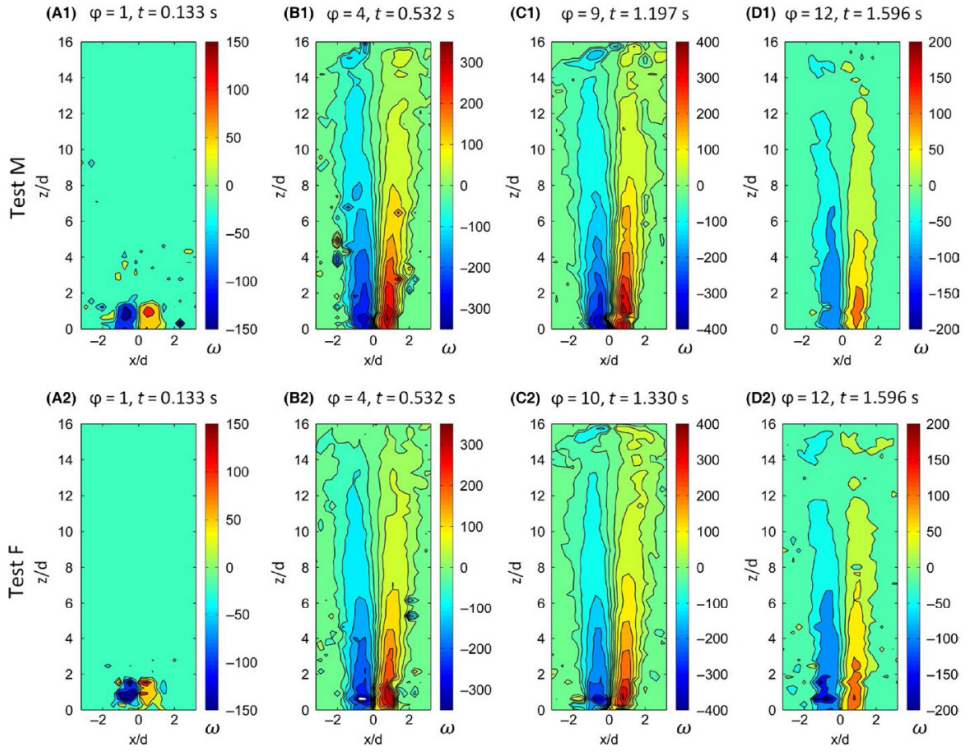


**FIGURE 9** Phase-averaged vorticity contours for test *M* and test *F*

At φ=1, two different vortices are created at each side of the jet. The right one shows clockwise rotation, while the left one shows counterclockwise rotation. These vortices are created because of the high velocity gradient generated by the exhalation. This initial rotation is developed by time increasing their vorticity value and its extension, as can be seen in the subsequent phases (φ=4 and φ=9). Vorticity intensity decreases with distance to the mouth, but its influence area increases. The maximum vorticity is always located near the exhalation point. The vorticity decreases at φ=12 for the two cases when the exhalation flow is decreasing.

While the structure of the vorticity remains similar for the two tests, the maximum values for test *M* are slightly higher than for test *F* during the whole exhalation process. This is due to the higher flow rate of the man's breathing, which induces a higher velocity gradient through the exhalation area. As Figures 6 and 9 show, the exhalation flow for test *M* and test *F* follows a straight vertical direction. It leads

to a symmetry of the velocity and vorticity values in both tests, which is generated by the dominating inertial forces of the exhalation. The upward convective flow of the manikin thermal plume is considered weak due to the supine position of the manikin and the low heat load generated in the head. An influence of the radiant wall might be expected in the direction of the exhalation. However, this feature has not been observed in the measurements. The large size of the room and the separation distance of the manikin with respect to the radiant wall may be helping to reduce that influence.

### 3.4 | Tracer gas concentration

Concentration was measured along the centerline and in the close influence area of the exhalation jet. The measurements are taken at 85 points organized in 5 columns and 17 rows in order to obtain the contaminant distribution (Figure 10). Each row consists of 5 $CO_2$ probes spaced at intervals of 15 mm, which are moved together to 17 vertical positions using a robotic arm system. The $CO_2$ measurements are taken over 10 min at each location, which corresponds to a total of 150 exhalations.

The average $CO_2$ concentration at each measuring point (*i*,*k*), has been normalized using the following equation.

$$c_{Ri,k} = \frac{c_{i,k} - c_{out}}{c_0 - c_{out}} \quad (5)$$

where $c_{i,k}$ is the tracer gas concentration into each measurement point, $c_{out}$ is the tracer gas concentration measured in the exhaust air of the experimental chamber, and $c_0$ is the maximum tracer gas concentration which is found in the mouth of the thermal manikin. Results are shown using contour lines in Figure 11.

Results show that the contaminant concentration distribution has similar symmetrical geometry for both tests. The maximum concentration values are found close to the manikin's mouth and their values quickly decrease with distance. The relative contaminant concentration reaches a further distance for test *F*. A relative contaminant concentration value of 0.2 is reached at $z/d$=12 for test *M*, while it is found at $z/d$=15 for test *F*. This means that the higher momentum obtained for test *M* exhalation increases contaminant dispersion, obtaining a lower centerline concentration compared to test *F*. The diffusion of the contaminants is directional, reaching the maximum values always at the centerline for test *M* and test *F*. This can be explained by the narrow angle of the jet and the influence of the temperature flow that confines the contaminants within the jet. For the concentration measurements shown in Figure 11, it is possible to see a deviation of the exhalation flow with respect to the vertical line, partly caused by the radiant wall. That leads to a not symmetrical dispersion of the exhaled contaminants, especially at distances larger than 10 $z/d$ from the manikin's mouth. The dispersion of exhaled $CO_2$ is measured during the exhalation and the inhalation periods of the manikin, not only for the exhalation periods as it happens for the velocity measurements. This fact may be producing an influence of the airflow pattern in the room on the dispersion of contaminants, particularly during the inhalation periods.

| Z | (mm) |
|---|---|
| 17 | 400 |
| 16 | 300 |
| 15 | 200 |
| 14 | 160 |
| 13 | 140 |
| 12 | 120 |
| 11 | 100 |
| 10 | 80 |
| 9 | 60 |
| 8 | 40 |
| 7 | 30 |
| 6 | 25 |
| 5 | 20 |
| 4 | 15 |
| 3 | 10 |
| 2 | 5 |
| 1 | 0 |

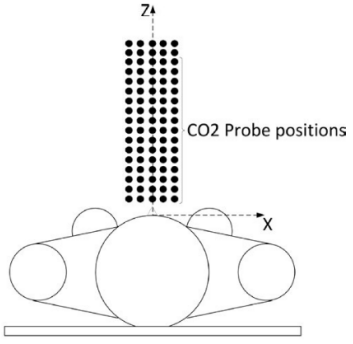


**FIGURE 10** $CO_2$ probe positions during tracer gas measurements. The table shows the distance of the probes from the mouth

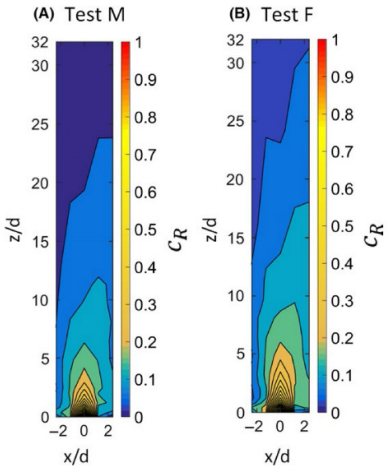


**FIGURE 11** $CO_2$ average concentration values in the breathing area. (A) test *M*. (B) test *F*

Recently, several authors[6,26,52] have shown that the exposure to exhaled contaminants by a person in indoor environments is dependent on the distance from the emission source and on the breathing mode. This study adds relevant information about the dispersion of exhaled contaminants when using different breathing functions, as such for an average female or male person. Results show how the contaminant concentration decreases with the distance to the source and how exhaled contaminants follow a further distance in the case of lower tidal volume analyzed, test *F*. As well, the opening angle of the exhalation changes the influence area of the contaminants. All these factors may directly influence the short-range airborne exposure to exhaled pathogens of a susceptible person placed in the same room, such as a nurse or a health worker.

### 3.5 | Velocity and concentration decay of the exhalation jet

Velocity and tracer gas concentration measurements are carried out along the centerline of the transient exhalation jet. Velocity has been registered using phase-averaged PIV technique, while tracer gas concentration values have been obtained using NDIR $CO_2$ probes. Relative maximum values obtained at each exhalation cycle for different distances from the origin of the jet (115 points for velocity and 17 points for tracer gas concentration) have been collected and averaged. Using these averaged values, the decay of velocity and concentration with respect to the distance to the manikin's mouth are calculated using the following expressions:

$$\frac{u_{cz}}{u_o} = K_v \left( \frac{z}{\sqrt{a_0}} \right)^{n_v} \tag{6}$$

$$\frac{c_{cz} - c_{out}}{c_0 - c_{out}} = K_c \left( \frac{z}{\sqrt{a_0}} \right)^{n_c} \tag{7}$$

In these expressions, $a_0$ represents the area of the manikin's mouth and $z$ the vertical distance from the measuring point to the mouth. About the velocity expression, $u_{cz}$ represents the centerline velocity at a $z$ vertical distance from the origin of the jet, while $u_0$ is the maximum velocity measured at the origin of the jet. For equation (7), $c_{cz}$ represents the concentration at $z$ along the centerline, $c_{out}$ is the concentration measured in the exhaust, and $c_0$ is the maximum concentration value measured at the origin of the jet. The parameters $K_v$, $n_v$, $K_c$, and $n_c$ are regression coefficients obtained from the fit of experimental data.

The characteristic constants for the velocity and concentration decay expressions are shown in Table 3.

Figure 12 shows the velocity and concentration decay of the exhalation jet in log–log coordinates.

It is possible to observe three different slope tendencies along the exhalation centerline. This is coherent with the behavior of a circular free jet where it is not possible to find the characteristic decay region.[53] The length of each zone is different for the concentration and the velocity results.

Looking at the velocity results, it is possible to recognize the potential core zone near the mouth. One of the major features is that the jet has the same width as the source orifice, as in a free isothermal jet. The following region can be identified as the axisymmetric decay zone where the slope is similar for the two tests with a value close to −0.5, which corresponds to the slope of a plane isothermal free jet. The mean characteristic of this zone is the presence of similarity of the local mean velocity profile in the region. It is possible to see that this region starts at a distance of around $z/\sqrt{a_0} = 2.5$ and ends at $z/\sqrt{a_0} = 5$ where the slope changes for the two tests. For distances higher than $z/\sqrt{a_0} = 5$ test *F* shows a slightly higher velocity decay rate that may be due to the lower initial velocity of the jet. It can also be noted that the tendency of the measurements becomes less clear in this zone, anticipating the typical behavior of the terminal zone.

Tracer gas concentration measurements also show three zones with different decay rates. Close to the origin of the jet, the tracer gas decay rate is negligible. This zone (until $z/\sqrt{a_0} = 1$) is shorter than the potential core zone that is found for velocity measurements, which may be due to the perturbation that the use of an invasive method to measure $CO_2$ concentration could have in flow development. Further, from $z/\sqrt{a_0} = 1$ to $z/\sqrt{a_0} = 10$, a nearly constant slope decay zone is found. From $z/\sqrt{a_0} = 10$ and further distances, the slope increases remarkably, showing behavior that can be compared with the terminal zone for velocity measurements. For the three zones of the concentration decay, test *F* shows lower slope values than test *M*, which leads to a higher dispersion of the contaminants in the air. This result is in accordance with $CO_2$ average concentration values already discussed and also shown in Figure 11.

## 4 | CONCLUSIONS

Experimental tests have been carefully carried out to analyze the characteristics of two different human exhalation flows corresponding to a standard male's (test *M*) and female's (test *F*) breathing functions. In view of the results of each test and the comparisons between them, the following conclusions can be stated.

**TABLE 3** Characteristic constants for velocity and concentration decay

| | $z/a_0^{0.5} < 2$ | | | $2 < z/a_0^{0.5} < 5$ | | | $z/a_0^{0.5} > 5$ | | |
|---|---|---|---|---|---|---|---|---|---|
| | $K_v$ | $n_v$ | $R^2$ | $K_v$ | $n_v$ | $R^2$ | $K_v$ | $n_v$ | $R^2$ |
| | Velocity Decay | | | | | | | | |
| test *M* | 0.953 | −0.014 | 0.293 | 1.284 | −0.515 | 0.994 | 1.955 | −0.710 | 0.974 |
| test *F* | 0.930 | −0.037 | 0.750 | 1.230 | −0.478 | 0.975 | 2.043 | −0.778 | 0.974 |
| | $z/a_0^{0.5} < 1$ | | | $1 < z/a_0^{0.5} < 10$ | | | $z/a_0^{0.5} > 10$ | | |
| | $K_c$ | $n_c$ | $R^2$ | $K_c$ | $n_c$ | $R^2$ | $K_c$ | $n_c$ | $R^2$ |
| | Concentration decay | | | | | | | | |
| test *M* | 0.627 | −0.197 | 0.967 | 0.589 | −0.742 | 0.998 | 2.620 | −1.383 | 0.985 |
| test *F* | 0.711 | −0.147 | 0.865 | 0.695 | −0.672 | 0.995 | 3.269 | −1.365 | 0.974 |

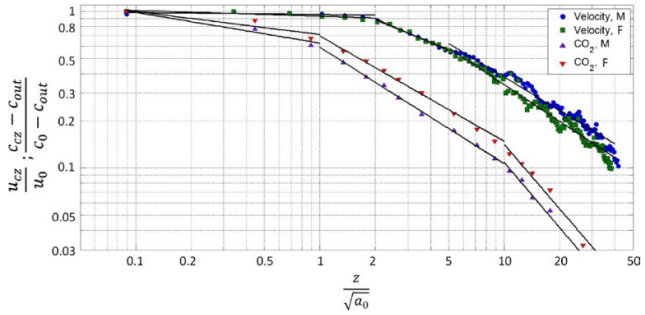


**FIGURE 12** Velocity and concentration decay experimental data and fitted expressions for both test *M* and test *F*

- The characteristics of the two exhalation jets are similar in terms of symmetrical geometry with respect to the centerline, vorticity, and velocity distribution along the jet. However, there are some important differences such as the penetration length, the jet opening angle, and the dispersion of contaminants.
- The sine breathing function of the male test has a higher amplitude and a larger number of cycles. This means a higher exhalation flow in a lower period of time, which produces a higher initial exhalation velocity and momentum. This fact makes the penetration length of the exhalation larger during the whole exhalation process, including the instant of maximum exhalation flow.
- The dispersion of contaminants for the female breathing case reaches a larger influencing area, the jet opening angle is wider, and the contaminant concentration decay is lower. This is due to the lower initial momentum that causes the exhaled contaminants to disperse in the surrounding air of the room more easily than that for test *M*.
- The velocity and vorticity distribution of the exhalation flow is symmetrical for both tests M and F. This fact may be due to the strong influence of the inertial forces of the exhalation flow, which makes the exhalation follow a vertical direction. The influence of the airflow pattern of the room is not noticeable on the exhalation velocity distribution. However, contaminant dispersion shows a non-symmetrical behavior for both tests, especially at 10 $z/d$ from the manikin's mouth. This fact may be due to an influence of the airflow pattern of the room, including the radiant wall, which directly affects the dispersion of contaminants.

Considering all the results, this paper shows that the PIV technique is a useful tool to characterize transient flows such as those associated with human exhalation. Therefore, it may be interesting to analyze other breathing functions or transient flows. All the results can help in understanding the development of an exhalation jet, the dispersion of exhaled contaminants, and the study of cross-infection risk situations. The dispersion of exhaled contaminants analyzed in this work may directly influence the exposure of another person in the same room, especially at short distances, where the microenvironment plays a crucial role. The experimental data obtained may be used as validation data or boundary conditions in CFD simulations.

## ACKNOWLEDGEMENTS

The authors acknowledge the financial support received from the Ministerio de Economia y Competitividad, Secretaría de Estado de Investigación, Desarrollo e Innovación, Spain, to the National R&D project TRACER with reference DPI2014-55357-C2-2-R, entitled "Ventilation system influence on airborne transmission of human exhaled bioaerosols. Cross infection risk evaluation." This project is cofinanced by the European Regional Development Fund (ERDF).

## NOMENCLATURE

| | |
|---|---|
| ACR | Air change rate ($h^{-1}$) |
| $a_0$ | Manikin's mouth area ($m^2$) |
| CFD | Computational fluid mechanics |
| $c$ | Tracer gas concentration (ppm) |
| $c_0$ | Maximum tracer gas concentration located at manikin's mouth (ppm) |
| $c_R$ | Normalized tracer gas concentration |
| $c_{out}$ | Tracer gas concentration at the exhaust of the experimental chamber (ppm) |
| $c_{cz}$ | Jet centerline tracer gas concentration at a vertical distance $z$ from the manikin's mouth (ppm) |
| $d$ | Diameter of manikin's mouth (m) |
| $F$ | Female test |
| $f$ | Focal length |
| HVAC | Heating, ventilation and air-conditioning systems |
| $H_R$ | Normalized height |
| $i$ | Position along X coordinate axis |
| $k$ | Position along Z coordinate axis |
| $K_c$ | Characteristic velocity constant for tracer gas concentration measurements |
| $K_v$ | Characteristic velocity constant for velocity measurements |
| $M$ | Male test |
| $n_c$ | Characteristic exponent for tracer gas concentration measurements |
| $n_v$ | Characteristic exponent for velocity measurements |
| $N$ | Total number of individual exhalations considered for phase-averaged PIV method. |

| | |
|---|---|
| NDIR | Non-dispersive infrared technology |
| $P$ | Thermal manikin |
| PIV | Particle image velocimetry |
| Pt | Vertical pole |
| $t$ | Each of the $N$ breathing measurements carried out during the experiment |
| $\bar{T}$ | Average temperature value (°C) |
| $\bar{T}_R$ | Dimensionless average temperature value |
| $\bar{T}_{in}$ | Average temperature of the ventilation air introduced to the experimental chamber during an experiment (°C) |
| $\bar{T}_{out}$ | Average temperature of the exhaust ventilation air of the experimental chamber during an experiment (°C) |
| $u$ | Mean instantaneous velocity of a given phase $\phi$ in a considered point (m/s) |
| $\bar{u}$ | Average absolute air velocity (m/s) |
| $u_0$ | Maximum jet velocity registered at the mouth of the thermal manikin during an exhalation (m/s) |
| $u_t$ | Instantaneous velocity of a phase in the $t$ breathing process in a considered point (m/s) |
| $u_{cz}$ | Jet centerline velocity at a $z$ vertical distance from the mouth (m/s) |
| $u_x$ | Horizontal component of a velocity vector (m/s) |
| $u_z$ | Vertical component of a velocity vector (m/s) |
| VOC | Volatile organic contaminant |
| $x$ | Transversal distance (m) |
| $x_{1/2}$ | Horizontal distance from centerline to the horizontal velocity field point where absolute velocity has been reduced to a half of its centerline value (m) |
| $X$ | Transversal coordinate axis |
| $y$ | Longitudinal distance (m) |
| $Y$ | Longitudinal coordinate axis |
| $z$ | Vertical distance (m) |
| $Z$ | Vertical coordinate axis |
| $\Delta X$ | Horizontal distance between two velocity vectors (m) |
| $\Delta Z$ | Vertical distance between two velocity vectors (m) |
| $\varphi$ | Phases, instants where PIV images are captured from the beginning of the exhalation |
| $\sigma_u$ (m/s) | Standard deviation of absolute velocity measurements |
| $\sigma_T$ | Standard deviation of temperature measurements (°C) |
| $\omega$ | Vorticity ($s^{-1}$) |

## REFERENCES


1. Benett JE, Dolin R, Blaser MJ. *Principles and Practice of Infectious Diseases*, 8th ed., Saunders, E. (ed.), Philadelphia: Elsevier; 2015.
2. Goldmann D. Transmission of viral respiratory infections in the home. *Pediatr Infect Dis J*. 2000;19:S97–S102.
3. Mao J, Gao N. The airborne transmission of infection between flats in high-rise residential buildings: a review. *Build Environ*., Elsevier Ltd. 2015;43:1805–1817.
4. Sun Y, Wang Z, Zhang Y, Sundell J. In China, students in crowded dormitories with a low ventilation rate have more common colds: evidence for airborne transmission. *PLoS ONE*. 2011;6:e27140.
5. Yu ITS, Li Y, Wong TW, et al. Evidence of airborne transmission of the severe acute respiratory syndrome virus. *N Engl J Med*. 2004;350:1731–1739.
6. Cao G, Nielsen PV, Jensen RL, Heiselberg P, Liu L, Heikkinen J. Protected zone ventilation and reduced personal exposure to airborne cross-infection. *Indoor Air*. 2015;25:307–319.
7. Gilkeson C, Camargo-Valero M, Pickin LE, Noakes CJ. Measurement of ventilation and airborne infection risk in large naturally ventilated hospital wards. *Build Environ*., Elsevier Ltd. 2013;65:35–48.
8. Qian H, Li Y, Nielsen PV, Hyldgaard CE, Wong TW, Chwang ATY. Dispersion of exhaled droplet nuclei in a two-bed hospital ward with three different ventilation systems. *Indoor Air*. 2006;16:111–128.
9. Tian L, Lin Z, Wang Q. Comparison of gaseous contaminant diffusion under stratum ventilation and under displacement ventilation. *Build Environ*., Elsevier Ltd 2010;45:2035–2046.
10. Jurelionis A, Gagytė L, Prasauskas T, et al. The impact of the air distribution method in ventilated rooms on the aerosol particle dispersion and removal: the experimental approach. *Energy Build*. 2015;86:305–313.
11. Knibbs LD, Morawska L, Bell SC, Grzybowski P. Room ventilation and the risk of airborne infection transmission in 3 health care settings within a large teaching hospital. *Am J Infect Control.*, Elsevier Inc. 2011;39:866–872.
12. Olmedo I, Nielsen PV, Ruiz de Adana M, Jensen RL, Grzelecki P. Distribution of exhaled contaminants and personal exposure in a room using three different air distribution strategies. *Indoor Air*. 2012;22:64–76.
13. Afshari A, Azadi S, Ebeling T, et al. Evaluation of cough using digital particle image velocimetry. In*: Proceedings of the Second Joint 24th Annual Conference and the Annual Fall Meeting of the Biomedical Engineering Society*, 2002;975–976.
14. Chao CYH, Wan MP, Morawska L, et al. Characterization of expiration air jets and droplet size distributions immediately at the mouth opening. *J Aerosol Sci*. 2009;40:122–133.
15. VanSciver M, Miller S, Hertzberg J. Particle image velocimetry of human cough. *Aerosol Sci Technol*. 2011;45:415–422.
16. Zhu S, Kato S, Yang J-H. Study on transport characteristics of saliva droplets produced by coughing in a calm indoor environment. *Build Environ*. 2006;41:1691–1702.
17. Tang J, Nicolle A, Klettner C, et al. Airflow dynamics of human jets: sneezing and breathing – potential sources of infectious aerosols. *PLoS ONE*. 2013;8:e59970.
18. Gupta JK, Lin C-H, Chen Q. Characterizing exhaled airflow from breathing and talking. *Indoor Air*. 2010;20:31–39.
19. Kwon S-B, Park J, Jang J, et al. Study on the initial velocity distribution of exhaled air from coughing and speaking. *Chemosphere*, Elsevier Ltd.2012;87:1260–1264.
20. Fabian P, McDevitt JJ, DeHaan WH, et al. Influenza virus in human exhaled breath: an observational study. *PLoS ONE*. 2008;3:e2691.
21. Milton DK, Fabian MP, Cowling BJ, Grantham ML, McDevitt JJ. Influenza virus aerosols in human exhaled breath: particle size, culturability, and effect of surgical masks. *PLoS Pathog*. 2013;9:e1003205.
22. Stelzer-Braid S, Oliver BG, Blazey AJ, et al. Exhalation of respiratory viruses by breathing, coughing, and talking. *J Med Virol*. 2009;81:1674–1679.
23. Morawska L, Johnson GR, Ristovski ZD, et al. Size distribution and sites of origin of droplets expelled from the human respiratory tract during expiratory activities. *J Aerosol Sci*. 2009;40:256–269.
24. Papineni RS, Rosenthal FS. The size distribution of droplets in the exhaled breath of healthy human subjects. *J Aerosol Med*. 1997;10:105–116.
25. Eames I, Tang JW, Li Y, Wilson P. Airborne transmission of disease in hospitals. *J R Soc Interface*. 2009;6(Suppl 6):S697–S702.

26. Liu L, Li Y, Nielsen PV, Wei J, Jensen RL. Short-range airborne transmission of expiratory droplets between two people. *Indoor Air*. 2016; doi: 10.1111/ina.12314.
27. Richmond-Bryant J. Transport of exhaled particulate matter in airborne infection isolation rooms. *Build Environ*. 2009;44:44–55.
28. Xie X, Li Y, Chwang ATY, Ho PL, Seto WH. How far droplets can move in indoor environments - revisiting the Wells evaporation-falling curve. *Indoor Air*. 2007;17:211–225.
29. Olmedo I, Nielsen PV, de Adana MR, Jensen RL, Ruiz de Adana M. The risk of airborne cross-infection in a room with vertical low-velocity ventilation. *Indoor Air*. 2013;23:62–73.
30. Qian H, Li Y, Nielsen PV, Hyldgaard CE. Dispersion of exhalation pollutants in a two-bed hospital ward with a downward ventilation system. *Build Environ*. 2008;43:344–354.
31. Bjørn E, Nielsen PV. Dispersal of exhaled air and personal exposure in displacement ventilated rooms. *Indoor Air*. 2002;12:147–164.
32. Melikov AK, Kaczmarczyk J. Measurement and prediction of indoor air quality using a breathing thermal manikin. *Indoor Air*. 2007;17:50–59.
33. Zhu S, Kato S, Murakami S, Hayashi T. Study on inhalation region by means of CFD analysis and experiment. *Build Environ*. 2005;40:1329–1336.
34. Gao N, Niu J. CFD study on micro-environment around human body and personalized ventilation. *Build Environ*. 2004;39:795–805.
35. Marr DR, Khan T, Glauser M, Higuchi H, Zhang JS. On Particle Image Velocimetry (PIV) measurements in the breathing zone of a thermal breathing manikin. *ASHRAE Trans*. ASHRAE, inproceedings, Atlanta, ASHRAE 2005;111:299–305.
36. Spitzer IM, Marr DR, Glauser M. Impact of manikin motion on particle transport in the breathing zone. *J Aerosol Sci*., Elsevier2010;41:373–383.
37. Berlanga FA, de Adana MR, Olmedo I. Diseño y construcción de maniquíes térmicos para la realización de ensayos experimentales de sistemas de climatización. In: *Proceedings of IX Congreso Nacional de Ingeniería Termodinámica, Cartagena*; 2015:1–8.
38. Tsoukias NM, Tannous Z, Wilson F, George SC. Single-exhalation profiles of NO and $CO_2$ in humans: effect of dynamically changing flow rate. *J Appl Physiol*. 1998;85:642–652.
39. Feng L, Yao S, Sun H, Jiang N, Liu J. TR-PIV measurement of exhaled flow using a breathing thermal manikin. *Build Environ*. 2015;94:683–693.
40. Cao X, Liu J, Pei J, Zhang Y, Li J, Zhu X. 2D-PIV measurement of aircraft cabin air distribution with a high spatial resolution. *Build Environ*., Elsevier Ltd. 2014;82:9–19.
41. Camargo-Valero M, Gilkeson CA, Noakes CJ. Tracer-gas technique as a surrogate for tracking airborne pathogen transport in indoor environments. In: *12th International Conference on Indoor Air Quality and Climate 2011*, Austin, vol. 2. 2011:1644–1613.
42. Camargo-Valero M. An experimental study of natural ventilation characteristics and pathogen transport in open and partitioned hospital wards, Proc. 9th UK Conf. Wind Eng.; 2010:8–11.
43. Chakroun W, Ghali K., Ghaddar N. Air quality in rooms conditioned by chilled ceiling and mixed displacement ventilation for energy saving. *Energy Build.*, Elsevier B.V. 2011;43:2684–2695.
44. Kanaan M, Ghaddar N, Ghali K. Simplified model of contaminant dispersion in rooms conditioned by chilled-ceiling displacement ventilation system. *HVAC&R Res*. 2010;16:765–783.
45. Suzuki T, Sagara K, Yamanaka T, Kotani H., Yamashita T. Vertical profile of contaminant concentration in sickroom with lyng person vetilated by displacement. In: *The 6th International Conference on Indoor Air Quality, Ventilation & Energy Conservation in Buildings IAQVEC*, Sendai; 2007:28–31.
46. Lee DD. Environmental gas sensors. *IEEE Sens J*. 2001;1:214–224.
47. Mendes L, Ogink N, Edouard N, van Dooren H, Tinôco I, Mosquera J. NDIR gas sensor for spatial monitoring of carbon dioxide concentrations in naturally ventilated livestock buildings. *Sensors*. 2015;15:11239–11257.
48. Zetterquist W, Marteus H, Johannesson M, et al. Exhaled carbon monoxide is not elevated in patients with asthma or cystic fibrosis. *Eur Respir J*. 2002;20:92–99.
49. Gong G, Han B, Luo H, Xu C, Li K. Research on the air stability of limited space. *Int J Green Energy*. 2010;7:43–64.
50. Xu C, Nielsen PV, Gong G, Jensen RL, Liu L. Influence of air stability and metabolic rate on exhaled flow. *Indoor Air*. 2015;25:198–209.
51. Guo Y, Jiang N, Yao S, Dai S, Liu J. Turbulence measurements of a personal airflow outlet jet in aircraft cabin. *Build Environ*., Elsevier Ltd 2014;82:608–617.
52. Villafruela JM, Olmedo I, San José JF. Influence of human breathing modes on airborne cross infection risk. *Build Environ*., Elsevier Ltd 2016;106:340–351.
53. Rajatman N. *Turbulent Jets*. Amsterdam: Elsevier: 1976.


## SUPPORTING INFORMATION

Additional Supporting Information may be found online in the supporting information tab for this article.

**How to cite this article:** Berlanga, F. A., Olmedo, I. and Ruiz de Adana, M. (2016), Experimental analysis of the air velocity and contaminant dispersion of human exhalation flows. Indoor Air, 00: 1-13. doi: 10.1111/ina.12357

# Paper V. Evaluation of the thermal comfort in a hospital room considering different air ventilation rates


10º Congreso Nacional
Ingeniería Termodinámica
Lleida, 28 al 30 de Junio de 2017

*This paper was presented in* the 10$^{th}$ *National Thermodynamics Engineering Conference, held from 28$^{th}$ to 30$^{th}$ June 2017in Lleida, (Spain) and was published in the proceedings of the congress.*

This research explores the influence that the increase of the air ventilation rate has on the thermal comfort of the occupants. A mixing ventilation considering a configuration consisting in a supply grilles places on the upper part of a wall and two position of two exhaust grilles placed in the opposite wall, in the upper part and in the lower part is tested.

Results show that both, the air ventilation rate and the ventilation airflow paths affect the comfort of the occupants. The increase of the air ventilation rate does not necessary lead to worse thermal comfort indices. Thermal comfort is highly dependent of the ventilation air paths created by the combination of the ventilation configuration and the air ventilation rate set.

10CNIT

10º Congreso Nacional de Ingeniería Termodinámica

10CNIT-20-134

# Evaluación del confort térmico en una habitación de hospital sometida a diferentes tasas de renovación de aire

F.A. Berlanga, I. Olmedo, M. Ruiz de Adana

Department of Physical Chemistry and Applied Thermodynamics, University of Córdoba, Córdoba, Spain, e-mail felix.berlanga@uco.es

## 1. Introduction

Los entornos hospitalarios son lugares en los que el riesgo de infección cruzada por vía aérea es alto. Diversas guías hospitalarias [1] animan a aumentar los caudales de ventilación para diluir y retirar los posibles patógenos presentes en el aire lo más rápidamente posible. Sin embargo, un aumento poco estudiado de la tasa de ventilación puede tener influencias negativas en el confort de los ocupantes de estos espacios. Este trabajo tiene como objetivo analizar la influencia de un aumento de la tasa de renovación de aire en el confort térmico en dos sistemas de ventilación por mezcla diferentes. Asimismo, se comparan los dos métodos de obtención de la temperatura radiante ($T_R$) descritos en la norma ISO 7726 [2].

## 2. Materiales y Métodos

El estudio experimental se ha llevado a cabo en la cámara de ensayos de ventilación y climatización de la Universidad de Córdoba, de 4,5 m de largo 3,3 metros de ancho y 2,75 metros de altura. Las cargas térmicas impuestas corresponden a un maniquí térmico (70W), respiración (5 W) y un panel radiante que simula una pared exterior (500W). El aire se impulsa a través de dos rejillas situadas en la pared a los pies del paciente, mientras que la extracción se realiza a través de dos rejillas situadas en la parte alta de la pared, caso a estudio E1, y dos rejillas en la parte baja, caso a estudio E2.

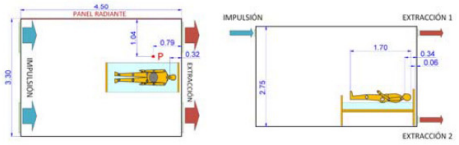


Figura 1. Planta y perfil de la cámara de ensayos.

Se estudian tres tasas de renovación de aire habituales en habitaciones de hospital diferentes, 3, 6 y 12 renovaciones de aire a la hora, ACH. El valor del voto medio previsto, PMV, y el porcentaje de personas insatisfechas, PPD, se han obtenido, en cada caso, empleando el método descrito en la norma UNE-EN ISO 7730 [3], basada en Fanger [4], a partir de las medidas de temperatura radiante, temperatura del aire, humedad relativa y velocidad del aire. La temperatura radiante se ha calculado mediante el método B.4.2 de la norma UNE-EN ISO 7726 [2], $T_R$, y mediante el método B2, $T`_R$.

## 3. Resultados y Discusión

Los valores de temperatura radiante obtenidos a través del método B.4.2, $T_R$, son ligeramente inferiores a los obtenidos a través del método B.2, $T'_R$, según se muestra en la figura 2a. Por tanto, se obtiene un mayor valor de PPD si se utiliza el método B.2, figura 2b.

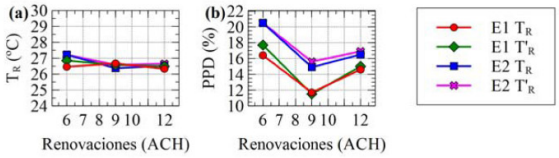


Figura 2. a) Temperatura radiante; b) PPD frente a tasa de renovación de aire.

En todos los casos analizados se obtiene un valor de PPD menor en el sistema de ventilación que extrae el aire por la parte superior de la sala, ver figura 2b. Se observa que la tasa de renovación de aire dentro de la sala tiene un impacto significativo sobre el PPD. Sin embargo, el valor del PPD no sigue una tendencia lineal con la misma, observándose un valor mínimo de PPD con 9 ACH.

## 4. Conclusiones

La obtención de la temperatura radiante a través del método B.2 o el método B.4.2 descritos en la norma ISO 7726 no tienen una influencia significativa en el cálculo del confort térmico en habitaciones de hospital. La posición de las rejillas de extracción en el sistema de ventilación en habitaciones de hospital tiene un papel importante en el confort que puedan experimentar los ocupantes de la misma, independientemente de la tasa de renovación de aire. La tasa de renovación de aire en la sala afecta al confort térmico de los ocupantes de forma no lineal.

## 5. Agradecimientos

Los autores agradecen el apoyo financiero recibido desde el Ministerio de Economía y Competitividad, Secretaria de Estado de Investigación, Desarrollo e Innovación, España, a través del Proyecto TRACER DPI2014-55357-C2-2-R, titulado "*Influencia del sistema de ventilación en la dispersión aérea de bioaerosoles exhalados por personas. Evaluación del riesgo de infección cruzada*". Este proyecto ha sido cofinanciado por el Fondo Europeo de Desarrollo Regional (FEDER).

## 6. Referencias

[1] J.D. Siegel, E. Rhinehart, M. Jackson, L. Chiarello, 2007 Guideline for Isolation Precautions, Am. J. Infect. Control. 35 (2007). doi:10.1016/j.ajic.2007.10.007.

[2] AEN/CTN 81, UNE-EN ISO 7726 Ergonomía en ambientes térmicos. Instrumentos de medida de las magnitudes físicas, 1st ed., AENOR, Madrid, 2002.

[3] AEN/CTN 81, UNE-EN ISO 7730. Ergonomía en ambiente térmico. Determinación analítica e interpretación del bienestar térmico mediante el cálculo de los índices PMV y PPD y los criterios de bienestar térmico local, Madrid, 2006.

[4] P.O. Fanger, Thermal comfort: analysis and applications in environmental engineering, McGraw-Hill, 1970.

# Paper VI. Influence of the breathing function on the airborne cross-infection risk in a hospital environment


*This paper was presented in* the 7th *European Congress for International Federation of Hospital Engineering, held from 29th to 31st May 2017in Bologne, (Italy) and was published in the proceedings of the congress.*

Once the influence of the breathing function is tested on the distribution of the exhaled contaminants in the short range, the influence of this exhalation is evaluated on a person standing close to the patient. The thermal manikin representing the health worker stands close to the patient, in a common situation that is usual in hospital rooms. The contaminants concentration is registered close to the inhalation of the thermal manikin. Both, the manikin that represents the patient and the patient that represents the health worker are performing complete breathings during the tests.

The results obtained permit the evaluation of the influence of the exhalation function on the relative amount of contaminants that reach health worker inhalation area.

# Influence of the breathing function on the airborne cross-infection risk in a hospital environment

F. A. Berlanga[#1], I. Olmedo[#2], M. Ruiz de Adana[#3]
[#]*Department of Physical Chemistry and Applied Thermodynamics University of Cordoba*
*Medina Azahara 5.1407 Cordoba, Spain*
[1]felix.berlanga@uco.es
[2]ines.olmedo@uco.es
[3]manuel.ruiz@uco.es

Keywords: Airborne Cross Infection; Breathing; Ventilation; Hospital Environments; Contaminant dispersion

Hospital environments are places where the airborne cross infection risk may be significant because infectious or immunocompromised patients and health workers share the same spaces. A correct ventilation design of these environments, such as hospital rooms, can reduce airborne cross infection risk between patients and health workers. Breathing exhalation and other respiratory events, such as cough and sneezing, are considered the source of biological contaminants that can originate airborne cross infections. People of different physical characteristics, such as gender or weight generate different breathing functions. The main objective of this paper is to analyze how different breathing functions of a contagious patient may influence the risk of cross-infection of a health worker placed in its surroundings in a hospital room.

For this purpose, two thermal manikins representing a patient and a health worker are placed inside an experimental chamber using a typical hospital room set up. One of the manikins (Patient) remain lying over a hospital bed while the other is standing close to one side of the bed (Health worker). Patient exhalation is considered the source of contaminants and the exhalation flow is seeded with a tracer gas in order to measure its concentration in the inhalation

of the health worker. The chamber is ventilated using a mixing ventilation system and a common air renovation rate in hospitals (6 ACH). Two different breathing flows and two different exhalation airways, mouth and nose, are considered in this study in order to evaluate the influence of the contaminant emission rate and the breathing function mode on the transport of exhaled contaminants in a hospital room The results are considered of significant relevance in order to gain knowledge about the airborne cross-infection risk in hospital environments.

# Paper VII. Can contaminant air quality indices be used to analyse the risk of airborne cross Infections in hospital environments?


*This paper was presented in* the AIVC 2017 *Workshop about Air Infiltration and Ventilation Centre held from 14th to 15st March 2017 in Brussels, (Belgium) and was published in the proceedings of the congress.*

This study focuses its attention on the possible relation between the air quality indexes and the possibility of the occurrence of an airborne cross infection. Since ventilation influences how exhaled contaminants distribute, it is possible to infer that the improvement on the ventilation efficiency indices could enhance the cross infection risk.

Results show that this relation is not always true because the exposure to contaminants is sometimes a transient process and ventilation efficiency indices do not reflect these particularities. Therefore, it is necessary to face the problem considering indices that reflect the high exposure punctual events that could lead to cross infections.

# CAN CONTAMINANT AIR QUALITY INDICES BE USED TO ANALYZE THE RISK OF AIRBORNE CROSS INFECTIONS IN HOSPITAL ENVIRONMENTS?

Félix Berlanga[1], Inés Olmedo[1], Manuel Ruiz de Adana[1]

*1 University of Cordoba - Department of Applied Thermodynamics*
*Campus of Rabanales – Leonardo Da Vinci Building - Ctra. Madrid Cádiz km396*
*Cordoba, Spain*

## ABSTRACT

Ventilation systems are designed to remove contaminants from hospital environments. Different air quality indices are used to express the ability of a system to remove airborne contaminants. However, indices related to peak exposure to contaminants can be used to characterize the risk of airborne cross infections in hospital environments. Local air quality index are compared to local exposure coefficient and local maximum exposure coefficient at different air changes rates using tracer gas measurements in an experimental setup with a mixing ventilation system.

## KEYWORDS

Ventilation; hospital environment; air quality indices; exposure to contaminants

## 1 INTRODUCTION

In a hospital environment one of the most important pathogen sources is due to the respiratory activity of a potentially infectious patient. Droplet nuclei are generally considered as the vehicles that transmit airborne transmissible diseases (Qian & et_al., 2008). Infection-control risk assessment in hospital environments requires the use of performance-based approaches in relation to spread of infectious diseases via the airborne route (CDC, 2003). Several contaminant removal indices can be used when detailed information is available on contaminant sources (Mundt E., 2004). Traditionally, indices that express the ability of a ventilation system to remove airborne contaminants are used. However, local maximum exposure to contaminants indices can be used to characterize the risk of airborne cross infections in hospital environments.

## 2 METHODOLOGY

The experimental setup at the HVAC Laboratory at the University of Cordoba correspond to a typical hospital room with two thermal breathing manikins, a patient (source of contaminants) and a health worker, figure 1. A mixing ventilation system is composed by a grille supply air, G, and a grille exhaust air, E2. Three different air changes rates are used, 6, 9 and 12 $h^{-1}$.

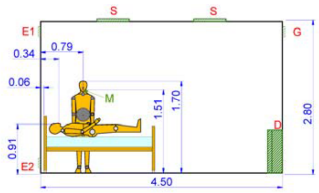


Figure 1: Profile view of the test room. Supply air grille (G); exhaust air grille (E2).

Tracer gas measurements, point M in figure 1, are used to evaluate different air quality indices. Indices representing the ability of a system to remove airborne contaminants such as local air quality index, $\epsilon_p^c$ and indices representing the exposure to contaminants such as exposure coefficient, $C_{exp}$, and the local maximum exposure coefficient, $C_{exp,max}$, are shown in table 1.

Table 1: Local air quality index and exposure coefficients.

| Local air quality index | Exposure coefficient | Local maximum exposure coefficient |
|---|---|---|
| $\epsilon_p^c = \frac{c_e}{c_p}$ | $C_{exp} = \frac{c}{c_e}$ | $C_{exp,max} = \frac{\bar{c}_{max}}{c_e}$ |

The local maximum exposure coefficient is obtained as the average of the maximum values registered in the specified point divided by the average concentration in the exhaust. A concentration measurement is considered as a maximum if its value exceeds a 25% the average concentration in the considered point.

## 3 RESULTS AND DISCUSSION

Time series analysis of exposure coefficient, figure 2a, show peak values. Concentration peak values are used to calculate local maximum exposure coefficient. Local air quality index, local exposure coefficient and local maximum exposure coefficient at different air changes rates are shown in figure 2b.

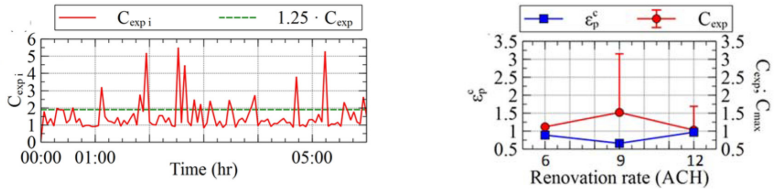


Figure 2: a) Exposure coefficient vs. time; b) Local air quality index, local exposure coefficient and local maximum exposure coefficient at different air changes rates.

## 4 CONCLUSIONS

The ability of the ventilation system to remove airborne contaminants is not always related to the exposure to contaminants. Indices representing peak exposure to contaminants can be used to characterize the risk of airborne cross infections in hospital environments.

## 5 ACKNOWLEDGEMENTS

The authors acknowledge the financial support received from the Ministerio de Economía y Competitividad, Secretaría de Estado de Investigación, Desarrollo e Innovación, Spain, to the National R&D project TRACER with reference DPI2014-55357- C2-2-R, entitled "*Ventilation system influence on airborne transmission of human exhaled bioaerosols. Cross infection risk evaluation*". This project is cofinanced by the European Regional Development Fund (ERDF).

## 6 REFERENCES

CDC. (2003). *Guidelines for Environmental Infection Control in Health-Care Facilities* (Vol. 2). Atlanta: Centers for Disease Control and Prevention.

Mundt E., M. H. (2004). *Ventilation effectiveness.* Brussels, Belgium: REHVA.

Qian, H., & et_al. (2008). Dispersion of exhalation pollutants in a two-bed hospital ward with a downward ventilation system. *Building and Environment*, 344-354.

# Paper VIII. Experimental measurements of the exposure to exhaled contaminants from different breathing modes


*This paper was presented in* the 2018 ROOMVENT / VENTILATION congress 2018 *held from 2nd to 5st June 2018 in Helsinki, (Finland) and was published in the proceedings of the congress.*

Once the influence of the breathing function is evaluated, the influence of the route that the exhalation air to reach the external environment is addressed. The airway through the two possible exhalation modes, through the nose or through the mouth have a different conduit geometry. This could lead to a different flow development once the air reaches the environment even if the breathing function remain constant. To evaluate the influence of this parameter, an experimental schedule of four tests resulting from the combination of two different breathing functions and the two different exhalation modes. The influence of the breathing mode on the contaminants distribution is evaluated considering the exposure of the health worker to the patient's exhaled contaminants. Results reinforce the idea that the exposure to the exhaled contaminants is a transient process. Even not existing high differences between the considered cases in average exposure indices, peak values show very different situations. According to the obtained results, peak exposure indices are developed in order to evaluate the maximum cross infection risk in each situation.

# EXPERIMENTAL MEASUREMENTS OF THE EXPOSURE TO EXHALED CONTAMINANTS FROM DIFFERENT BREATHING MODES

**F.A. Berlanga[1,*] , I. Olmedo[1], M. Ruíz de Adana[1]**

[1]Universidad de Córdoba, Córdoba, España
[*]*Corresponding email: felix.berlanga@uco.es*

## SUMMARY

This experimental study analyses the contaminants exposure of a health worker (HW) to the contaminants exhaled by a lying patient (P) inside a hospital room using breathing thermal manikins. The two possible exhalation ways of P, though the nose (N) or through the mouth (M) are considered while HW always inhales through its nose. In addition, two different respiration functions are tested for P breathing, one corresponding to a 1,8 m height and 80 kg weight male (H) and another corresponding to a 1,5 m height and 50 kg weight female (L). The room is ventilated using a mixing ventilation strategy with 6 ACH as ventilation rate. A tracer gas (R134A) is used to surrogate the contaminants emitted through P exhalation, being the only source of contaminants inside the room. Using field measurements data, the value of contaminant exposure ($e_{HW}^{c}$) and the intake fraction ($IF$) are obtained together with the peak concentration intensity and frequency as the indices to compare the different experimental combinations. Results are intended to be extrapolated, considering the limitations, to the possible exposition of HW to the pathogens released by P exhalation.

**Keywords**: Hospital, Human breathing, Personal exposure, Exhalation airway, Breathing functions

## 1 INTRODUCTION

It is well known that hospitals are risky places for cross infection. This is because patients that suffer from contagious illnesses are in close contact with other patients and health workers. Airborne cross infections can spread quickly in these indoor spaces because their occupants move from a place to the other constantly interacting with different people, especially the medical staff. So it is important to avoid the possible infection of their personnel.

Pathogens that are responsible of the contagion can be emitted in respiratory events such as cough, sneezing and breathing (Fabian et al. 2008). They are expelled in droplets, falling if their size is higher than 60 $\mu m$ (Liu et al. 2016) or following the air current if not (Ji et al. 2018). Once these droplets get out the body they start to lose mass because of evaporation and can be transformed in droplets nuclei. These low mass particles can reach further distances following ventilation flows (Liu et al. 2016).

This study uses a tracer gas (R134A) to study the diffusion of these particles as they were contaminants. It is performed in a typical hospital room set-up (Bivolarova et al. 2014). Inside the averaged size hospital room, two thermal breathing manikins surrogate the presence of a patient (P) as a source of pathogens and a health worker (HW) as the target. P lies on a bed while HW stands close to it. Two different exhalation functions, female 1,5 m height 50 kg weight (L) and male 1,8 m height and 80 kg weight (H) and two airways, nose (N) and mouth (M) are tested for P exhalation.

This study uses two different contaminant exposition indices to determine the exposition of HW to the contaminants exhaled by P. Contaminants exposure ($e_{HW}^{c}$) determines the amount of contaminants present in HW inhalation referred to the exhaust. On the contrary the intake fraction ($IF$) determines contaminants quantity in HW airway referred to the contaminants emitted into the room. Furthermore, the peak concentrations registered in HW are analysed so that its frequency and scale are compared in order to describe in which cases HW is more exposed to the contaminants released by P. Since between

these contaminants could be infectious pathogens, the exposure values obtained could be related with HW cross infection risk.

## 2 METHODS

The experiments have been performed in an experimental chamber of 4.5 m length, 3.3 m wide and 2.8 m height. The chamber is ventilated using mixing ventilation strategy with a ventilation rate of 6 air changes per hour (ACH). Fresh air is introduced through S and exhausted through E grilles. Figure 1 show the experimental set-up.

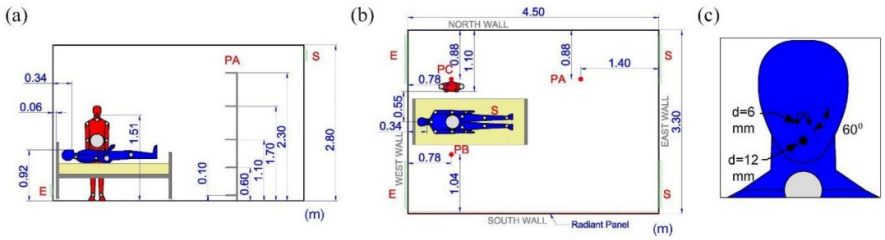


*Figure 1. Experimental setup. (a) Side view of the experimental chamber. (b) Plane view of the experimental chamber. (c) Detail view of the positions of the exhaling points of the thermal manikins.*

Two thermal manikins (Berlanga et al. 2015) represent a lying patient (P) and an standing health worker (HW). The body of the manikins is heated to reach a surface temperature of 34 ºC. The manikins head is equipped with two different airways a 12 mm diameter circular mouth and two 6 mm diameter circular nostrils. The nostrils and its conduct are oriented following the indications of previous studies (Gupta et al. 2010). An illustration of manikin airways is shown in Figure 1 (c).

The manikins perform different breathing functions as is summarized in Table 1. P manikin performs two different exhalation functions, H corresponding to a 1.8 m 80 kg male and L corresponding to a 1.5 m 50 kg female, exhaling through the nose (N) and through the mouth (M). Its breathing is heated to obtain 34 ºC just in the airway opening. On the contrary, HW manikin only performs HW inhalation function, always inhaling through the mouth. The nomenclature of the experiments performed are the combination of the P exhaust possibilities.

*Table 1. Breathing function properties of the three different exhalations present in the experiment.*

| Manikin which perform the breathing | Breathing function | Respiration frequency ($min^{-1}$) | | Minute volume (l/min) | Tidal Volume (l) |
|---|---|---|---|---|---|
| | | In | Out | | |
| HW | HW | 17.90 | 16.43 | 9.46 | 0.552 |
| P | L | 18.16 | 16.25 | 6.62 | 0.387 |
| P | H | 17.22 | 14.26 | 10.43 | 0.669 |

Apart from the heat gains that the manikins represent (85 W HW manikin and 75 W P manikin), a radiant wall is present in the room behaving like an external wall load (Figure 1). This element represent a heat gain of 500 W. Thus, the total heat gains in the chamber amount to 660 W. In order to compensate the heat gains, ventilation air is supplied at 18.2 ºC, this way the exhaust temperature reaches 25 ºC.

To obtain the room temperature conditions, J thermocouples (2% accuracy in the range of 20-40ºC) are installed along the height of the chamber. Dimensionless temperatures are obtained at a specific height ($T_z$) using the supply ($T_i$) and the exhaust ($T_e$) temperatures. Results are presented against the dimensionless height respect to the total height of the chamber ($H$).

In pursuance of analyse the dispersion of the exhalation droplets, a constant amount of tracer gas (R134a) is seeded into P exhalation. To dose and measure the tracer gas a dosing and measurement equipment is used (Innova 1303 and 1412, LumaSense Technologies, California). Tracer gas concentration is registered in four different points, ventilation supply ($c_s$), and exhaust ($c_e$), P exhalation airway ($c_p$) and in HW inhalation airway ($c_{HW}$). The value of $c_s$ is always null because the tracer gas used in this study can't be found naturally in the atmosphere and the air renovation rate is zero. These individual values are averaged to obtain the corresponding mean concentration values ($\bar{c}_s, \bar{c}_e, \bar{c}_p$ and $\bar{c}_{HW}$).

Peak concentrations registered in the airway the of HW are defined as the measurements that exceed the 25% the value of $\bar{c}_{HW}$. These values are averaged to obtain the mean peak concentration in HW airway ($\bar{c}_{HW,125\%}$). The frequency of the occurrence of these peaks ($f_{125\%}$) is quantified so that the periodicity of these events could be studied.

Using the average concentration values, four different indices are defined to describe HW mean and peak tracer gas exposure.

The exposure to contaminants ($e^c_{HW}$) is an index that express the punctual exposure referred to the one in the exhaust. This index is also obtained for the value of $\bar{c}_{HW,125\%}$ to study the peaks occurred. The equations used to obtain the values are shown in the Equation 1.

$$e^c_{HW} = \frac{\bar{c}_{HW} - \bar{c}_s}{\bar{c}_e - \bar{c}_s} \quad , \quad e^c_{HW,125\%} = \frac{\bar{c}_{HW,125\%} - \bar{c}_s}{\bar{c}_e - \bar{c}_s} \tag{1}$$

The intake fraction ($IF$) is an index that is used to determine the effective amount of contaminants inhaled by HW. The value corresponding to the peak concentrations ($IF_{125\%}$) is also obtained. The equations used to obtain the indices are shown in the Equation 2.

$$IF = \frac{\int Q_{HW} \cdot c_{HW} \cdot \mathrm{d}t}{\int Q_P \cdot c_P \cdot \mathrm{d}t} = \frac{MV_{HW} \cdot \bar{c}_{HW}}{MV_P \cdot \bar{c}_P} \quad , \quad IF_{125\%} = \frac{MV_{HW} \cdot \bar{c}_{HW,125\%}}{MV_P \cdot \bar{c}_P} \tag{2}$$

Being $MV_{HW}$ and $MV_P$ the minute volume (L/min) of the breathings performed by HW and P respectively.

## 3 RESULTS AND DISCUSSION

Dimensionless temperature along the height of the room in three different positions, PA, PB and PC, Figure 1, is shown in Figure 2. The data were obtained during the performance of the four tests carried out for this study.

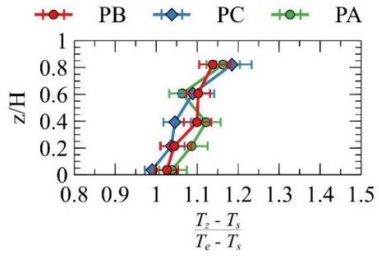


*Figure 2. Dimensionless temperature profiles along the height of the room in the three positions considered*

Figure 2 show that the temperature registered inside the chamber is quite homogeneous no matter the height where is registered nor the plane position inside the chamber chosen. This situation is typical for

mixing ventilation strategies such the used in this case. The error bars show a low variability of the temperature during the data gathering. This assure that the tracer gas measurements recollected for each test are comparable.

The values of the variables $c_{HW}$ and $c_e$ obtained during the complete test period (6 h) of each experimental case are shown in Figure 3. Not all the registered data are considered, the measurements obtained before to reach a stationary concentration in each point are not included in the index calculations. The data are considered from time = 50 min.

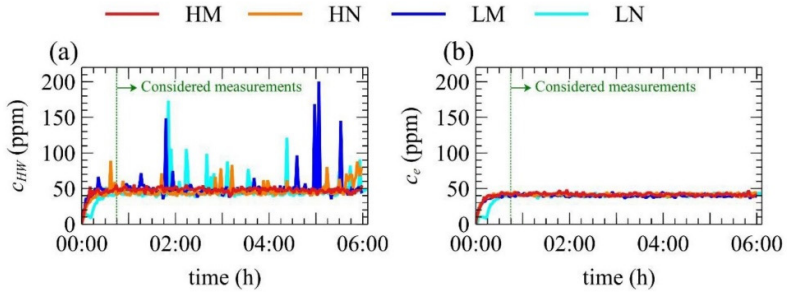


*Figure 3. Contaminant concentrations measured over time. (a) Inhalation of HW. (b) Ventilation exhaust.*

Results show that once the contaminant is seeded into P airway, the concentration in the considered points increase progressively. This process ends once the contaminants reach a definite concentration in each point. Once that happens the average value of the concentration remains nearly constant over time. This phenomenon is more evident for $c_e$. Nearly no difference is obtained for $\bar{c}_e$ between experiments, that the contaminants are removed to the exhaust in the same amount for all the tests. In contrast to the homogeneous data obtained in $c_e$, instantaneous sudden high registers that break the uniformity of the records appears for $c_{HW}$ though time. These peak concentration registers are not obtained with the same intensity nor the same frequency in all the tests.

To determine the average and peak HW exposition differences between the experiments carried out, the average ($e^c_{HW}, IF$) and peak ($e^c_{HW,125\%}, IF_{125\%}$) exposition indices are shown in Figure 4 together with the peak occurrence frequency ($f_{125\%}$). Peak values are shown in form of error bars over the average bars.

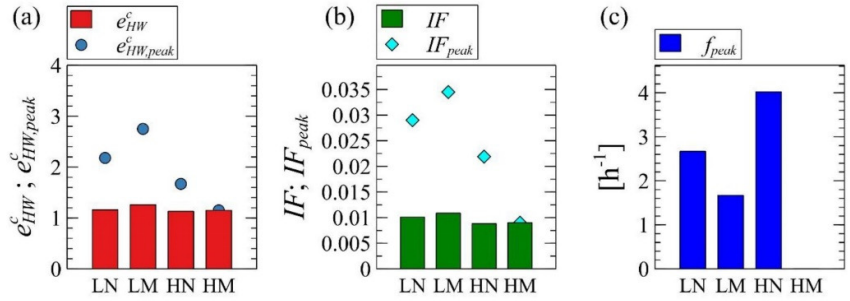


*Figure 4. Contaminant exposure. (a) Average ($e^c_{HW}$) and maximum ($e^c_{HW,125\%}$) contaminants exposure. (b) Intake Fraction, average ($IF$) and maximum ($IF_{125\%}$). (c) Peak frequency ($f_{125\%}$).*

Contaminant exposure ($e^c_{HW}$) maintain values slightly over the unit for all the tests. That means that the value obtained for $\bar{c}_{HW}$ is always higher than the one obtained for $\bar{c}_e$, which indicates that HW is overexposed respect to the exhaust. Being $e^c_{HW}$ value very homogeneous between the cases tested, a slight tendency to be higher in L cases is obtained. It is also noticeable that the exposition to contaminans is higher in M cases. So, the higher exposition is found for LM case.

The values obtained for $IF$ reveals the same tendency observed for $e^c_{HW}$, being again LM case the worse in terms of contaminants exposition. The amount of contaminant effectively inhaled by HW stands always around 1% of the contaminants seeded into the chamber thouth P exhalaton.

The values obtained for $e^c_{HW,125\%}$ and $IF_{125\%}$ reveal higher differences between the cases studied. The worst situation appears again for LM case where $e^c_{HW,125\%}$ reveals peak concentrations till nearly 3 times higher than the obtained in the exhaust and that reach nearly the 4% of the contaminants seeded through P exhalation. In general peak indices reinforces the differences shown by the mean indices. Nevertheless, it is noticeable that under HM experimental configuration any peak is registered.

The higher exposure values obtained for the LM case could be explained by two facts. L exhalation cases high HW exposition could be related with the lower momentum of the breathing. In contrast with H cases, contaminants diffusion is lower, promoting higher concentrations in HW inhalation surroundings. When M is used, contaminants are projected directly upwards by P exhalation in unlike in N cases. This shorten the distance to reach HW airways.

Peak occurence, $f_{125\%}$, show higher values for N cases, even in HM case any peak is reached. It can be observed that the higher the peak frequency is the lower the peak exposure indices are. The different values obtained for this index show that the parameters modified between experiments have an influence on this value. When N airway is used, $f_{125\%}$ is higher, but at the same time the scale of the peaks is lower. That could be related with the fact that, in this case, contaminanst are projected in a oblique direction that move contaminans away from HW body.

## 4 CONCLUSIONS

Considering the obtained results, a number of conclusions can be stated:

- A certain correlation has been found between the exposition indices $e^c_{HW}$ and $IF$. Both indices provide exposure information but referred to different reference concentrations. While $e^c_{HW}$ is referred to the exhaust, $IF$ refers to the source of contaminants. The correlation found between them suggests that both can be used to describe HW exposition to a punctual indoor contaminant emission in ventilated spaces.
- HW exposition depends on the P exhalation airway and its breathing function performed. P exhalation through the mouth (M) and a low momentum exhalation function (L) increase HW exposition. The differences are slight but the results are consistent between the two parameters considered. This reveals the importance of the way contaminants are released by the source into their distribution inside the indoor space and thus the exposure of the rest of the occupants.
- Peak and average exposure indices show differences in the information retrieved. A more precise description of the HW exposure characteristics is obtained when peak exposition and the exposition frequency are considered. These values contribute to better describe the phenomenon and should be considered in future exposure studies. In addition, since infectious pathogens can be found between the contaminants released through exhalation the average, peak and peak frequency exposure values can be directly related with cross infection risk.
- Since a number of peak exposure records are registered during the measurements, the use of quicker response sensors would provide useful information about the transient processes that seems to appear in situations like the presented.

The conclusions stated for the presented hospital room setup could be extrapolated to different indoor scenarios since breathing is a constant activity for humans and the indoor ventilation strategy performed is quite common. Exhaled air is continuously released through breathing and have an influence on the rest of occupants of indoor environments. The exhaled air could contain infectious pathogens, so the exposure values obtained could be related with cross infection risk of the occupants. Therefore, a more precise description of the exposure of the occupants under different situations could aid to design more effective ventilation systems for indoor spaces reducing the problems created by a poor ventilation design.

## ACKNOWLEDGEMENTS

The authors acknowledge the financial support received from the Ministerio de Economia y Competitividad, Secretaría de Estado de Investigación, Desarrollo e Innovación, Spain, to the National R&D project TRACER with reference DPI2014- 55357- C2- 2- R, entitled "Ventilation system influence on airborne transmission of human exhaled bioaerosols. Cross infection risk evaluation." This project is cofinanced by the European Regional Development Fund (ERDF).

## REFERENCES

Berlanga, F.A., M. Ruiz de Adana, and I. Olmedo. 2015. "Diseño Y Construcción de Maniquíes Térmicos Para La Realización de Ensayos Experimentales de Sistemas de Climatización." In *Proceedings of IX Congreso Nacional de Ingeniería Termodinámica*, 1–8. Cartagena.

Bivolarova, M. P., Arsen Krikor Melikov, Monika Kokora, Chiyomi Mizutani, and Zhecho Dimitrov Bolashikov. 2014. "Novel Bed Integrated Ventilation Method for Hospital Patient Rooms." *13th SCANVAC International Conference on Air Distribution in Rooms*, 49–56.

Fabian, Patricia, James J. McDevitt, Wesley H. DeHaan, Rita O. P. Fung, Benjamin J. Cowling, Kwok Hung Chan, Gabriel M. Leung, and Donald K. Milton. 2008. "Influenza Virus in Human Exhaled Breath: An Observational Study." *PLoS ONE* 3 (7): e2691.

Gupta, J. K., Chao-Hsin Lin, and Q. Chen. 2010. "Characterizing Exhaled Airflow from Breathing and Talking." *Indoor Air* 20 (1): 31–39.

Ji, Yichen, Hua Qian, Jin Ye, and Xiaohong Zheng. 2018. "The Impact of Ambient Humidity on the Evaporation and Dispersion of Exhaled Breathing Droplets: A Numerical Investigation." *Journal of Aerosol Science* 115 (October 2017). Elsevier Ltd: 164–72.

Liu, Li, Yuguo Li, P. V. Nielsen, Jianjian Wei, and Rasmus L Jensen. 2016. "Short-Range Airborne Transmission of Expiratory Droplets between Two People." *Indoor Air*, no. February: 1–11.

# Paper IX. Experimental evaluation of thermal comfort, ventilation performance indices and exposure to airborne contaminant in an airborne infection isolation room equipped with a displacement air distribution system

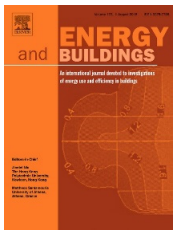


*The paper has been published in Energy and Buildings journal (10.1016/J.ENBUILD.2017.09.100)*

Once the transient nature of health worker exposure is revealed, a systematic study on the exposure to patient exhaled contaminants is carried out considering displacement ventilation strategy and different air ventilation rates. Three different air ventilation rates are tested. From 6 ACH considered for common patient hospital rooms, going through the intermediate value of 9 ACH and to 12 ACH, required for airborne infection isolation rooms.

Results show that this innovative ventilation strategy permits gathering good ventilation efficiency indices and acceptable exposure indices for reduced air ventilation rates. Global and local comfort indices indicate that the maintenance of the highest thermal comfort standards for all the occupants of the room is a challenge.

Energy and Buildings 158 (2018) 209–221

Contents lists available at ScienceDirect

Energy and Buildings

journal homepage: www.elsevier.com/locate/enbuild

# Experimental evaluation of thermal comfort, ventilation performance indices and exposure to airborne contaminant in an airborne infection isolation room equipped with a displacement air distribution system

F.A. Berlanga[a,*], M. Ruiz de Adana[a], I. Olmedo[a], J.M. Villafruela[b], J.F. San José[b], F. Castro[b]

[a] Department of Chemical Physics and Applied Thermodynamics, University of Córdoba, 14014 Córdoba, Spain
[b] Department of Energy and Fluid Mechanics, University of Valladolid, 47011 Valladolid, Spain

ARTICLE INFO

*Article history:*
Received 21 July 2017
Received in revised form
24 September 2017
Accepted 29 September 2017
Available online 7 October 2017

*Keywords:*
Air distribution
Displacement ventilation
Isolation room
Personal exposure
Human breathing
Ventilation effectiveness
Thermal plume
Thermal comfort

ABSTRACT

This study is focused on determining the convenience of the use of displacement ventilation strategy in airborne infection isolation rooms (AIIRs). Thermal comfort of the occupants of the chamber, ventilation and contaminant performance indices and the exposure of the health worker (HW) to the contaminants exhaled by the confined patient (P) are considered in a typical AIIR set up with two thermal breathing manikins and a radiant wall simulating an external wall. Three air renewal rates are tested to determine their influence in the studied variables. Results show that ventilation performance, contaminants and general comfort indices for both manikins perform well in the cases studied. Lockup phenomenon associated with displacement ventilation occurs above P but it has a low influence on contaminant exposure of HW because of the influence of the convective boundary layer of HW. The influence of the radiant wall could lock the air path near the exhaust grille.



## 1. Introduction

Hospitals and medical facilities are risky places for cross infection between their occupants [1–3], whether they are patients, health workers or visitors. Some of these infections could be transmitted through the air [4], where pathogens are transported from infected people and spread the illness. Pathogens can be found in droplets of different sizes that are emitted through respiratory exhalation processes [5,6] such as breathing [7] coughing [8] and sneezing [9]. This study is focused to analyze the emissions released though exhalation as the most common and continuous respiratory event [10]. Once these droplets are released, they suffer an evaporative process that transform them into droplet nuclei [11–13]. Depending on the size of the resulting particle they can deposit quickly because of the effect of gravity, if their diameter is greater than 10 μm [14]; or be suspended following the ventilation induced effects, if their diameter lower than 10 μm. These small particles can be spread over long distances and generate cross infections [11]. For example, transmission by small droplets or droplet nuclei (<5 μm diameter) is the dominant mode for influenza spreading [15].

Patients that develop an infectious disease that is found to be capable of spreading through air, and in this way are considered a threat for the rest of the occupants of the health facility, need to be confined in an isolated environment [16]. Airborne Infection Isolation Rooms (AIIR) are isolation spaces in hospitals provided with negative differential pressure with respect to the rest of the building [17]. This way, the pathogens can be confined in the AIIR if the room doors are closed. A convenient ventilation strategy can reduce the possibility of these infections [18]. In addition, AIIRs are ventilated using high renewal rates according to guides published by different National Health Committees [16,19–22].

These recommendations are based on the belief that high renewal rates could reduce cross infection risk between patients and health workers in such spaces by diluting and removing pathogens. Nevertheless, recent research focusses attention on providing a good air distribution rather than on maintaining high renewal rates as being the most important factor in reducing cross infection risk [23–25]. Thus, current strategies to reduce energy usage [26] in ventilation systems typically involve lowering airflow

* Corresponding author.
*E-mail address:* felix.berlanga@uco.es (F.A. Berlanga).

https://doi.org/10.1016/j.enbuild.2017.09.100
0378-7788/

**Nomenclature**

| | |
|---|---|
| ACH | Air changes per hour ($h^{-1}$) |
| AIIR | Airborne infection isolation room |
| <c> | Mean tracer gas concentration of contaminant of the chamber (ppm) |
| $c_e$ | Average tracer gas concentration of the exhaust air (ppm) |
| $c_i$ | Average tracer gas concentration in a determined point (ppm) |
| $c_{exh}$ | Average contaminant concentration emitted through the P exhalation (ppm) |
| $c_{inh}$ | Average contaminant concentration inside the inhalation airway of the HW manikin (ppm) |
| $c_{i,max}$ | Average of the maximum tracer gas concentration values registered in a determined point (ppm) |
| $c_s$ | Average tracer gas concentration in the supply air (ppm) |
| D | Displacement diffuser |
| DV | Displacement ventilation |
| E | Exhaust grille |
| $e^c_{P,max}$ | Local relative maximum exposure coefficient |
| $f_{e^c_{P,max}}$ | Local maximum exposure frequency ($h^{-1}$) |
| IAQ | Indoor air quality |
| IF | Intake fraction |
| H | Total height of the chamber (m) |
| $HR_i$ | Average relative humidity in a determined point (%) |
| HW | Health worker |
| MV | Mixing ventilation |
| P | Patient |
| P3 | Pole located far from thermal loads |
| PHW | Pole located near health worker |
| PMV | Predicted mean vote |
| PP | Pole located near patient |
| PPD | Predicted percentage of dissatisfied (%) |
| $Q_{b,exh}$ | Breathing rate of P (l/min) |
| $Q_{b,inh}$ | Breathing rate of HW (l/min) |
| $T_i$ | Average ambient temperature in a determined point ($^a$C) |
| $T_{globe}$ | Globe temperature (°C) |
| z | Height along the z axis of the chamber (m) |
| $V_i$ | Average absolute air velocity in a determined point (m/s) |
| $\Delta T_{prN\text{-}S}$ | Radiant temperature asymmetry due to the south radiant wall (°C) |
| $\Delta T_{h\text{-}f}$ | Temperature difference between head level (1.1 m or 1.7 m height) and feet level (0.1 m height) (°C) |
| $\varepsilon^a$ | Air change efficiency index |
| $\varepsilon^a_P$ | Local air change index for a determined point |
| $\varepsilon^c$ | Contaminant removal effectiveness index |
| <$\tau$> | Mean age of air in the room (min) |
| $\tau_n$ | Nominal time constant (min) |
| $\tau_P$ | Local mean age of air in a determined point (min) |

rates and/or heating/cooling capacity. The ventilation performance [27] and thermal comfort [28] can be compromised if the design it is not appropriate [26].

Maintaining a comfortable environment [27] is an important issue to be taken into account in designing AIIRs because patients have to remain confined for long periods of time in these spaces [29]. Recent research has focused its attention on comfort in hospital environments, for both health workers [30] and patients [31,32] who usually spend a lot of time asleep lying down [33,34]. It has been determined that patients' thermal comfort [35,36] is reached at higher temperatures than in other environments.

Different ventilation strategies can be used in AIIR indoor environments [13], while the most widely applied is mixing ventilation (MV) [37]. However, this strategy can reduce thermal comfort in the occupied zone of the ventilated space and can spread contaminants and pathogens [38]. In recent times displacement ventilation (DV) has arisen as an alternative ventilation strategy to improve both the thermal comfort and IAQ of the occupied space. The inward air flow is delivered at low velocity using diffusers placed at relative low height; when this slow moving air mass encounters a heat load, it rises and carries the heat and pollutants towards the ceiling of the room [39,40]. This strategy is used extensively in different ventilation applications and its use is particularly recommended for high renewal rates requirement applications [41] such as AIIR. Well-designed DV systems have been found to be especially effective in removing contaminants [13,42,43].

Ventilation performance indices [18] have been defined to evaluate both the ability of a system to exchange the air in the room and the ability of a system to remove airborne contaminants [14]. These values have been used widely used in recent ventilation studies to determine how ventilation can dilute and remove pathogens and in this way reduce cross infection risk of health workers [23,44,45].

Tracer gas technique is recommended [18] and has been used extensively to analyze ventilation performance and contaminant removal in indoor places [45,46]. This technique has also been used to determine cross infection risk between people in indoor environments [47–50]. Tracer gases are seeded in the air simulating the presence of pathogens. Its concentration in a defined location is used to determine pathogens' exposure and hence cross infection risk at that point. This technique has been validated by comparing with tracer aerosol particles technique (1 μm to 3 μm) close to the source of contaminants [50,51].

This study is intended to experimentally analyze the use of DV strategy resolving some of the limitations found in other ventilation studies. Exhalation of the lying thermal manikin is considered the source of contaminants in this study. These contaminants are seeded completely mixing with the breathing exhalation air flow. This method is considered a more realistic way to perform than other approaches carried out previously [46,50]. The study of exhaled contaminants distribution is more important in low velocity ventilation systems (DV) than in the cases where ventilation is based on mixing strategies [52,53]. This study implements a radiant panel on a wall simulating an external wall. The heat load of this wall can have an important influence on a thermally driven ventilation system such as DV [46] that needs to be considered. Three air renewal rates ranging from 6 ACH to 12 ACH are considered in this study. Recent experimental ventilation studies in hospital rooms have been carried out with a ventilation rate below 12 ACH [19,47,52,53]. Other experimental ventilation studies in hospital rooms have been carried out with a ventilation rate of 12 ACH but they don't use DV systems [45,54]. Nevertheless different national committees recommend higher renewal rates for such spaces, 9 ACH in the case of Canada, 12 ACH in the case of USA, UK, Japan and Denmark [19] and 15 ACH in the case of Australia [20,55].

This paper presents an experimental analysis of the use of DV strategy in AIIR as an alternative to the most extended MV strategy, using a representative case of study of an AIIR set up. The objectives of this investigation are, for three different high air renewal rates, (1) to assess the thermal comfort for a representative case of study of an AIIR by using DV (2) to analyze ventilation performance indices and (3) to determine contaminant exposure by studying local mean exposure, local peak exposure, its frequency and effective contaminant intake for health workers (HW) being the only source of contaminants the exhalation of the patient (P). This way, the convenience of the use of DV strategy in AIIRs can be evaluated.

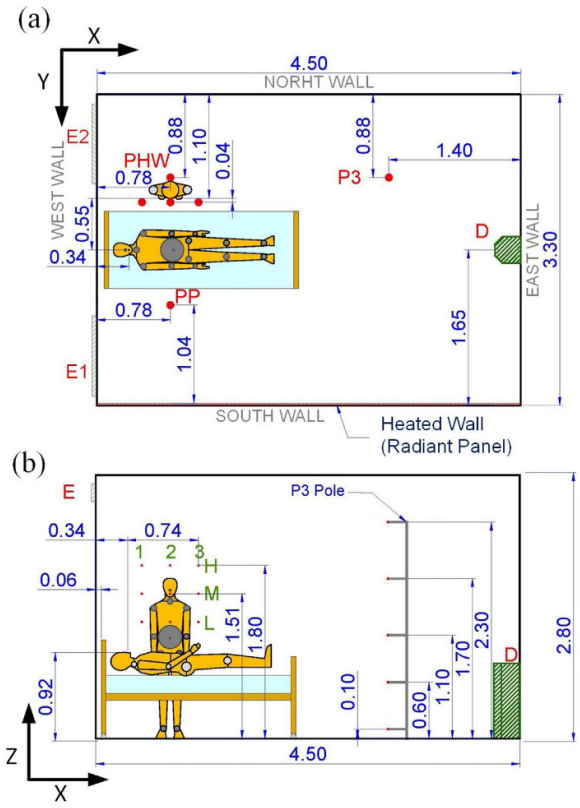


**Fig. 1.** (a) Plan view of the test room. (b) Profile view of the test room. Displacement air diffuser (D); Exhaust grilles (E); Vertical Poles (PP, PHW and P3); Columns of the point matrix of tracer gas measurements (1, 2 and 3); Rows of the point matrix of tracer gas measurements (H, M, L).

## 2. Methods

### 2.1. Test room and experimental setup

This study was carried out in an experimental chamber within the HVAC (heating, ventilation and air-conditioning systems) laboratory at the University of Cordoba. The experimental setup corresponds to a typical AIIR, which consists of a room 4.50 m in length, 3.3 m in width, and 2.8 m in height (H). The dimensions of the room are compatible with the recommendations the different national committees consulted [16,19–22]. Two breathing thermal manikins located inside the chamber represent a patient lying on a hospital bed (P) and a health worker standing close to the first one (HW), (Fig. 1).

### 2.2. Thermal loads and breathing thermal manikins

The two breathing thermal manikins have the same geometry, with a height of 1.70 m and a surface of 1.6 $m^2$ [7,56]. Each breathing thermal manikin has four independent thermal zones: head, arms, torso and legs. The total sensible heat emitted for each manikin is obtained from the ASHRAE Fundamentals Handbook [10] according to the metabolic rate of 1 met in the case of the standing manikin (HW) and 0.7 met in the case of the lying manikin (P). The distribution of the total sensible heat is set according to Tanabe [57], as shown in Table 1.

An external heat gain in the South wall of 500 W is imposed by means of a hydronic wall radiant system. The radiant panel emits a heat flux of 39.68 $W/m^2$ and maintains a mean inner surface temperature of 29.1 °C in the South wall of the chamber. This heat gain could represent the heat gains of an external wall exposed to sun radiation. Heat gains would be thus dependent of a number of factors such the location of the building, the season of the year and the time of the day. Hence, this case corresponds with an specific combination of these factors and its results should not be generalized. The rest of the walls of the chamber are considered adiabatic as the chamber is inside a lab at the same temperature.

The HW manikin emits 80 W through its body and 5 W through its breathing, while the P manikin emits 70 W through its body and 5 W through its breathing as shown in Table 1.

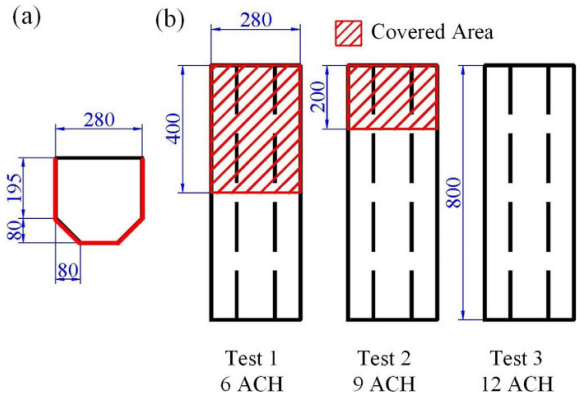


**Fig. 2.** Displacement diffuser dimensions (mm) and covered area for each test performed. (a) Plant view. (b) Front view.

**Table 1**
Thermal loads in the experimental chamber.

| Source | | | Load (W) | |
|---|---|---|---|---|
| Radiant Panel | | | | 500 |
| HW manikin | Body | Head | 5.6 | 85 |
| | | Arms | 14.4 | |
| | | Torso | 19.2 | |
| | | Legs | 40.8 | |
| | Breathing | | 5 | |
| P manikin | Body | Head | 4.9 | 75 |
| | | Arms | 12.6 | |
| | | Torso | 16.8 | |
| | | Legs | 35.7 | |
| | Breathing | | 5 | |
| Total | | | | 660 |

**Table 2**
Breathing function characteristics.

| Respiration frequency ($min^{-1}$) | | Minute volume (l/min) | Tidal volume (l) |
|---|---|---|---|
| In | Out | | |
| 17.90 | 16.43 | 9.46 | 0.55 |

The total thermal loads present in the room during the experiments, considering the thermal radiant panel (500 W) and the thermal manikins (160 W) reach 660 W, which corresponds to 44.44 $W/m^2$.

The breathing thermal manikins have their own independent breathing system that can simulate different breathing flows. Breathing function has been calculated according to the studies carried out by Gupta [58] who obtained that the breathing function of a subject is dependent on its gender, its weight and its height. In this study both manikins perform the same breathing function obtained considering a male 1.70 m tall and 70 kg weight. The resulting breathing function characteristics can be seen at Table 2.

HW inhales through the nose while the P exhales through the mouth. This way P manikin can be considered the only source of contaminants in the experimental chamber in contaminant exposure experiments while HW can be considered the target where the contaminant exposure is measured. Exhalation of P is situated at a relative height of z/H = 0.328 while the inhalation point of HW it is located at z/H = 0.539, as can be observed at Fig. 1.

**Table 3**
Experimental conditions of the tests performed.

| Tests | Renewal Rate (ACH) | Supply air flow rate ($m^3/h$) | Supply air temperature (°C) |
|---|---|---|---|
| Test 1 | 6 | 250 | 18.2 |
| Test 2 | 9 | 375 | 20.6 |
| Test 3 | 12 | 500 | 21.8 |

### 2.3. Ventilation system

Clean air is supplied through a displacement diffuser, D, located in the East wall of the chamber and extracted by two exhaust grilles, E1 and E2, located in the upper part of the West wall of the chamber (Fig. 1).

The ventilation system has been set at three different air change rates of 6, 9 and 12 ACH, supplying air at 18.2 °C, 20.6 °C and 21.8 °C respectively to maintain a mean temperature in the exhaust of 25 ± 1 °C. This is done in order to reproduce comparable and realistic AIIRs conditions for the test [59]. A summary of the conditions of the three tests performed can be seen at Table 3.

Part of the effective area of the displacement diffuser (QLV-180-200-800, Trox, Germany) is partially covered during Test 1 and Test 2. It is necessary to maintain the same supply velocity and thus the same air throw in the room for all the three tests performed despite the ventilation airflow. The area covered in each case is shown in Fig. 2. Low supply temperatures together with reduced diffusor areas could lead to local draught discomfort issues, but in this case, they have not been found. Supplementary information B contains a specific study about the local draught discomfort of the occupants of the room.

### 2.4. Measuring instruments

Three vertical poles (PHW, PP and P3) are located inside the experimental chamber (Fig. 1). PHW and PP are close to HW manikin and P manikin respectively. P3 is placed far from the breathing thermal manikins. Along the length of these poles, temperature, humidity and air velocity probes are disposed as can be seen at Table 4.

Ambient temperature probes ($T_i$) consist of J-type thermocouples, with an accuracy of 2% at the considered temperature range (15–45 °C). These air temperature sensors are protected from radiation by a cylindrical reflective metal device. Absolute air velocity

**Table 4**
Probes position along the height of each pole.

| Height (m) | P3 Pole | PHW Pole | PP Pole |
|---|---|---|---|
| 2.3 | $T_i$ | $T_i$, $V_i$ | $T_i$, $V_i$ |
| 1.7 | $T_i$ | $T_i$, $V_i$, $HR_i$ | $T_i$, $V_i$, $HR_i$, $T_{globe}$ |
| 1.1 | $T_i$ | $T_i$, $V_i$ | $T_i$, $V_i$ |
| 0.6 | $T_i$ | $T_i$, $V_i$ | $T_i$, $V_i$ |
| 0.1 | $T_i$ | $T_i$, $V_i$ | $T_i$, $V_i$ |

($V_i$) is measured using hot-sphere anemometers (TSI Air Velocity Transducer 8475, TSI, Minnesota). These probes can measure an instantaneous velocity range from 0.02 to 2.5 m/s with a calibration accuracy of 3%. Ambient relative humidity ($HR_i$) has been measured using air humidity sensors (HMT100, Vaisala, Finland) with a calibration accuracy of 1.7%.

Inner surface temperature of all the enclosures has been also measured during the tests. 15 resistive temperature probes (PT100, TC Direct, UK) have been distributed for all the internal wall surfaces of the chamber. These sensors have been calibrated in the range between 15 °C and 40 °C in order to ensure an uncertainty of measurement of ±0.3 °C. Radiant temperature is calculated by using these inner surface temperatures and the method B.4.2 of EN ISO 7726 standard [60]. A globe temperature probe ($T_{globe}$) has been placed along the PP pole (Table 4) to compare radiant temperature obtained by using Method B.4.2 and that obtained by Method B.2 from ISO 7726 standard [60]. The globe is a black sphere of 150 mm diameter (SFT-SCB-10-6-100, KIMO, France) at the center of which is the temperature probe, a J-Type thermocouple with an accuracy of 2% in the range of 15–45 °C. The comparative is added as additional information in Supporting information A.

Tracer gas equipment is used to measure the exposure of manikin HW to the contaminants exhaled by P manikin. R134a is used as a tracer gas [46,61]. To dose the tracer gas emitted through P exhalation and measure the presence of tracer gas in the surroundings of the HW manikin, a multipoint sampler and doser (Innova 1303, LumaSense Technologies, California) together with a photoacoustic gas monitor (Innova 1412, LumaSense Technologies, California) are used. The uncertainty of the repeatability of the measurement provided by the manufacturer of the photoacoustic gas monitor is 1% of the measured value.

### 2.5. Thermal comfort indices

Temperature, air velocity, and humidity data obtained from the poles PP and PHW together with the radiant temperature obtained from the inner surface temperature of the internal chamber enclosures are used to determine different thermal comfort indices for the position of P and HW following the procedures detailed in ISO EN 7730 [36].

Operative temperature ($T_O$) has been obtained to evaluate thermal comfort for P and HW. General thermal comfort is determined by obtaining the values of predicted mean vote (PMV) and predicted percentage of dissatisfied (PPD). These values are obtained for a standing person in the position of HW and a sitting person in the position of P after steady state conditions are obtained in the experimental room. Current standards do not provide a method to obtain such indices for a lying person, so the closest body posture has been selected. PP pole stands close to the bet where P lies. Airflow patterns and thermal conditions could differ from the position of P because of the geometry of the bed. Nevertheless, the range of variation is not expected to be such that the broader range of thermal comfort is violated. A clothing level of 0.5 clo is selected for both manikins according to the usual clothing conditions in hospitals. The metabolic activity considered for HW manikin is that which corresponds with a standing person performing light activity while P manikin is considered to be seated and at rest. Local thermal comfort indices are also evaluated. Asymmetric thermal radiation as a source of thermal discomfort is studied for P and HW positions by obtaining its value between the South Wall, where the radiant wall is located, and North wall ($\Delta T_{prN\text{-}S}$). The temperature difference between head and feet level ($\Delta T_{h\text{-}f}$), 1.1 m and 0.1 m above the floor in the case of P and 1.7 and 0.1 m in the case of HW is also obtained.

### 2.6. Ventilation performance indices

Ventilation performance indices, widely used in the research literature [18,62,63], have been obtained by using tracer gas technique for the conditions of the three tests performed, air change efficiency ($\varepsilon^a$) and local air change index ($\varepsilon_P^a$). These indices are defined as:

$$\varepsilon^a = \frac{\tau_n}{2 \cdot \tau} \cdot 100 \quad (1)$$

$$\varepsilon_P^a = \frac{\tau_n}{\tau_P} \cdot 100 \quad (2)$$

Where $\tau_n$ is the nominal time constant, $\tau_P$ is the local mean age of air in a determined point and $<\tau>$ is the mean age of air in the room. These indices have been obtained by using the step down method [18] using 40 ppm as the initial concentration. Supply air, as the only source of contaminant in the chamber in this experiment, is seeded with tracer gas setting ventilation system into a configuration of full recirculation until the selected concentration is achieved. After that, seeding is stopped and the ventilation system operates again at 100% outside air and the contaminant concentration decay curve is registered. Contaminant concentration is registered in the exhaust grilles to obtain $\varepsilon^a$ and in three different points in the surroundings of HW breathing area, M1, M2 and M3 to obtain $\varepsilon_P^a$.

### 2.7. Contaminants distribution

The distribution of contaminants emitted through the exhalation of P has been studied under the conditions of the three tests carried out. Each experiment is performed stationary during 6 h after steady state conditions are obtained in the experimental room. P inhales clean air from the exterior of the experimental chamber. Then, tracer gas is injected into the breathing system of P. This manikin exhales air inside the experimental chamber with the contaminant completely mixed. The concentration of tracer gas in the P exhalation flow is 7382 ppm of R134A.

In order to determine the general contaminant removal performance of the ventilation system configuration, contaminant removal effectiveness index ($\varepsilon^c$) is obtained. This value has been used in different recent research [46,61,64,65] and is defined as:

$$\varepsilon^c = \frac{c_e - c_s}{c - c_s} \quad (3)$$

Where $c_e$ is the average concentration of the exhaust air, $c_s$ is the average concentration in the supply air, $<c>$ is the mean concentration of contaminant of the chamber. The concentration in the supply air ($c_s$) is registered but its value is always null because the tracer gas used is not naturally present in the atmosphere. The mean concentration in the chamber ($<c>$) is obtained immediately after the stationary experiment is finished. At that moment, the ventilation system is shut down as well as the tracer gas seeding into the chamber while the air inside the experimental chamber is completely mixed using an auxiliary fan. The concentration values obtained from all the measurement points inside the chamber are averaged during at least 15 min to obtain the mean contaminant concentration value. The concentration in all the measurement points inside

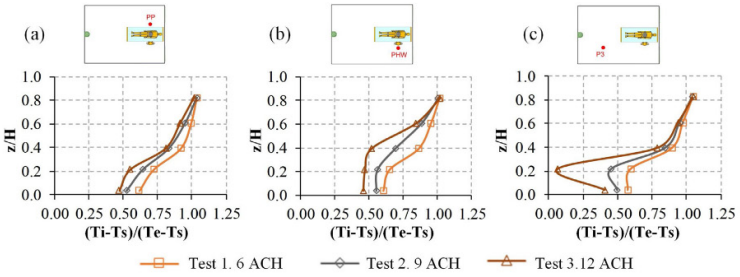


**Fig. 3.** Dimensionless temperature at different heights. (a) Pole PP. (b) Pole PHW. (c) Pole P3.

the chamber tends to a specific value that does not change during the time considered.

Ventilation performance guides [18] define the local air quality index to determine localized contaminant removal ventilation system efficiency. This value is defined as the inverse of local contaminant exposure defined in this study.

The exposure to contaminants around the breathing point of HW is determined through the local relative contaminant exposure $\left(e_p^c\right)$ index. This value has been used in similar studies [66–68] and is defined as:

$$e_p^c = \frac{c_i - c_s}{c_e - c_s} \tag{4}$$

Where $c_i$ is the average tracer gas concentration in a determined point inside the chamber. This concentration is measured inside the chamber to obtain $e_p^c$ in 10 different points around HW microenvironment. 9 points distributed in a vertical plane in front of HW manikin allocated in a $3 \times 3$ matrix, separated 4 cm from the HW inhalation point as can be seen at Fig. 1(a) and an extra point inside the inhalation airway (Inh) of HW breathing.

Local relative contaminant exposure index is a useful value to determine contaminant exposure during the whole experiment. However, to analyze peak exposure to contaminants in such points, a new index, the local relative maximum exposure coefficient $\left(e_{p,\max}^c\right)$ is defined as follows:

$$e_{p,\max}^c = \frac{c_{i,\max} - c_s}{c_e - c_s} \tag{5}$$

Where $c_{i,\max}$ is the average of the maximum values registered in a measurement point. A concentration measurement register is considered as a maximum if its value exceeds 25% of the average concentration. The frequency of such events has been also registered in time for each experiment $\left(f_{e_{p,\max}^c}\right)$, this way the possibility of having a peak concentration can be compared for the tests carried out.

The average concentration obtained in the inhalation airway of HW referred to the average concentration emitted by the source, P manikin exhalation, is defined as the intake fraction ($IF$) index [65]. Its value is obtained as:

$$IF = \frac{\int Q_{b,inh}\ c_{inh}\ \mathrm{d}t}{\int Q_{b,exh}\ c_{exh}\ \mathrm{d}t} \tag{6}$$

Where $Q_{b,inh}$, and $Q_{b,exh}$ (l/min) are the breathing rate of HW (Target) and P (Source) manikins respectively which are the same for this study, $c_{inh}$ is the average contaminant concentration inside the inhalation airway of the HW manikin and $c_{exh}$ is the average contaminant concentration emitted through the P exhalation.

### 2.8. Smoke test

Smoke visualization experiments have been carried out to determine supply air distribution inside the experimental chamber. These three experiments have been carried out under the three test conditions considered in this study once the environment conditions have reached its stationary state. Smoke is introduced into the room through the displacement diffuser completely mixed with supply air (Fig. 1) during 60 s. Smoke is created by a smoke machine (F2010Plus, Safex, Germany) using its standard fog fluid (Normal Power Mix, Safex, Germany). The images are recorded using a digital camera (DSC-H50, SONY, Japan). Supporting information C contents tests videos of smoke distribution inside the room.

## 3. Results and discussion

### 3.1. Experimental conditions

Temperature is registered at five different heights, Table 4, in three different locations, Fig. 1, using vertical poles PHW, PP and P3. The dimensionless value of the temperature has been obtained taking into account the average value of the temperature measurements ($T_i$), the supply average air temperature ($T_s$), and the exhaust average air temperature ($T_e$). Fig. 3 shows the results:

The increase of air renewal rate leads to temperature profiles displaced to lower relative temperatures, especially in the lower parts of the chamber. Temperature profiles show the general temperature distribution along the height of the room for three different points. They show a typical displacement ventilation distribution, where a positive relative temperature gradient are found. The temperature at the upper part of the chamber is around the unit in all cases. This is due to the position of the exhaust grilles, which are situated close to the ceiling height of the room. The diffuser throw has an influence in relative temperature profiles under z/H = 0.2. Under this height, the vertical positive temperature slope changes. In the case of PP, Fig. 3(a), the temperature gradient slope decreases noticeably, while in the case of PHW it disappears, Fig. 3(a). This temperature homogeneity in the lower part of HW pole reaches z/H = 0.4 in Test 3. This is because of the direct action of the supply air throw. In this case, it reaches a higher height because of the increase of the uncovered area of the diffuser. The consequences of this increase of the uncovered area can be also seen in P3 relative temperature profiles, Fig. 3(c), where a sudden decrease of relative temperature is found at z/H = 0.2.

### 3.2. Smoke tests

Smoke tests were performed for the three tests carried out in this study. The three videos taken during the three experiments

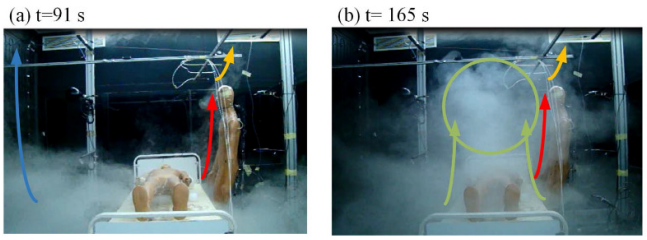


**Fig. 4.** Smoke test pictures taken under the conditions of Test 1 at different time instants. Time since smoke is introduced in the chamber is shown in the images. (a) time = 91 s, (b) time = 165 s.

(a)

| | Units | HW | | | P | | |
|---|---|---|---|---|---|---|---|
| | | Test1 6 ACH | Test 2 9 ACH | Test 3 12 ACH | Test1 6 ACH | Test 2 9 ACH | Test 3 12 ACH |
| $T_o$ | °C | 25.2 | 25.0 | 24.8 | 25.6 | 25.6 | 25.2 |
| PMV | - | 0.62 | 0.53 | 0.52 | -0.42 | -0.55 | -0.54 |
| PPD | % | 13.1 | 11.0 | 10.7 | 11.3 | 11.2 | 19.1 |
| $\Delta T_{pr\,N\text{-}S}$ | K | 0.9 | 0.9 | 1.1 | 2.7 | 2.6 | 2.9 |
| $\Delta T_{h\text{-}f}$ | K | 2.4 | 1.5 | 1.1 | 2.7 | 1.4 | 1.0 |

(b)

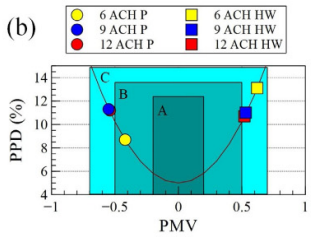


**Fig. 5.** (a) General and local thermal comfort indices. (b) Predicted percentage of dissatisfied as a function of predicted mean vote.

carried out are shown as Supporting information C1, C2 and C3 for Test 1, Test 2 and Test 3 respectively. Two photographs taken during one of the tests carried out are shown in Fig. 4 to illustrate details of the airflow pattern.

In general terms, supply air ventilation behaves in a similar way for the three tests carried out. Although, some differences derived from the different air renewal rate and the change in the free area of the diffuser for each test are found. It can be observed that the dynamics of the process are faster when the renewal rate is increased. Supply air is introduced in the chamber through the displacement diffuser and advances though the floor of the room in radial form from this point though North, South and West walls (Fig. 1) gaining height with the distance to the diffuser [62]. When the flow reaches the South wall, equipped with a radiant heating panel, the flow rises through the wall reaching the ceiling, blue arrow in Fig. 4(a). It happens in the closest section of the wall to the supply diffuser. This is due to the natural convective forces originated by the temperature difference between the radiant panel and the air temperature inside the chamber. Once the South wall air flow reaches the ceiling the smoke is displaced close to the exhaust grilles placed in the upper part of the West wall. Because of the convective flow on the South wall, the smoke is displaced preferentially to the E2 grille. This process is more evident in Test 2 and Test 3 than in Test 1. The rest of the supply flow, that is not caught by the radiant panel, advances from the East wall to the West wall, gaining height when it increases in temperature. When the air reaches the legs of HW it rises through its body captured by its convective thermal boundary layer. This current is originated by the temperature difference between the surface of HW and the air in the chamber, red arrow in Fig. 4. This flow is dragged upwards until, once it leaves behind the head of the manikin, forms a thermal plume, orange arrow in Fig. 4. The time the smoke reaches the body of P manikin, it is warmed by P heat load and rises developing a thermal plume [69,70]. This phenomenon is noted by green arrows in Fig. 4(b). The ascension of this flow is locked upwards, being stacked up above the height of HW, green circle in Fig. 4(b). This is caused by the intense slope of the positive temperature gradient at these heights that generate a lock-up phenomenon. This phenomenon has been reported in other studies that use the similar DV strategy [67,71]. The height and the stability of this stacked flow vary between the three tests carried out because of the differences in the temperature gradients obtained for each test, Fig. 3.

### 3.3. Thermal comfort

General and local thermal comfort indices have been obtained. Results are shown in Fig. 5.

According to the results, $T_O$ decreases with the air renewal rate for P and HW. The values obtained are situated in the comfort zone for summer clothing and sedentary activity for low relative humidity situations [36].

The presence of the radiant panel in the North wall of the chamber creates a significant radiant temperature asymmetry for the N-S plane in all the cases. This radiant temperature asymmetry is higher for P than for HW. It is due to the geometric proximity with the radiant wall. The temperature asymmetry increases with the air renewal rate in all cases. The increase of the air change rate implies an increment of the free area of the diffuser. This makes the temperature on North wall surface decrease. This phenomenon is less evident in the South wall, which is equipped with the radiant panel. Thus, the radiant temperature asymmetry for the N-S plane increases. The temperature difference between the head and feet level decreases with the increase of air renewal rate. This is because an increment in the renewal rate promotes temperature homogeneity in the occupied zone of the chamber. This increase of the homogeneity is directly related to the increase of the free surface of the diffuser with the increase of the ventilation rate, as was noted earlier. More specific research should be carried out to determine the influence of the bed over the comfort of P. Previous research on the comfort of sleeping lying persons determines that under standard ventilation conditions a high degree of thermal comfort can be achieved at 25 °C set point temperature.

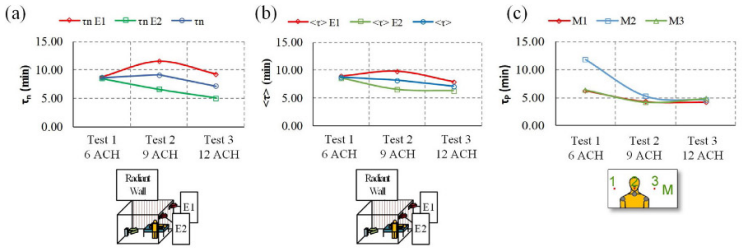


**Fig. 6.** Ventilation performance indices. (a) Nominal time for each exhaust grille ($\tau_n E1$ and $\tau_n E2$) and the averaged exhaust nominal time ($\tau_n$). (b) Room mean age of air for each exhaust grille (<τ> *E1* and <τ> *E2*) and averaged room mean age of air <τ>. (c) Local mean age of air in three different points close to the exhalation point of HW, M1, M2 and M3.

General thermal comfort indices have been plotted in Fig. 5(b), where thermal comfort categories are defined according to the standard EN ISO 7730 [29]. According to the resultscomfort indices PMV for P and HW differs in all the cases. PMV indices for P reflects a slightly cold sensation, being always located between the thermal comfort categories B and C depending on the test. However, PMV indices for HW shows a slightly hot sensation. In this case the thermal comfort category is always C. This situation reflects that the two occupants have different thermal sensations in the same ambient conditions. This is directly related with the different metabolic rate of P and HW cause by the different activities carried out.

### 3.4. Ventilation efficiency

Nominal time constant ($\tau_n$), and the room mean age of air (<τ>) have been obtained by the step down method in each exhaust grille (E1, and E2). Since the exhaust flow rate is equilibrated for both grilles, the time values obtained for them are averaged to obtain representative values for the air exhaust of the chamber. Results obtained for the three tests carried out can be observed in Fig. 6(a) and (b). Local mean age of air ($\tau_P$) has been obtained in three points near the inhalation point of HW, the results for the three tests carried out can be seen at Fig. 6(c).

The values obtained for $\tau_n$ and <τ> for each exhaust grille are different for Test 2 and Test 3. This is due to the effect of the natural convection generated by the radiant panel placed in the North wall. The vertical flow originated by the temperature difference of the wall locks the path of the fresh inward air from the displacement diffuser to E1 grille. This way the decay of contaminant is less pronounced in E1 than in the E2 grille. Consequently, $\tau_n$ and <τ> obtained for E1 grille are higher than the ones for E2. Therefore, results suggest that E2 grille became the preferential path for the inward fresh air. Both characteristic times, $\tau_n$ and <τ>, register a decrease of their value when the air ventilation rate is increased from Test 2 to Test 3. It is due to a weaker influence of the convective flow of the South wall when the airflow rate is increased. The values of $\tau_n$ and <τ> do not differ between grilles in Test 1. It indicates that nothing locks the path of the supply air to the E1 grilles. This difference respect to the other tests might be due to the low air ventilation rate set in this occasion. The reduced supply flow rate avoid the presence of the preferential path between the displacement diffuser and the E1 grille.

Local mean age of air ($\tau_P$) for the three points considered near HW mouth presents the similar decreasing tendency with the increase of air renewal rate. Nevertheless, while the $\tau_P$ values obtained for M1 and M3 are very similar for the three tests, the values obtained for M2 are higher than the rest for Test 1 and Test 2. This difference is especially noticeable in Test 1, while it decreases in Test 2. This is due to the different intensity of the convective air layer around HW body for each test. When the air ventilation rate increases, the free height of the air diffuser is incremented, Fig. 2, while the air temperature inside the chamber decreases, Fig. 3. This promotes the convective flow around HW and thus makes easier for fresh air to reach M2.

Air change efficiency ($\varepsilon^a$) and local air change index ($\varepsilon_P^a$) have been obtained by using the values of $\tau_n$, <τ>, and $\tau_P$ obtained previously. Results are shown in Fig. 7(a) and (b) respectively.

Air change efficiency presents a nearly flat tendency for the three tests, being in all cases around 50%. The value obtained for Test 2 is slightly higher than the rest. It can be explained through the $\tau_n$ and <τ> values obtained for E1 and E2 grilles. In the case of Test 2, these values are very different in each grille. While the times obtained for E1 are high, because of the lock of the supply air path to this grille phenomenon explained previously, the values obtained for E2 are especially low. The resulting mean values for these two variables results in a slight increase of the value of $\varepsilon^a$. This circumstance shows a lower impact in Test 3, and $\varepsilon^a$ has a value close to the one of Test 1. The of $\varepsilon^a$ are lower than expected for displacement ventilation strategy [18]. It may be due to the impact of the supply air path lock phenomenon present in E1 for Test 2 and Test 3.

The values of $\varepsilon_P^a$, Fig. 7(b), are higher than 100% in nearly all cases. This suggests that the ventilation system presents a good local performance. The only exception is found for M2 in Test 1, whose value is noticeably lower than 100%. The tendencies of $\varepsilon_P^a$ for the tests are dependent of the location. The values obtained at M1 and M3 locations show similar values for the three tests carried out. On the contrary, the results obtained for M2 show a different tendency, being lower in Test 1 and Test 2. This is a direct consequence of the values of $\tau_P$ and $\tau_n$ obtained as discussed previously.

### 3.5. Contaminant distribution and exposure to contaminants

Contaminant removal effectiveness ($\varepsilon^c$) is obtained as an index of the performance of the ventilation system in removing the locally emitted contaminants for the three tests. Fig. 8 shows the results.

The results obtained for <c> show a descending tendency with the increase of air renewal rate. Nevertheless, the decrease from Test 1 to Test 2 is very slight. The average concentrations in the exhaust ($c_e$) show an important decrease from Test1 to Test 2 while from Test 2 to Test 3 the trend reverses. The significant drop of $c_e$ from Test 1 to Test 2 does not result in a decrease of <c>, so it can be concluded that part of the emitted contaminants are accumulated into the experimental chamber in Test 2. This could be due to the partial lock of the supply air path to E1 exhaust registered in Test 2. Test 3 shows a decrease of <c> with respect to the values obtained in Test 1 and Test 2 while $c_e$ reaches an intermediate value between Test 1 and Test 2. These results suggest that the increase of venti-

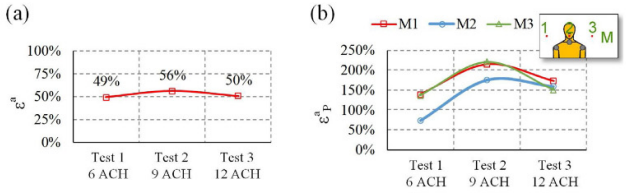


**Fig. 7.** Ventilation effectiveness indices. (a) Air change efficiency ($\varepsilon^a$). (b) Local air change index for three points placed near HW inhalation area.

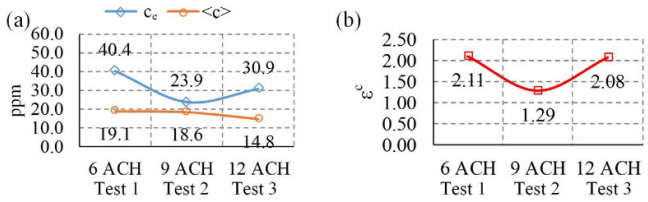


**Fig. 8.** (a) Average contaminant concentration in the exhaust together with the mean contaminant concentration in the experimental chamber for the three tests performed. (b) Contaminant removal effectiveness ($\varepsilon^c$) for the three tests performed.

lation flow rate decreases the influence of the lock of the air path from the diffuser to E1 exhaust, as it was introduced previously.

According to the results obtained, contaminant removal effectiveness ($\varepsilon^c$) presents values that are higher than the unit for the three tests performed, as shown in Fig. 8(b). A value higher than the unit means that contaminants remain for a short period of time in the room before they are removed by the exhaust [18]. The obtained values are comparable to the ones obtained in other AIIR ventilation studies where other ventilation strategies are used [23,64]. Test 1 and Test 3 present similar values higher than that obtained in Test 2. The value of $\varepsilon^c$ is strongly influenced by the position of the source of contaminants [18,23,46]. Since the source stands in the same point for all the three tests performed, its variation in Test 2 could be related with a local change in the airflow pattern inside the chamber that reduces the ventilation system performance in this matter. According to the results obtained for ventilation efficiency indices, the lock of the supply air path phenomenon in E1 found in Test 2 makes $\varepsilon^c$ decrease. The increase of air renewal rate in Test 3 makes this phenomenon less intense and thus, the value of $\varepsilon^c$ increases.

Relative contaminant exposure index $\left(e_P^c\right)$ and maximum exposure coefficient $\left(e_{P,\max}^c\right)$ results for the 10 different points around HW inhalation are shown in Fig. 9.

According to the results obtained for the 10 probes placed in the surroundings of HW inhalation area, Fig. 9(a)–(c), relative contaminant exposure index show different behaviors depending on the probe position. Natural convection, due to the difference in temperature of the exhaled flow with respect to the ambient temperature of the chamber, combined with exhalation flow momentum, turbulent diffusion and ventilation air movements, are the forces that disperse the contaminants seeded in P exhalation [67]. For the three tests performed, the most exposed zone to contaminants is L1, located near the exhalation of P. Values corresponding to M1 and H1 show also high values due to the location with respect to the source of contaminants. This area near the West wall shows higher values as the ventilation strategy is not effective in this area. However, region 3 keeps cleaner for all the three tests. This suggests that in this area fresh air is arriving from the diffuser. In Test 1, Fig. 9(a), the $e_P$ values are higher in the lower part (L) due to the proximity to the source and to a lock-up phenomenon that confine the exhaled contaminants at this height. For Test 2, Fig. 9(b), it is still possible to observe a high concentration of contaminants in the lower part of the room, influenced by the direct exhalation of the manikin, but the contaminant concentration also increases close to the ceiling of the chamber. The lock-up phenomenon observed in the case of Test 1 may have changed due to the different height of the diffuser and the increase of air renewal rate. In the same way, for 12 ACH, Fig. 9(c), the lower height of the room remains clean due to a more direct influence of the fresh air from the diffuser. This clean air displaces the contaminants to M1. This way the lock-up phenomenon occurs at a higher height from the P manikin, corresponding to M region, which is consistent with the temperature profiles registered, as can be seen at Fig. 3. The thermal plume of the HW may also be directly influencing the dispersion of the exhaled contaminants in a different way, as contaminant concentration registered in column 2 points increases with their height for the three tests. This could be due to the dragging effect that the upward vertical convective current over the manikin body has over the contaminants, displacing them to higher heights.

The exposure in the inhalation of the HW manikin, Fig. 9, is low, less than 1 for all the tests carried out. It suggests that the ventilation strategy is maintaining contaminants far from the inhalation of HW. The relative position of HW with respect to the diffuser and P exhalation location, could explain these low values, as it is located in the path of the flow of air from the diffuser to the exhaust in the opposite wall. Another phenomenon that can explain the relative low exposure is the vertical convective layer around HW originated by the temperature difference between the surface of HW and the temperature of the air in the chamber. That layer prevents the inhalation from contaminants, making it difficult for them to penetrate the inhalation region of HW. The value of $e_P$ for the air inhaled by HW (Inh) in Test 2 is higher than that obtained for Test 1 and Test 3. This phenomenon could be related with the contaminant accumulation inside the chamber detected in this test and detailed previously.

The values of $e_{P,\max}^c$ for all the three tests performed show in general terms, a similar tendency than the values of $e_P^c$. The higher the values of $e_P^c$ are, the higher the values of $e_{P,\max}^c$ are too. The higher concentration peaks can be found at column 1, where they

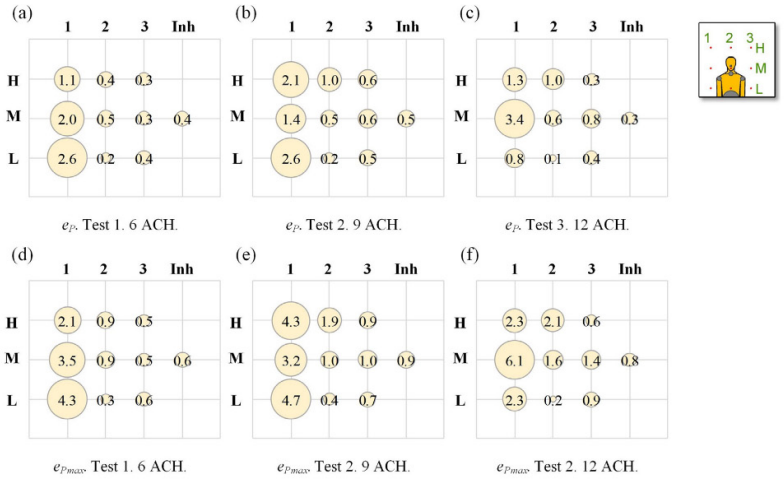


**Fig. 9.** Local relative contaminant exposure index $e_P^c$ together with the corresponding local maximum relative exposure index $e_{P,max}^c$ to contaminants for the 9-point array situated in HW microenvironment and Inh point inside the inhalation airways. (a) and (d) Test 1; (b) and (e) Test 2; (c) and (f) Test 3.

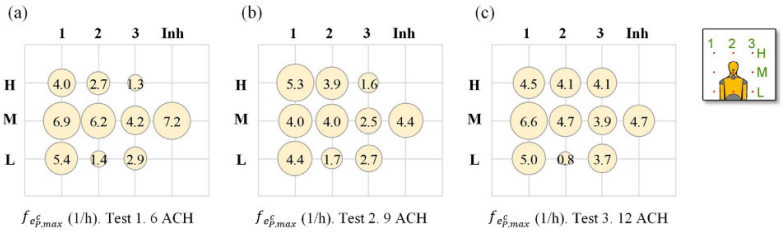


**Fig. 10.** Frequency of maximum exposure coefficients for each test performed.

can double the values of $e_P^c$. The value of $e_{P,\max}^c$ for columns 2 and 3 is lower than the values obtained for column 1 but, in some cases they exceed the unit, which is contrary to that of the values of $e_P^c$. These results show that it is possible to register peak concentrations over the unit even if the value of $e_P^c$ is lower than the unit. Therefore, a short exposure to relative peak exposure can lead to a situation with a higher exposure to contaminants.

Local maximum exposure coefficient frequency $\left(f_{e_{P,\max}^c}\right)$ is obtained for all the points where contaminant exposure is registered. Fig. 10 shows the obtained results.

In general, the points placed closer to the contaminants source present higher $f_{e_{P,\max}^c}$ values than the ones that are farther which is consistent with the results of $e_P^c$ and $e_{P,\max}^c$, where the same dependence with distance is found. The reliance of $f_{e_{P,\max}^c}$ with air renewal rate is not as strong as in the case of $e_P^c$ and $e_{P,\max}^c$. A generalized decrease of $f_{e_{P,\max}^c}$ is found when the air renewal rate is increased from Test 1 to Test 2. This suggests that contaminants concentration is more homogeneous over time under these conditions. These results, together with the values obtained for $e_P^c$ and $e_{P,\max}^c$, suggest that contaminants spread more easily in Test 2. Although, the increment of air renewal Test 3 leads to higher $f_{e_{P,\max}^c}$ values. That situation could be explained by the instability in contaminant concentration values created by the influence of the fresh air rising through the West wall. The values of $f_{e_{P,\max}^c}$ obtained inside the inhalation airways of HW (Inh) are similar to that obtained in the point M2, immediately outside the inhalation point of HW. These results suggest that at the time a peak concentration occurs, it is registered inside and outside the inhalation point.

The intake fraction (*IF*) index has been obtained in two different points, immediately in front of the inhalation point (M2), and inside the inhalation airways of the manikin (Inh). Fig. 11 shows the obtained results.

The tendency of *IF* for the three tests performed is the same for the two positions considered. Even so, the values obtained for the point Inh are always lower than the obtained in the point M2. These results suggest that by selecting a point out of the inhalation airways to determine the contaminants intake of the manikin, the resulting index could be overestimated [65]. This situation may be originated by the action of the human convective boundary layer as it has been described in other studies [70,72]. Test 1 presents the higher values of *IF*, coinciding with the lower air ventilation rate. The increase of the renewal rate from Test 1 to Test 2 reduces the value of *IF*, and thus the contaminants intake of the HW manikin

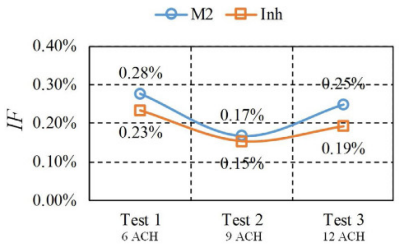


**Fig. 11.** Intake fraction referred to the concentration of the only source of contaminants, P breathing.

decreases. The ease for contaminants to disperse far from HW in Test 2 based on the data obtained for $\varepsilon^c$ and $\varepsilon^a$ can explain the decrease of *IF*. Although, when the renewal rate increases again in Test 3, the tendency changes, and the obtained values are comparable to the ones obtained in Test 1. It can be explained by the direct influence of fresh ventilation air rising through West wall displacing contaminants upwards to the inhalation region of HW.

## 4. Conclusions

Experimental tests have been carried out to determine thermal comfort, ventilation performance and contaminant exposure in a representative case of study of an AIIR configuration using displacement ventilation strategy. Three air renewal rates have been tested to determine its impact on these three issues.

In view of the results of each test and the comparisons between them, the following conclusions can be stated:

- The air renewal rates tested in this experimental study have an impact on the environment conditions of the experimental chamber and thus on the comfort situation of the people inside it. According to the general thermal comfort indices obtained, the occupants have different thermal sensations under the same ambient conditions; that is, while HW identifies a hot environment, PP registers a cold one. This is due to their different activity level. This could be problematic because the relatively hot sensation of HW can discourage the use of personal protective equipment and thus limit its effectiveness [59].
- A lock of the air path of the exhaust grille closer to the radiant panel, to the access of fresh inward ventilation air has been identified in Test 2 and Test 3. Radiant panel convective flow locks the access of the fresh supply ventilation air to this grille, finding this air to be a preferential path to E2. This situation can cause a contaminant accumulation in this area due to the lack of fresh air in the zone. The relative importance of this fact decreases when the air ventilation renewal rate is increased.
- A "lock-up" phenomenon has been identified above of P head. The height of the lock-up is dependent on the temperature gradient present in the chamber. The presence of this stagnant zone can stop the rise of the contaminants, generating a high contaminant concentration zone above P. This situation does affect, but not significantly, the exposure of the different points around HW inhalation. This lack of effect is due to the effect of the convective boundary layer, which provides fresh air from the lower part or the chamber to the inhalation zone of HW, avoiding the penetration of contaminants in HW microenvironment.
- The relative exposure to contaminants $\left(e_p^c\right)$ in a point around HW inhalation is dependent on its position with respect to the source. In general, the closest area to the source presents a higher relative contaminant concentration. Relative exposure in this area is very dependent on the ventilation air distribution in the area. The zone influenced by the thermal convective layer around HW shows low $e_p^c$ values. This is due to the effect of the convective current that brings fresh ventilation air from the lower part of the room. The zone situated between the diffuser and HW presents lower relative exposure to contaminants, ventilation drag contaminants to the zone situated between the P exhalation and the exhaust. Relative peak exposure to contaminants $\left(e_{P,\max}^c\right)$ can register a high variation to its average value, that can even double it in points close to the source. It can happen several times each hour. This is especially significant if the cross infection risk of HW is evaluated, the exposure can be underestimated if the average values are considered.
- Intake fraction *IF* and relative local contaminant exposure indices $\left(e_p^c\right)$ show that the ventilation strategy is effective. The emitted contaminant that reaches the surroundings of HW inhalation is low. In addition, it has been found that the contaminant concentration in the surroundings of the inhalation point is always higher than that obtained in the inhalation airways. So, if contaminants measurements are performed out of the inhalation airway, the real exposure can be overestimated.
- The increase of the air ventilation rate leads to different air distribution scenarios that modify the ventilation performance and contaminant distribution indices. Results have shown that the increase of air ventilation rate does not imply a direct improvement of such indices. In fact, the results obtained in Test 1 and Test 3 are quite similar. It is necessary to analyze all the indices to understand completely how the designed ventilation system behaves. For instance, results obtained for Test 2 are good in terms of ventilation performance indices and in *IF* but the value of contaminant removal effectiveness indicates that P emitted contaminants must be accumulated inside the room, somewhere out of the reach of HW. A specific study of these aspects can lead to a decrease of energy consumption since the air renovation rate can be adjusted to the real necessities of the ventilated space. In this case of study air ventilation rate can be reduced by half, from the recommended 12 ACH to 6 ACH without a significant change of the air quality, exposure nor thermal comfort indices.

Considering all the results, this paper shows that displacement ventilation is a real alternative to mixing ventilation as a strategy for AIIRs. Comfort for patients and health workers can be achieved as well as acceptable ventilation performance indices and HW contaminant exposure by using this strategy. However, and according to the results, special attention to the air distribution inside the room must be paid. Aspects such as the distribution of the thermal loads and the relative position of P and HW determine the ventilation performance of the system.

## Acknowledgments

The authors acknowledge the financial support received from the Ministerio de Economía y Competitividad, Secretaría de Estado de Investigación, Desarrollo e Innovación, Spain, to the National R&D project TRACER with reference DPI2014-55357-C2-2-R, entitled "Ventilation system influence on airborne transmission of human exhaled bioaerosols. Cross infection risk evaluation". This project is cofinanced by the European Regional Development Fund (ERDF).

## Appendix A. Supplementary data

Supplementary data associated with this article can be found, in the online version, at https://doi.org/10.1016/j.enbuild.2017.09.100.

## References


[1] M.-F. King, C.J. Noakes, P.A. Sleigh, Modeling environmental contamination in hospital single- and four-bed rooms, Indoor Air (2015) 1–14, http://dx.doi.org/10.1111/ina.12186.

[2] C.B. Beggs, L.D. Knibbs, G.R. Johnson, L. Morawska, Environmental contamination and hospital-acquired infection: factors that are easily overlooked, Indoor Air 25 (2015) 462–474, http://dx.doi.org/10.1111/ina.12170.

[3] J. Richmond-Bryant, Transport of exhaled particulate matter in airborne infection isolation rooms, Build. Environ. 44 (2009) 44–55, http://dx.doi.org/10.1016/j.buildenv.2008.01.009.

[4] L. Liu, Y. Li, P.V. Nielsen, J. Wei, R.L. Jensen, Short-range airborne transmission of expiratory droplets between two people, Indoor Air (2016) 1–11, http://dx.doi.org/10.1111/ina.12314.

[5] S. Stelzer-Braid, B.G. Oliver, A.J. Blazey, A. Elizabeth, T.P. Newsome, W.D. Rawlinson, et al., Exhalation of respiratory viruses by breathing, coughing, and talking, J. Med. Virol. 81 (2009) 1674–1679, http://dx.doi.org/10.1002/jmv.

[6] D.K. Milton, M.P. Fabian, B.J. Cowling, M.L. Grantham, J.J. McDevitt, Influenza virus aerosols in human exhaled breath: particle size, culturability, and effect of surgical masks, PLoS Pathog. 9 (2013) e1003205, http://dx.doi.org/10.1371/journal.ppat.1003205.

[7] F.A. Berlanga, I. Olmedo, M. Ruiz de Adana, Experimental analysis of the air velocity and contaminant dispersion of human exhalation flows, Indoor Air (2016) 1–13, http://dx.doi.org/10.1111/ina.12357.

[8] J.K. Gupta, C.H. Lin, Q. Chen, Flow dynamics and characterization of a cough, Indoor Air 19 (2009) 517–525, http://dx.doi.org/10.1111/j.1600-0668.2009.00619.x.

[9] J.W. Tang, A. Nicolle, C. Klettner, J. Pantelic, L. Wang, A. Suhaimi, et al., Airflow dynamics of human jets: sneezing and breathing—potential sources of infectious aerosols, PLoS One 8 (2013) e59970, http://dx.doi.org/10.1371/journal.pone.0059970.

[10] American Society of Heating and Air-Conditioning Engineers, Thermal comfort, in: ASHRAE Handb. Fundam., 2013, ASHRAE, Atlanta, GA, p. 9. 1–9.32.

[11] X. Xie, Y. Li, A.T.Y. Chwang, P.L. Ho, W.H. Seto, How far droplets can move in indoor environments—revisiting the wells evaporation-falling curve, Indoor Air 17 (2007) 211–225, http://dx.doi.org/10.1111/j.1600-0668.2007.00469.x.

[12] W.F. Wells, On air-borne infection. II. Droplets and droplet nuclei, Am. J. Hyg. 20 (1934) 611–618.

[13] A. Jurelionis, L. Gagytė, T. Prasauskas, D. Čiužas, E. Krugly, L. Šeduikytė, et al., The impact of the air distribution method in ventilated rooms on the aerosol particle dispersion and removal: the experimental approach, Energy Build. 86 (2015) 305–313, http://dx.doi.org/10.1016/j.enbuild.2014.10.014.

[14] K. Lyngby, T.H. Kuehn, H.E.B. Burroughs, C.O. Muller, D. Tompkins, W.J. Fisk, et al., ASHRAE Position Document on Airborne Infectious Diseases, 2015.

[15] M.P. Atkinson, L.M. Wein, Quantifying the routes of transmission for pandemic influenza, Bull. Math. Biol. 70 (2008) 820–867, http://dx.doi.org/10.1007/s11538-007-9281-2.

[16] J.D. Siegel, E. Rhinehart, M. Jackson, L. Chiarello, 2007 guideline for isolation precautions: preventing transmission of infectious agents in health care settings, Am. J. Infect. Control 35 (2007), http://dx.doi.org/10.1016/j.ajic.2007.10.007.

[17] N.J. Adams, D.L. Johnson, R.A. Lynch, The effect of pressure differential and care provider movement on airborne infectious isolation room containment effectiveness, Am. J. Infect. Control 39 (2011) 91–97, http://dx.doi.org/10.1016/j.ajic.2010.05.025.

[18] E. Mundt, H.M. Mathisen, P.V. Nielsen, A. Moser, Ventilation Effectiveness, 2004.

[19] E. Lingaas, J.P. Rydock, Best practice in design and testing of isolation rooms in Nordic hospitals, Round Table Ser. – R. Soc. Med. (2007) 87–107.

[20] Victorian Advisory Committee on Infection Control, Guidelines for the Classification and Design of Isolation Rooms in Health Care Facilities, 1st ed., Victorian Government, Melbourne, 2007.

[21] Centers for Disease Control and Prevention, Guidelines for preventing the transmission of Mycobacterium tuberculosis in health-care facilities, MMWR Morb. Mortal. Wkly. Rep. 43 (1994) 1–132, http://dx.doi.org/10.2307/42000931.

[22] L. Sehulster, R.Y.W. Chinn, Guidelines for environmental infection control in health-care facilities, Morb. Mortal. Wkly. Rep. 52 (2003) 1–42.

[23] F. Memarzadeh, W. Xu, Role of air changes per hour (ACH) in possible transmission of airborne infections, Build. Simul. 5 (2012) 15–28, http://dx.doi.org/10.1007/s12273-011-0053-4.

[24] P. Kalliomäki, P. Saarinen, J.W. Tang, H. Koskela, Airflow patterns through single hinged and sliding doors in hospital isolation rooms—effect of ventilation, flow differential and passage, Build. Environ. 107 (2016) 154–168, http://dx.doi.org/10.1016/j.buildenv.2016.07.009.

[25] A. Jurelionis, L. Gagyte, L. Seduikyte, T. Prasauskas, D. Ciuzas, D. Martuzevicius, Combined air heating and ventilation increases risk of personal exposure to airborne pollutants released at the floor level, Energy Build. 116 (2016) 263–273, http://dx.doi.org/10.1016/j.enbuild.2016.01.011.

[26] P. Kumar, C. Martani, L. Morawska, L. Norford, R. Choudhary, M. Bell, et al., Indoor air quality and energy management through real-time sensing in commercial buildings, Energy Build. 111 (2016) 145–153, http://dx.doi.org/10.1016/j.enbuild.2015.11.037.

[27] A. Kabanshi, H. Wigö, M. Sandberg, Experimental evaluation of an intermittent air supply system—part 1: thermal comfort and ventilation efficiency measurements, Build. Environ. 95 (2016) 240–250, http://dx.doi.org/10.1016/j.buildenv.2015.09.025.

[28] W. Yu, B. Li, H. Jia, M. Zhang, D. Wang, Application of multi-objective genetic algorithm to optimize energy efficiency and thermal comfort in building design, Energy Build. 88 (2015) 135–143, http://dx.doi.org/10.1016/j.enbuild.2014.11.063.

[29] F. Memarzadeh, A. Manning, Thermal comfort, uniformity, and ventilation effectiveness in patient rooms: performance assessment using ventilation indices, ASHRAE Trans. 106 (2000).

[30] R. Van Gaever, V.A. Jacobs, M. Diltoer, L. Peeters, S. Vanlanduit, Thermal comfort of the surgical staff in the operating room, Build. Environ. 81 (2014) 37–41, http://dx.doi.org/10.1016/j.buildenv.2014.05.036.

[31] C.A. Balaras, E. Dascalaki, A. Gaglia, HVAC and indoor thermal conditions in hospital operating rooms, Energy Build. 39 (2007) 454–470, http://dx.doi.org/10.1016/j.enbuild.2006.09.004.

[32] S. Del Ferraro, S. Iavicoli, S. Russo, V. Molinaro, A field study on thermal comfort in an Italian hospital considering differences in gender and age, Appl. Ergon. 50 (2015) 177–184, http://dx.doi.org/10.1016/j.apergo.2015.03.014.

[33] L. Lan, L. Pan, Z. Lian, H. Huang, Y. Lin, Experimental study on thermal comfort of sleeping people at different air temperatures, Build. Environ. 73 (2014) 24–31, http://dx.doi.org/10.1016/j.buildenv.2013.11.024.

[34] S. Zhu, W. Cai, J.D. Spengler, Control of sleep environment of an infant by wide-cover type personalized ventilation, Energy Build. 129 (2016) 69–80, http://dx.doi.org/10.1016/j.enbuild.2016.07.064.

[35] P.O. Fanger, Thermal Comfort: Analysis and Applications in Environmental Engineering, McGraw-Hill, 1970.

[36] ISO—AEN/CTN 81, ISO 7730, Ergonomics of the Thermal Environment—Analytical Determina- Tion and Interpretation of Thermal Comfort Using Calculation of the PMV and PPD Indices and Local Thermal Comfort Criteria, 2005, ISO, Geneva.

[37] X. Ye, H. Zhu, Y. Kang, K. Zhong, Heating energy consumption of impinging jet ventilation and mixing ventilation in large-height spaces: a comparison study, Energy Build. 130 (2016) 697–708, http://dx.doi.org/10.1016/j.enbuild.2016.08.055.

[38] M. Behne, Indoor air quality in rooms with cooled ceilings. Mixing ventilation or rather displacement ventilation? Energy Build. 30 (1999) 155–166, http://dx.doi.org/10.1016/S0378-7788(98)00083-8.

[39] N.M. Mateus, G.C. Da Graça, Simplified modeling of displacement ventilation systems with chilled ceilings, Energy Build. 108 (2015) 44–54, http://dx.doi.org/10.1016/j.enbuild.2015.08.054.

[40] E. Mundt, Contamination distribution in displacement ventilation-influence of disturbances, Build. Environ. 29 (1994) 311–317, http://dx.doi.org/10.1016/0360-1323(94)90028-0.

[41] S. Cho, P. Im, J.S. Haberl, Literature Review of Displacement Ventilation, Energy Syst. Lab. Texas A&M Univ. Syst., 2005, pp. 23.

[42] D. Spengler, J.M. Samet, J.F. McCarthy, Disinfecting air, in: Indoor Air Qual Handb., 2001.

[43] J. Wang, Y. Chen, Concentration characteristics of ozone and product for indoor occupant surface chemical reaction under displacement ventilation, Energy Build. 130 (2016) 378–387, http://dx.doi.org/10.1016/j.enbuild.2016.08.065.

[44] J.M. Villafruela, I. Olmedo, M. Ruiz de Adana, C. Méndez, P.V. Nielsen, CFD analysis of the human exhalation flow using different boundary conditions and ventilation strategies, Build. Environ. 62 (2013) 191–200, http://dx.doi.org/10.1016/j.buildenv.2013.01.022.

[45] Y.C. Tung, S.C. Hu, T.I. Tsai, I.L. Chang, An experimental study on ventilation efficiency of isolation room, Build. Environ. 44 (2009) 271–279, http://dx.doi.org/10.1016/j.buildenv.2008.03.003.

[46] R. Tomasi, M. Krajčík, A. Simone, B.W. Olesen, Experimental evaluation of air distribution in mechanically ventilated residential rooms: thermal comfort and ventilation effectiveness, Energy Build. 60 (2013) 28–37, http://dx.doi.org/10.1016/j.enbuild.2013.01.003.

[47] J.P. Rydock, P.K. Eian, Containment testing of isolation rooms, J. Hosp. Infect. 57 (2004) 228–232, http://dx.doi.org/10.1016/j.jhin.2004.01.032.

[48] D. Than, J. Decker, Case studies evaluation of isolation rooms in health care settings using tracer gas analysis, Appl. Occup. Environ. Hyg. 10 (1995) 887–891, http://dx.doi.org/10.1080/1047322X.1995.10387707.

[49] J. Yang, S.C. Sekhar, K.W.D. Cheong, B. Raphael, Performance evaluation of a novel personalized ventilation-personalized exhaust system for airborne infection control, Indoor Air 25 (2015) 176–187, http://dx.doi.org/10.1111/ina.12127.

[50] Y. Yin, W. Xu, J.K. Gupta, A. Guity, P. Marmion, A. Manning, et al., Experimental study on displacement and mixing ventilation systems for a patient ward, HVAC&R Res. 15 (2009) 1175–1191, http://dx.doi.org/10.1080/10789669.2009.10390885.

[51] M. Bivolarova, J. Ondráček, A. Melikov, V. Ždímal, A comparison between tracer gas and aerosol particles distribution indoors: the impact of ventilation rate, interaction of airflows, and presence of objects, Indoor Air (2017) 1–12, http://dx.doi.org/10.1111/ina.12388.

[52] H. Qian, Y. Li, P.V. Nielsen, C.E. Hyldgaard, T.W. Wong, A.T.Y. Chwang, Dispersion of exhaled droplet nuclei in a two-bed hospital ward with three different ventilation systems, Indoor Air 16 (2006) 111–128, http://dx.doi.org/10.1111/j.1600-0668.2005.00407.x.

[53] A. Guity, M. Nash, L. Burch, P. Marmion, Healthcare Ventilation Research Collaborative: Displacement Ventilation, 2009.

[54] H. Qian, Y. Li, Removal of exhaled particles by ventilation and deposition in a multibed airborne infection isolation room, Indoor Air 20 (2010) 284–297, http://dx.doi.org/10.1111/j.1600-0668.2010.00653.x.
[55] C.W. Branch, Building and Refurbishment, Infection Control Guidelines January 2002, 2002.
[56] F.A. Berlanga, M. Ruiz de Adana, I. Olmedo, Diseño y construcción de maniquíes térmicos para la realización de ensayos experimentales de sistemas de climatización, in: Proc. IX Congr. Nac. Ing. Termodinámica, Cartagena, 2015, pp. 1–8 (978-84-606-8931-7).
[57] S. Tanabe, E.A. Arens, F. Bauman, H. Zang, T. Madsen, Evaluating thermal environments by using a thermal manikin with controlled skin surface temperature, ASHRAE Trans. 100 (1994) 39–47.
[58] J.K. Gupta, C. H. Lin, Q. Chen, Characterizing exhaled airflow from breathing and talking, Indoor Air 20 (2010) 31–39, http://dx.doi.org/10.1111/j.1600-0668.2009.00623.x.
[59] J.W. Tang, Y. Li, I. Eames, P.K.S. Chan, G.L. Ridgway, Factors involved in the aerosol transmission of infection and control of ventilation in healthcare premises, J. Hosp. Infect. 64 (2006) 100–114, http://dx.doi.org/10.1016/j.jhin.2006.05.022.
[60] Technical Comitee for Ergonomics of the physical environment, ISO 7726 Ergonomics of the Thermal Environment—Instruments for Measuring Physical Quantities, 2nd ed., ISO, 1998, 2017.
[61] M. Krajčík, A. Simone, B.W. Olesen, Air distribution and ventilation effectiveness in an occupied room heated by warm air, Energy Build. 55 (2012) 94–101, http://dx.doi.org/10.1016/j.enbuild.2012.08.015.
[62] H.B. Awbi, Ventilation of Buildings, 2nd ed., Spon Press, London, 2003, http://dx.doi.org/10.1080/02786820490519234.
[63] H. Amai, A. Novoselac, Experimental study on air change effectiveness in mixing ventilation, Build. Environ. 109 (2016) 101–111, http://dx.doi.org/10.1016/j.buildenv.2016.09.015.
[64] J.M. Villafruela, F. Castro, J.F. San Jose, J. Saint-Martin, Comparison of air change efficiency, contaminant removal effectiveness and infection risk as IAQ indices in isolation rooms, Energy Build. 57 (2013) 210–219, http://dx.doi.org/10.1016/j.enbuild.2012.10.053.
[65] J. Laverge, M. Spilak, A. Novoselac, Experimental assessment of the inhalation zone of standing, sitting and sleeping persons, Build. Environ. 82 (2014) 258–266, http://dx.doi.org/10.1016/j.buildenv.2014.08.014.
[66] G. Cao, P.V. Nielsen, R.L. Jensen, P. Heiselberg, L. Liu, J. Heikkinen, Protected zone ventilation and reduced personal exposure to airborne cross-infection, Indoor Air 25 (2015) 307–319, http://dx.doi.org/10.1111/ina.12142.
[67] I. Olmedo, P.V. Nielsen, M. Ruiz de Adana, R.L. Jensen, P. Grzelecki, Distribution of exhaled contaminants and personal exposure in a room using three different air distribution strategies, Indoor Air 22 (2012) 64–76, http://dx.doi.org/10.1111/j.1600-0668.2011.00736.x.
[68] I. Olmedo, P.V. Nielsen, M. Ruiz de Adana, R.L. Jensen, The risk of airborne cross-infection in a room with vertical low-velocity ventilation, Indoor Air 23 (2013) 62–73, http://dx.doi.org/10.1111/j.1600-0668.2012.00794.x.
[69] D. Licina, A.K. Melikov, C. Sekhar, K.W. Tham, Human convective boundary layer and its interaction with room ventilation flow, Indoor Air 25 (2015) 1–15, http://dx.doi.org/10.1111/ina.12120.
[70] D. Licina, A. Melikov, C. Sekhar, K.W. Tham, Transport of gaseous pollutants by convective boundary layer around a human body, Sci. Technol. Built Environ. (2015), http://dx.doi.org/10.1080/23744731.2015.1060111, 00–00.
[71] C. Xu, P.V. Nielsen, G. Gong, R.L. Jensen, L. Liu, Influence of air stability and metabolic rate on exhaled flow, Indoor Air 25 (2015) 198–209, http://dx.doi.org/10.1111/ina.12135.
[72] S. Zhu, S. Kato, S. Murakami, T. Hayashi, Study on inhalation region by means of CFD analysis and experiment, Build. Environ. 40 (2005) 1329–1336, http://dx.doi.org/10.1016/j.buildenv.2004.11.009.

# Paper X. Experimental assessment of different mixing air ventilation systems on ventilation performance and exposure to exhaled contaminants in hospital rooms

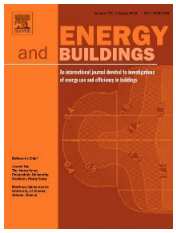


*The paper has been published in Energy and Buildings journal (10.1016/j.enbuild.2018.07.053)*

After performing the analysis of displacement ventilation strategy, other mixing ventilation strategies are tested. Mixing ventilation strategy can be faced by supplying and exhausting air from different points inside the indoor space. This study focuses its attention in two different ways to supply air, using swirl diffusers and wall grilles, and two different exhaust grille heights located in the upper part of the wall and in the lower part of it.

Results highlight the importance of the ventilation flow currents on the dispersion of the exhaled contaminants. Different ventilation configurations and flow rates lead to diverse results on contaminant dispersion inside the indoor space. In accordance with the results obtained together with the obtained for the same set up using displacement ventilation, it is possible to discuss the optimum ventilation configuration and the air ventilation rate that leads to reduce health worker cross infection risk.

Energy & Buildings 177 (2018) 207–219

Contents lists available at ScienceDirect

Energy & Buildings

journal homepage: www.elsevier.com/locate/enbuild

# Experimental assessment of different mixing air ventilation systems on ventilation performance and exposure to exhaled contaminants in hospital rooms

F.A. Berlanga[a,*], I. Olmedo[a], M. Ruiz de Adana[a], J.M. Villafruela[b], J.F. San José[b], F. Castro[b]

[a] Department of Chemical Physics and Applied Thermodynamics, University of Córdoba, Córdoba 14014, Spain
[b] Department of Energy and Fluid Mechanics, University of Valladolid, Valladolid 47011, Spain

ARTICLE INFO

*Article history:*
Received 3 May 2018
Revised 18 July 2018
Accepted 24 July 2018
Available online 11 August 2018

*Keywords:*
Mixing ventilation
Hospital room
Personal exposure
Ventilation effectiveness thermal comfort
Airborne transmission of diseases

ABSTRACT

This study evaluates the convenience of the use of four different mixing ventilation configurations in individual hospital rooms (IHR) based on ventilation performance and health workers (HW) exposure to the contaminants released by a confined patient (CP). Two supply configurations: grilles in the upper part of a wall (G) and swirl ceiling diffusers (S), combined with two different exhaust grilles positions in the opposite wall: upper part (U) and lower part (D) are tested using typical IHR set up. Occupants are represented by thermal breathing manikins, CP lies on a bed while HW stands close to it. Three air renewal rates are tested to determine their influence in the studied variables, 6, 9 and 12 ACH covering the whole range of ventilation requirements of such spaces. The experimental conditions considering the thermal comfort of the occupants are taken into account. Different ventilation configurations create different air distribution patterns inside the room. G configurations lead to high HW transient exposure values while S maintain low values that decrease when ACH is increased, so this second configuration is preferred for IHRs. Results are also compared with a displacement ventilation (DV) study highlighting the convenience of this strategy for IHRs.



## 1. Introduction

Hospitals environments are risky places for cross infections because of the close interaction of healthy and infected people [1]. Health workers successively visit different patients and, if they are infected, can become disease vector [2]. Visitors are also in contact with patients and they can spread the disease out of the hospital environment. Pathogens that spread diseases such as influenza and tuberculosis can be transported through the air [3–5] being respiratory events such breathing [6], sneezing [7] and coughing [8] the main exit route for it. Together with other bioeffluents, emitted droplets of different size transport pathogens through the air [9]. These particles suffer an evaporative effect that reduce their size until they are transformed into droplet nuclei [10–13]. Depending on the size of the resulting particle, it can precipitate quickly because of the effect of the gravity (if its diameter is greater or 10 μm) or move through the air by means of the ventilation-induced effects (in the case that its diameter is lower than 10 μm) [10]. These small particles can be spread over long distances and be the cause of cross infections between people [13]. The dispersion of these particles is influenced by ventilation flows [14]. Thus, a convenient ventilation strategy can reduce the possibility of these infections [12,15] since it has an influence on particle dynamics [16].

Different types of spaces with different ventilation requirements can be present in hospitals [17]. Focusing our attention in individual hospital rooms (IHRs), airborne infectious isolation rooms (AIIRs) as a specific configuration of IHRs, present specific ventilation requirements. While recovery rooms minimal ventilation rate is fixed in 6 ACH, the requirements for AIIRs increase this value to 12 ACH [17]. Patients considered highly contagious, or especially sensible to infections, are confined in AIIRs. These spaces maintain a negative pressure differential with respect of the rest of the building, in addition to other security measures [18] in order to maintain the patients isolated from the rest of the building. Different National Health committees have published guides about AIIRs design [5,19–22]. Regarding the prevention of airborne cross infections, these regulations focus their attention in assuring a high ventilation air renewal rate. These recommendations are based on the belief that high renewal rates could reduce cross infection risk in such spaces by diluting and removing pathogens. Nevertheless, recent research focuses attention on providing a good air distribu-

* Coresponding author.
*E-mail address:* felix.berlanga@uco.es (F.A. Berlanga).

https://doi.org/10.1016/j.enbuild.2018.07.053
0378-7788/

**Nomenclature**

| | |
|---|---|
| ACH | Air changes per hour ($h^{-1}$) |
| AIIR | Airborne infection isolation room |
| CFD | Computational fluid mechanics |
| CP | Patient |
| D | Exhaust grille placed on the lower part of the West wall |
| DR | Percentage of dissatisfied people as a result of draught |
| DV | Displacement ventilation |
| G | Supply grille diffuser placed on the East wall of the room |
| GD | Ventilation system configuration combining G supply and D exhaust |
| GU | Ventilation system configuration combining G supply and U exhaust |
| IHR | Individual hospital room |
| $IF$ | Intake fraction |
| $IF_{max}$ | Maximum intake fraction |
| $IF_{125\%}$ | Peaks average intake fraction |
| S | Supply swirl diffuser placed on the ceiling of the room |
| SD | Ventilation system configuration combining S supply and D exhaust |
| SU | Ventilation system configuration combining S supply and U exhaust |
| U | Exhaust grille placed on the upper part of the West wall |
| $\langle \bar{c} \rangle$ | Mean tracer gas concentration of contaminant of the chamber (ppm) |
| $\bar{c}_e$ | Average tracer gas concentration of the exhaust air (ppm) |
| $\bar{c}_P$ | Average tracer gas concentration in a determined point (ppm) |
| $\bar{c}_{P,\ 125\%}$ | Average peaks tracer gas concentration in a determined point (ppm) |
| $c_{P,\ max}$ | Maximum tracer gas concentration in a determined pint (ppm) |
| $\bar{c}_{CP,exh}$ | Average contaminant concentration emitted through the CP exhalation (ppm) |
| $\bar{c}_s$ | Average tracer gas concentration in the supply air (ppm) |
| $\epsilon^c_P$ | Local relative exposure coefficient |
| $\epsilon^c_{P,125\%}$ | Local relative average peaks concentration exposure coefficient |
| $\epsilon^c_{P,max}$ | Local relative maximum exposure coefficient |
| $f_{P,\ 125\%}$ | Local maximum exposure frequency ($h^{-1}$) |
| H | Total height of the chamber (m) |
| $HR_i$ | Average relative humidity in a determined point (%) |
| HW | Health worker |
| IAQ | Indoor air quality |
| $IF$ | Intake fraction |
| Inh | Point located inside the inhalation airway of HW manikin |
| MV | Mixing ventilation |
| P3 | Pole located far from thermal loads |
| PHW | Pole located near health worker location |
| PCP | Pole located near patient location |
| PMV | Predicted mean vote |
| PPD | Predicted percentage of dissatisfied (%) |
| ppm | Particles per million |
| $Q_{b,\ exh}$ | Exhaled volume of CP (l/min) |
| $Q_{b,\ inh}$ | Inhaled volume rate of HW (l/min) |
| $T_i$ | Average ambient temperature in a determined point (°C) |
| $T_{globe}$ | Globe temperature (°C) |
| U | Exhaust grilles placed in the upper part of the West wall |
| Z | Height along the Z axis of the chamber (m) |
| $V_i$ | Average absolute air velocity in a determined point (m/s) |
| $\Delta T_{prN\ S}$ | Radiant temperature asymmetry due to the South radiant wall (°C) |
| $\Delta T_{h\text{-}f}$ | Temperature difference between head level (1.1 m or 1.7 m height) and feet level (0.1 m height) (°C) |
| $\varepsilon^a$ | Air change efficiency index |
| $\varepsilon^a_P$ | Local air change index for a determined point |
| $\varepsilon^C$ | Contaminant removal effectiveness index |
| $\langle \tau \rangle$ | Mean age of air in the room (min) |
| $\tau_n$ | Nominal time constant (min) |
| $\tau_P$ | Local mean age of air in a determined point (min) |

tion rather than on maintaining high renewal rates as being the most important factor in reducing cross infection risk [15,23,24]. Thus, if this requirement is met, strategies to reduce energy usage in ventilation systems by lowering airflow rates can be achieved [25]. These strategies should not compromise the thermal comfort of the occupants [26,27].

Recent studies have tested innovative ventilation strategies such displacement ventilation (DV) [28,29] and personalized ventilation [30–32] in health environments. Furthermore, more efficient ventilation methods based on source control that reduce substantially the risk of exposure have been suggested [17]. Nevertheless, nowadays, mixing ventilation (MV) is the most used indoor ventilation strategy in such spaces, especially in IHR [19,33].

The configuration of the ventilation of an indoor space system has a direct influence on ventilation effectiveness [34]. The ventilation efficiency in an AIIR like room has been registered for mixing ventilation and 12 and 24 ACH through the local air quality index [35]. This value has been also obtained numerically for different ventilation rates switching between linear and radial supply diffusers for a hospital room set-up. Another numerical study analyzed ventilation efficiency values for a number of combinations of wall and ceiling supply and exhaust cases in hospital rooms [36]. These studies highlight the influence of the relative position of the supply diffusers and exhausts on the flow dynamics and hence on the ventilation performance inside the room. An experimental research has been also carried out using a hospital room setup but using DV for a range of ventilation rates from 6 to 12 ACH [37], showing the potential of this ventilation strategy for these spaces if it is well designed, highlighting the high importance of the heat loads in air distribution for this case. Different studies have obtained different occupants exposure to the exhaled contaminants of patients in hospital rooms. The role of the ventilation rate in the exposure index of a health worker has been studied numerically for a ceiling supply mixing configuration [23]. An experimental research have been performed to evaluate the exposure the other patient in two bed hospital rooms using tracer gases for MV and DV [28]. The problem has been also studied numerically for downward ventilation [38] and for ceiling mixing ventilation [39]. The exposure in the positions where a health worker could locate inside an isolation room have been also obtained for high ventilation rates [35], finding a dependence with the negative pressure differential level in AIIRs. All these studies agree in the influence of ventilation strategy and ventilation flow dynamics on patient exhaled contaminants distribution. That distribution has a determinant effect on

the exposure of the rest of the occupants of the room. However, none of these researches studies the influence of different ventilation strategies and air ventilation rates on the exposure of exhaled contaminants in a hospital room.

This paper presents an experimental analysis of the use of different mixing ventilation configurations in a representative case of study of an IHR setup. Two different supply air configurations, through grilles (G) situated at a lateral wall or through two swirl diffusers (S) placed at the ceiling. Two ways to remove the exhaust air of the room have been also tested, by using two grilles placed in the upper part of a lateral wall (U) or by using two grilles placed in the lower part of the same wall (D). The combination of these tests make four different mixing ventilation system configurations. Three different air ventilation rates have been used for each ventilation configuration. The air changes per hour (ACH) is switched from 6 ACH, recommended for recuperation rooms to 9 ACH and to 12 ACH indicated for AIIRs. The experimental setup reproduce a realistic IHR where two thermal manikins representing a lying confined patient (CP) and a health worker standing close to it (HW).

## 2. Methods

Two different indicators are gathered to determine the convenience of each ventilation configuration. (1) Ventilation efficiency indices and (2) HW exposure to CP exhaled contaminants and aerosols. Specific experiments are carried out to determine these indicators for each ventilation configuration and air ventilation rate. Ventilation efficiency indices are obtained to determine the ventilation performance of each case for the IHR set-up implemented following standard methods [40]. Specifically air change efficiency ($\varepsilon^a$) and the local air change index ($\varepsilon_P^a$) together with the contaminant removal effectiveness ($\varepsilon^c$) are obtained. HW exposure to the contaminants exhaled by CP is determined by seeding CP exhalation flow with R134A as tracer gas to surrogate them. Tracer gas exposition is registered in several points inside the experimental chamber and around HW inhalation area. This way, the average and peak HW exposure is evaluated though different exposure to contaminants ($e_P^c$) and intake fraction ($IF$) indices. To assess the transient nature of HW contaminants exposure, the average of the concentration peaks and the maximum peak concentration registered are also considered to obtain derived exposure indices, ($e_{P,max}^c$ and $e_{P,125\%}^c$) and ($IF_{ma}$ and $IF_{125\%}$) respectively.

### 2.1. Test room and experimental set-up

This study is carried out in an experimental chamber with a typical IHR configuration setup [37] within the HVAC (heating, ventilation and air-conditioning systems) laboratory at the University of Cordoba. The experimental setup can be seen at Fig. 1.

The nine points that register tracer gas concentration around the inhalation point of HW are distributed in three columns (1, 2 and 3) and three rows (H, M and L) in the same vertical plane. Rows and columns are spaced at 300 mm between each other, being the point M2 placed just in front of the mouth, center of HW, with a 4 cm gap between them, being it the inhalation point. Contaminant exposure in these points help to infer the distribution of contaminants around the breathing zone of HW and hence the routes followed by the contaminants from the exhalation of CP to HW inhalation.

### 2.2. Ventilation configurations

Clean air is supplied through two swirl diffusers, S, (VDW 400 × 16, Trox, Germany) or through two wall grilles, G (AEH 1008 × 158, Trox, Germany), depending on the test carried out. Likewise, the exhaust is realized through two grilles placed in the upper part of the West wall, U, or through two grilles placed in the lower part of the same wall, D. U and D grilles are the same model than G ones. Fig. 2 shows the diagrams of the four ventilation system configurations tested in this study.

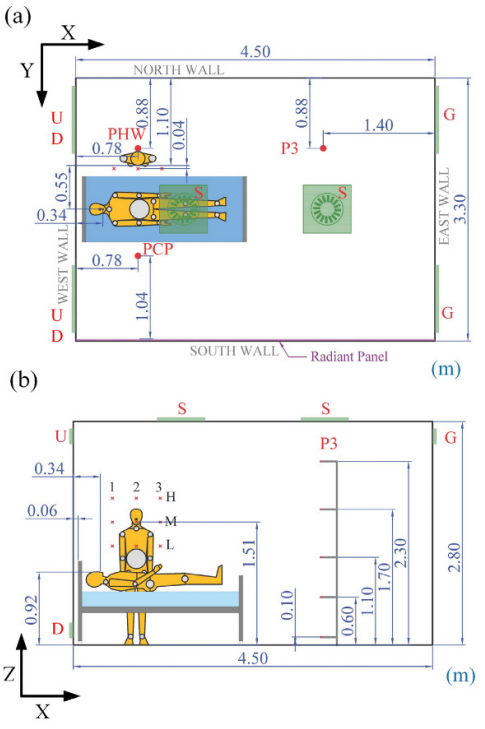


**Fig. 1.** (a) Plan view of the test room; (b) Profile view of the test room. Ceiling swirl air diffuser (S). Wall grille air diffuser (G). Upper exhaust grilles (U). Lower exhaust grilles (D). Vertical Poles (PCP, PHW and P3). Columns of the point matrix of tracer gas measurements (1, 2 and 3). Rows of the point matrix of tracer gas measurements (H, M, L).

The ventilation system has been set at three different air change rates, *ACH*, 6, 9 and 12 $h^{-1}$ supplying air at a supply temperature, $T_s$, of 18.2 °C, 20.6 °C and 21.8 °C respectively in order to maintain a mean temperature in the exhaust, $T_e$, of 25 ± 1 °C. This is done to reproduce comparable and realistic IHR conditions for the tests [41]. A summary of the conditions of the three tests performed can be seen at Table 1.

Part of the effective area of the supply diffusers is covered when 6 and 9 ACH ventilation tests are performed, Fig. 3. This is necessary in order to maintain the same supply velocity and thus the same air throw in the room for all the experimental tests.

### 2.3. Thermal loads and breathing thermal manikins

Inside the experimental chamber there are two thermal manikins representing a patient, CP, and a health worker, HW. Both manikins have the same geometry, and have been used previously in other research studies [6,37,42]. The body of the manikins is

**Table 1**
Experimental conditions of the tests performed.

| Renewal rate (ACH) | Supply air flow rate ($m^3/h$) | Supply air temperature (°C) |
|---|---|---|
| 6 | 250 | 18.2 |
| 9 | 375 | 20.6 |
| 12 | 500 | 21.8 |

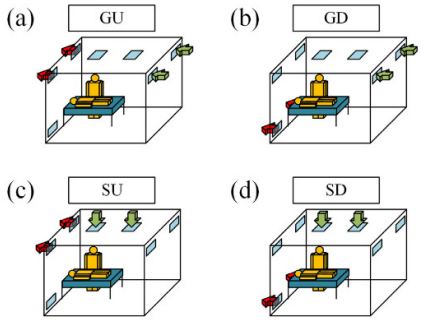


**Fig. 2.** Ventilation system configurations tested in this study: (a) Wall grille supply combined with upper wall exhausts (GU); (b) Wall grille supply combined with lower wall exhausts (GD); (c) Ceiling swirl supply combined with upper wall exhausts (SU); (d) Ceiling swirl supply combined with lower wall exhausts.

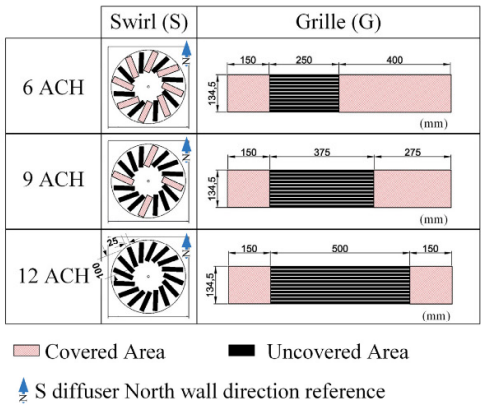


**Fig. 3.** Supply diffuser covered area for each test performed.

heated to achieve a homogeneous surface temperature of 34 °C which lead to the thermal gains summarized in Table 2.

The South wall is covered by an hydronic wall radiant system to simulate an external wall heat gain of 500 W [37]. The rest of the walls of the chamber are considered adiabatic because the temperature out of the chamber is maintained at the inward set point temperature. A summary of the thermal gains inside the experimental chamber, thermal manikins and radiant wall, can be seen at Table 2.

Each thermal manikin has its own independent breathing system with the capability of performing different breathing flows. The breathing functions characteristics of both thermal manikins are shown in Table 3.

**Table 2**
Thermal gains in the experimental chamber.

| Source | | Load (W) | |
|---|---|---|---|
| Radiant Panel | | 500 | |
| HW Manikin | Head | 5.6 | 85 |
| | Arms | 14.4 | |
| | Torso | 19.2 | |
| | Legs | 40.8 | |
| | Breathing | 5 | |
| CP Manikin | Head | 4.9 | 75 |
| | Arms | 12.6 | |
| | Torso | 16.8 | |
| | Legs | 35.7 | |
| | Breathing | 5 | |
| Total | | | 660 W |

**Table 3**
Breathing function of both thermal manikins.

| Respiration frequency ($min^{-1}$) | | Minute volume (l/min) | Tidal volume (l) |
|---|---|---|---|
| In | Out | | |
| 17.90 | 16.43 | 9.46 | 0.55 |

**Table 4**
Probes position along the height of each pole.

| Height (m) | P3 Pole | PHW Pole | PCP Pole |
|---|---|---|---|
| 2.3 | $T_i$ | $T_i$, $V_i$ | $T_i$, $V_i$ |
| 1.7 | $T_i$ | $T_i$, $V_i$, $HR_i$ | $T_i$, $V_i$, $HR_i$ |
| 1.1 | $T_i$ | $T_i$, $V_i$ | $T_i$, $V_i$ |
| 0.6 | $T_i$ | $T_i$, $V_i$ | $T_i$, $V_i$ |
| 0.1 | $T_i$ | $T_i$, $V_i$ | $T_i$, $V_i$ |

CP exhales fresh air taken from the exterior of the experimental chamber conveniently seeded with tracer gas. In the same way HW inhales through the nose and, after analyze the tracer gas concentration of the inhaled air, it is expelled far from the experimental chamber. This way, CP manikin exhalation is the only source of contaminants present inside the experimental chamber during contaminant exposure experiments. In the same way HW can be considered the target where the contaminant exposure is evaluated.

### 2.4. Measuring instruments

Temperature, humidity and air velocity measurements are registered at different heights along three different poles (PHW, PCP and P3). Table 4 summarizes the height of the different measurement points, while its position on the chamber plane can be seen in Fig. 1.

Ambient temperature probes ($T_i$) consist of J-type thermocouples with an accuracy of 2% in the range 15 – 45 C. Absolute air velocity ($V_i$) is measured using hot-sphere anemometers (TSI Air Velocity Transducer 8475, TSI, Minnesota) with a 3% accuracy in the range of 0.02 to 2.5 m/s. Ambient relative humidity ($HR_i$) has been measured using air humidity sensors (HMT100, Vaisala, Finland) with a calibration accuracy of 1.7% on the full range 0–100%.

The temperature of the inner surfaces of the chamber is registered during the tests by means of 15 resistive temperature probes

(PT100, TC Direct, UK). Using the inner enclosure average temperatures, radiant temperature is calculated using the method B.4.2 of EN ISO 7726 standard [43]. These probes have been calibrated in the range form 20 to 40 °C to assure an accuracy of ±0.3°C.

Tracer gas equipment is used to study the exposure of manikin HW to the contaminants exhaled by CP manikin. R134a is selected as a tracer gas as it has been done in similar previous studies [37,44,45]. To dose the tracer gas emitted through CP exhalation and register tracer gas concentration around HW manikin close environment, a multipoint sampler and doser (Innova 1303, LumaSense Technologies, California) along with a photoacoustic gas monitor (Innova 1412, LumaSense Technologies, California) are used.

Smoke has been introduced in the room completely mixed with the supply ventilation air through the diffusers in order to analyze airfow distribution inside the chamber in each case. A commercial specific fluid (Normal Power Mix, Safex, Germany) is used on the smoke generator machine (F2010Plus, Safex, Germany). Videos have been recorded using a digital video camera (DSC–H50, SONY, Japan). All the edited videos have been added as Supplementary Information.

### 2.5. Thermal comfort indices

The procedures detailed in ISO EN 7730 [46] are used to determine different thermal comfort indices for the position of PCP and PHW poles. A standing person performing a light activity, standing (1.4 met), is considered in PHW pole position while for the PCP pole a sitting one is considered, seated quiet (1 met). According to the usual light clothing conditions in hospitals, a clothing level index of 0.57 clo, trousers and short sleeved T-shirt, is assumed [47].

In order to determine general thermal comfort operative temperature ($T_o$) and the predicted mean vote (PMV) - predicted percentage of dissatisfied (PPD) values are obtained. Local thermal discomfort is also considered by means of the gathering of different indices. The radiant temperature asymmetry between the South and North the walls ($\Delta T_{pr,N-S}$), where a radiant panel simulates an external thermal gain . The draft discomfort is evaluated through the draught local discomfort (*DR*). Finally, the temperature difference between the head and feet ($\Delta T_{hf}$) is gathered to assess the discomfort due to the temperature gradient along the height of the chamber.

### 2.6. Ventilation performance indices

In order to determine the effectiveness of the ventilation, two ventilation efficiency indices have been used, air change efficiency ($\varepsilon^a$) and the local air change index ($\varepsilon_P^a$). The first index evaluates the ventilation efficiency globally while and the second determines its performance in a determined point. The expressions used to define these indices are:

$$\varepsilon^a = \frac{\tau_n}{2 \cdot \langle \tau \rangle} \cdot 100 \tag{1}$$

$$\varepsilon_P^a = \frac{\tau_n}{\tau_P} \cdot 100 \tag{2}$$

Being, $\tau_n$ the nominal time constant, $\tau_P$ the local mean age of air and $\langle \tau \rangle$ is the chamber mean age of air. The step down method [40] is used to determine the times involved in the indices, being 40 ppm the initial concentration chosen. Tracer gas concentration is registered over time in the exhaust to obtain $\varepsilon^a$ and in three different points around HW inhalation surroundings (M1, M2, and M3) to obtain $\varepsilon_P^a$.

The contaminant removal effectiveness index ($\varepsilon^c$) is obtained for the whole chamber with the purpose of determining global contaminant removal performance of the contaminants emitted through CP exhalation. Contaminants are surrogated by R134A as a tracer gas witch is seeded completely mixed with CP exhalation flow at a concentration of 7382 ppm. Contaminant removal effectiveness index has been previously obtained in recent studies [36,44,45,48]. Its value is obtained as follows:

$$\varepsilon^c = \frac{\bar{c}_e - \bar{c}_s}{\langle \bar{c} \rangle - \bar{c}_s} \tag{3}$$

where $\langle \bar{c} \rangle$ represents the mean concentration of contaminant of the chamber and $\bar{c}_e$ and $\bar{c}_s$ represents the mean contaminant concentrations in the exhaust and in the supply respectively. The value of $\langle \bar{c} \rangle$ is obtained immediately after the stationary experiment finishes by shutting down the ventilation system and mixing the air inside the chamber using an auxiliary fan [40].

### 2.7. HW tracer gas exposure

In order to determine the exposure of HW to the contaminants emitted by CP, its exhalation is seeded with tracer gas as it was previously detailed in $\varepsilon^c$ evaluation method. Tracer gas concentration is registered in 9 points around HW inhalation surroundings distributed in three columns (1, 2 and 3) and 3 rows (H, M and L) as can be seen in Fig. 1. Additionally, the concentration is also recorded inside the inhalation of HW airway. Each test is performed stationary during 6 h after steady state conditions are obtained inside the chamber. In order to be sure that the experimental exposure time is enough to obtain representative values of the tracer gas exposure, a detailed analysis have been carried out. The results are shown in a Supplementary Information section.

The concentration measurement along the time in each point (*P*) is used to calculate the concentration mean value, ($\bar{c}_P$), and the concentration maximum value, ($c_{P,\,max}$). Since it has been observed that concentration peaks arise in different points in a transitory way, the average peaks concentration ($\bar{c}_{P,125\%}$) and its frequency ($f_{P,\,125\%}$) are defined to describe this circumstance. A peak is considered when its value exceed the 125% of the average value of the concentration.

Two derived exposure indices, exposure to contaminants ($e_P^c$) and intake fraction (*IF*) are obtained to evaluate the exposition of HW to the contaminants released by CP.

The exposure to contaminants ($e_P^c$) relates the local contaminant concentration with the difference between average one obtained in the exhaust ($\bar{c}_e^c$) and in the supply ($\bar{c}_s^c$). Contaminant concentration in the supply is always is always null because the tracer gas used can't been found naturally in the atmosphere. This index is obtained for each contaminant index $\bar{c}_P$, $\bar{c}_{P,125\%}$ and $c_{P,\,max}$, to obtain $e_P^c$, $e_{P,125\%}^c$ and $e_{P,\,max}^c$ as follows:

$$e_P^c = \frac{\bar{c}_P - \bar{c}_s}{\bar{c}_e - \bar{c}_s};\; e_{P,125\%}^c = \frac{\bar{c}_{P,125\%} - \bar{c}_s}{\bar{c}_e - \bar{c}_s};\; e_{P,max}^c = \frac{\bar{c}_{P,max} - \bar{c}_s}{\bar{c}_e - \bar{c}_s} \tag{4}$$

Additionally, intake fraction (*IF*), which is the ratio of the mass of a pollutant inhaled to the mass of the pollutant emitted seeded in CP exhalation at a certain concentration ($\bar{c}_{CP,exh}$), is evaluated for the measuring point placed inside the inhalation airway of HW (*Inh*). This index is obtained for each contaminant value $\bar{c}_P$, $c_{125\%}$ and $\bar{c}_{P,maxk}$, to obtain *IF*, $IF_{125\%}$ and $IF_{max}$:(*Inh*). The equations used are the following:

$$IF = \frac{\int Q_{b,inh} \cdot c_{inh}\, dt}{\int Q_{b,exh} \cdot c_{CP,exh}\, dt};\; IF_{125\%} = \frac{\int Q_{b,inh} \cdot c_{inh,125\%}\, dt}{\int Q_{b,exh} \cdot c_{CP,exh}\, dt};$$
$$IF_{\max} = \frac{\int Q_{b,inh} \cdot c_{inh,\max}\, dt}{\int Q_{b,exh} \cdot c_{CP,exh}\, dt} \tag{5}$$

where $Q_{b,\,inh}$ and $Q_{b,\,exh}$ are the inhaled and exhaled breathing flows of the manikins respectively. Since both manikins perform the same breathing function, the intake fraction expression can

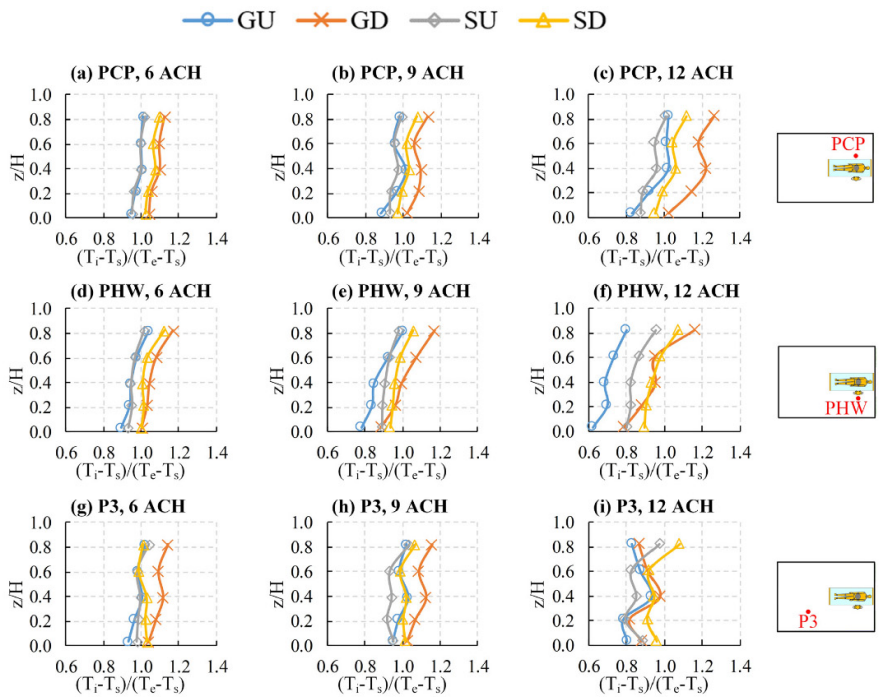


**Fig. 4.** Non dimensional profiles of temperature along the three vertical poles of the room, PCP, PHW and P3 for different ventilation system configurations, GU, GD, SU and SD, and different air change rates, 6 9, and 12 ACH.

be simplified to the quotient between the average tracer gas concentration value in the inhalation airway of HW ($\bar{c}_{inh}$) and the tracer gas concentration emitted through CP exhalation ($\bar{c}_{CP,exh}$). The value of $\bar{c}_{CP,exh}$ is obtained averaging the tracer gas concentration measurements registered inside the exhalation airways of CP during a 6 h experiment. The values of $IF_{125\%}$ and $IF_{max}$ are calculated replacing $\bar{c}_{inh}$ by $\bar{c}_{inh,125\%}$ and $\bar{c}_{inh,max}$ respectively.

## 3. Results and discussion

### 3.1. Experimental conditions

The vertical temperature gradients measured for the four experiments at the three poles of the room: PCP, PHW and P3 are shown in Fig. 4.

Results show a similar temperature distribution along the three temperature poles for each experiment. Dimensionless temperature profiles show, in general, a slight positive gradient with height in all cases, that is higher when the extraction of the air is made by the lower exhaust grilles (D). This may be due to a difficult of the warm air to find the exhaust in an area affected by the thermal convection of the manikins. According to the results, the use of the upper exhaust grilles (U) lead to lower relative temperature values. The differences between the obtained profiles are more evident when the ventilation rate is increased especially for PCP and PHW profiles. These differences could be a consequence of different airflow distributions patterns generated by each ventilation system.

Global and local comfort indices are evaluated for two positions inside the chamber, PHW and PCP, see Fig. 1. Results have been summarized in Table 5.

Results show that $T_o$ decreases slightly when air ventilation rate increases. That means that the increase of the air ventilation rate has an impact on the $T_o$ at the poles positions. This effect is more evident when G supply is used, being both PCP and PHW pole positions exposed to this effect. This is due to the increase of the air velocity in the occupied zone when the air ventilation rate is increased as the increment of the DR index for G tests indicates. It does not happen in S tests presumably because of the different flow distribution originated by this diffuser. Anyway, the values obtained are situated in the comfort zone for summer clothing and sedentary activity for low relative humidity situations [46,49].

General thermal comfort indices summarized in Table 5 have been plotted in Fig. 5 for better understanding, where thermal comfort categories are defined according to the standard EN ISO 7730 [46].

According to the results, thermal comfort indices PMV for PCP and PHW positions differs in all the cases. PMV indices for PCP position reflects a slightly cold sensation, in most cases between the categories A and B. Nevertheless, for PHW position, this index reflects a warm sensation, which even overpass C category in some cases as it can be seen at Fig. 5(c). This is directly related with the different activity levels considered in each pole. Results suggest that the increase in ventilation rate lead to colder sensations in all cases.

**Table 5**
General and local thermal comfort indices for health worker (PHW) and patient (PCP) under different ventilation configuration and different air changes per hour, ACH.

| | | PHW | | | | | | PCP | | | | | |
|---|---|---|---|---|---|---|---|---|---|---|---|---|---|
| | | *To* °C | *PMV* – | *PPD* % | $\Delta T_{prN\text{-}S}$ K | $\Delta T_{h\,f}$ K | *DR* % | *To* °C | *PMV* – | *PPD* % | $\Delta T_{prN\text{-}S}$ K | $\Delta T_{h\,f}$ K | *DR* % |
| **GU** | **6** | 25.7 | 0.71 | 15.6 | 0.8 | 0.5 | 2.6 | 26.0 | −0.18 | 5.7 | 2.3 | 0.4 | 1.1 |
| | **9** | 25.4 | 0.56 | 11.6 | 0.6 | 0.6 | 7.3 | 25.8 | −0.27 | 6.5 | 2.2 | 0.6 | 3.4 |
| | **12** | 24.6 | 0.28 | 6.6 | 0.7 | 0.3 | 13.9 | 25.5 | −0.52 | 10.6 | 2.4 | 0.6 | 7.5 |
| **GD** | **6** | 26.1 | 0.72 | 16 | 0.7 | 0.5 | 7.0 | 26.3 | −0.07 | 5.1 | 2.1 | 0.4 | 2.0 |
| | **9** | 25.6 | 0.63 | 13.3 | 0.5 | 0.7 | 6.1 | 25.8 | −0.31 | 6.9 | 2.2 | 0.3 | 5.5 |
| | **12** | 25.2 | 0.39 | 8.1 | 0.7 | 0.4 | 15.5 | 25.9 | −0.2 | 5.8 | 2.1 | 0.5 | 5.5 |
| **SU** | **6** | 25.7 | 0.71 | 15.7 | 0.3 | 0.3 | 0.0 | 26.0 | −0.2 | 5.8 | 1.9 | 0.3 | 3.5 |
| | **9** | 25.6 | 0.69 | 15 | 0.4 | 0.2 | 4.6 | 25.9 | −0.27 | 6.5 | 1.9 | 0.2 | 5.6 |
| | **12** | 25.4 | 0.6 | 12.6 | 0.4 | 0.3 | 6.1 | 25.8 | −0.32 | 7.1 | 2.0 | 0.3 | 5.8 |
| **SD** | **6** | 25.7 | 0.7 | 15.4 | 0.4 | 0.3 | 0.0 | 26.0 | −0.19 | 5.7 | 2.0 | 0.3 | 0.0 |
| | **9** | 25.8 | 0.72 | 16 | 0.3 | 0.3 | 2.2 | 26.0 | −0.22 | 6 | 1.9 | 0.3 | 6.4 |
| | **12** | 25.7 | 0.7 | 15.5 | 0.4 | 0.3 | 2.3 | 26.0 | −0.32 | 7.1 | 1.9 | 0.3 | 7.5 |

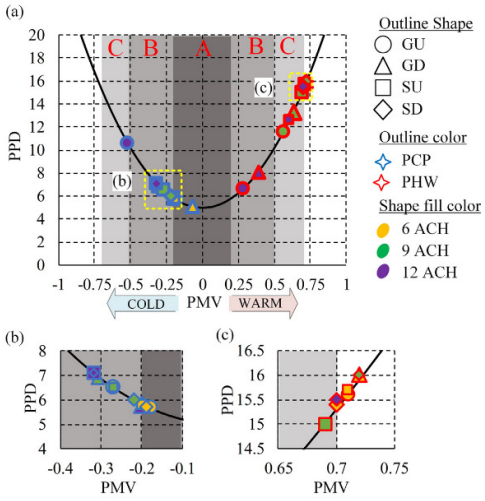


**Fig. 5.** Predicted percentage of dissatisfied (PPD) as a function of predicted mean vote (PMV) for different ventilation configurations and different air changes per hour; (a) Full range of results; (b) Detail view of some of PCP results; (c) Detail view of some PHW results.

To assess completely comfort in the room, different local discomfort indices have been obtained and presented in Table 5. Radiant temperature asymmetry due to South radiant wall, $\Delta T_{prN\text{-}S}$, is higher in PCP position due to its proximity to the South wall. The increase of the ventilation rate does not lead to different values of $\Delta T_{prN\text{-}S}$. It can be also noted that the use of the S supply reduces $\Delta T_{prN\text{-}S}$ and $\Delta T_{h\text{-}f}$ indices. It can be due to the effect of the S diffuser on the radiant wall. The value of *DR* increases with the air ventilation rate. It is because the increase of the average air velocity generated by the increase of the air ventilation rate. The effect is more evident for G supply ventilation configurations and PHW position. The different ventilation airflow rate could modify the air distribution patterns inside the room making the air reach directly the standing person head height at PHW position, increasing local discomfort in this case.

### 3.2. Ventilation performance

The values of $\tau_n$, $\langle\bar{\tau}\rangle$ and $\varepsilon^a$ have been obtained for each ventilation configuration. Results are shown in Fig. 6.

According to the results obtained, the value of $\varepsilon^a$ is around 50% in all cases. If this value is reached, a perfect mixing situation is found [40]. The values of $\tau_n$ and $\langle\bar{\tau}\rangle$ times tend to decrease when the ventilation rate increases. This decreasing tendency is different for each ventilation configuration. The value of $\langle\bar{\tau}\rangle$ is higher than $\tau_n$ in all cases except for G supply when 12 ACH is tested, being this the only case where $\varepsilon^a$ exceeds 50%. That means that the contaminants are evacuated quickly through the exhaust remaining short time inside the room. However, it is found that $\varepsilon^a$ barely reach 45% when G supply is used in 9 ACH tests. That means that the contaminants take more time to leave the room, this way contaminants have the possibility of being stacked inside.

When S supply is chosen, the value of $\varepsilon^a$ remains close but under 50% for all the air changes used. It can be noted that the increase of air ventilation rate improve $\varepsilon^a$ value in SD cases but not in SU ones. Even so, in both configurations, the differences of $\varepsilon^a$ for the different ACH tested are lower than in G supply cases.

The results of $\varepsilon_p^a$ values are obtained in three points in the near surrounding of HW inhalation area, M1, M2 and M3 and are shown in Fig. 7.

The values of $\varepsilon_p^a$ remains close to 100% for all the tests performed. It means that the air is well mixed in the local area around HW inhalation area as in the whole room. Differences in $\varepsilon_p^a$ between the configurations tested are found especially at higher ventilation rates. When G supply is used the value of $\varepsilon_p^a$ tends to decrease for 9 ACH, especially for GD test in M2, to afterward increase to about 120% for 12 ACH one. That means that contaminants remain more time in the surroundings of HW when 9 ACH are performed than in the cases of 6 and 12 ACH. These fluctuations in $\varepsilon_p^a$ values can be due to changes in air distribution patterns inside the room when the ACH value is modified.

In S supply cases, a higher dispersion of results is found under 12 ACH ventilation rate, in contrast with the data homogeneity of the 6 and 9 ACH tests. When the ventilation rate is high, a stronger swirl downward flow from the diffusers could be breaking the arising convective flow from CP manikin body. This way, the horizontal spreading of contaminants is promoted, leading to different contaminants concentration in the three points considered.

In both G and S supply configurations, no improvement is found in $\varepsilon_p^a$ when the ventilation rate is increased from 6 to 9 ACH. When the ventilation rate is increased to 12 ACH the value of $\varepsilon_p^a$ increases under G supply configuration while in S cases its value becomes dependent on the position.

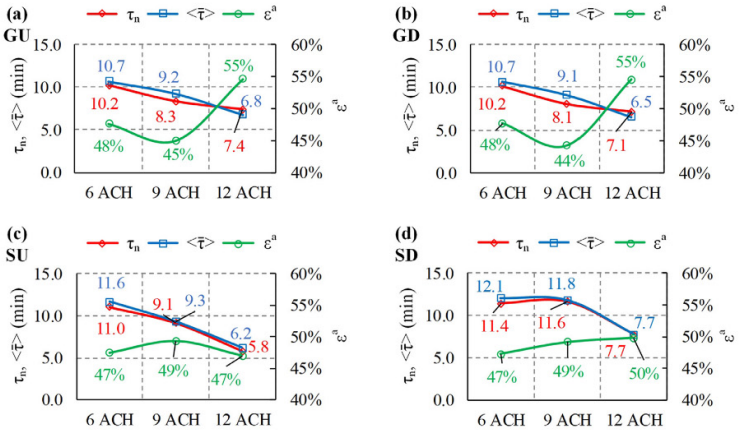


**Fig. 6.** Air change efficiency ($\varepsilon^a$), nominal time constant ($\tau_n$) and room mean age of air $\bar{\tau}$ for the four ventilation configurations considered at different air change rates. (a) GU; (b) GD; (c) SU; (d) SD.

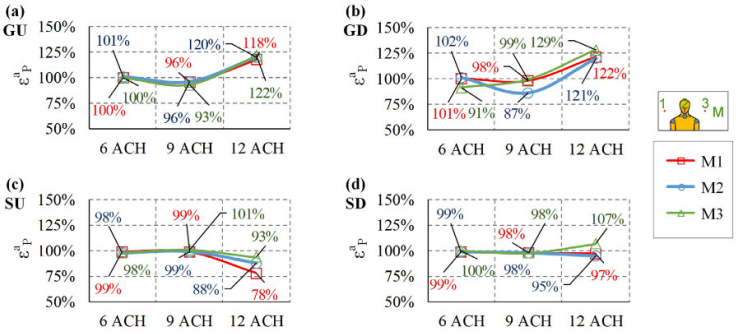


**Fig. 7.** Local air change index ($\varepsilon^a_p$) for three points around HW inhalation point at different air change rates. (a) GU ventilation strategy; (b) GD ventilation strategy; (c) SU ventilation strategy; (d) SD ventilation strategy.

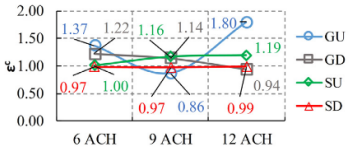


**Fig. 8.** Contaminant removal effectiveness ($\varepsilon^c$) index for the four ventilation configuration tested.

In order to analyze how contaminants are globally removed by each ventilation configuration, $\varepsilon^c$ index is obtained. To do this, the average contaminant concentration in the room ($\langle\bar{c}\rangle$) and in the exhaust ($\bar{c}_e$) have been registered for all the tests carried out. Results are shown in Fig. 8.

According to the results, the values of $\varepsilon^c$ remains around 1 for nearly all the tests. The values for GD and SU maintain values over the unit while SD values are slightly under the unit. This might be due to the difficult of the upward exhaled contaminants to reach the D exhaust placed in the lower part of the room. The case of GU is different to the rest, for 12 and 6 ACH it performs the highest values of $\varepsilon^c$. This is positive because it means that the contaminants path to the exhaust is relatively short and quick. However, for GU with 9 ACH the lowest value of $\varepsilon^c$ is obtained. It can be due to the short circuit generated between the G supply grilles and the exhausts grilles placed at the same height in the opposite wall. In that way, the airflow from the supply grilles is not able to reach the CP exhalation area and remove efficiently the contaminants exhaled.

### 3.3. HW tracer gas exposure

Tracer gas exposure is evaluated in 9 points around the inhalation of HW and in the inhalation of HW (*Inh*), as it can be seen in Fig. 1. Fig. 9 shows the values of $e^c_P$, $e^c_{P,125\%}$, and $e^c_{P,max}$ for these points.

According to the results, there is a notable difference between the results obtained for G supply tests and the ones obtained for S supply. In general terms, it can be noted that the exposure indices are higher in the cases where G supply is used. S supply tests

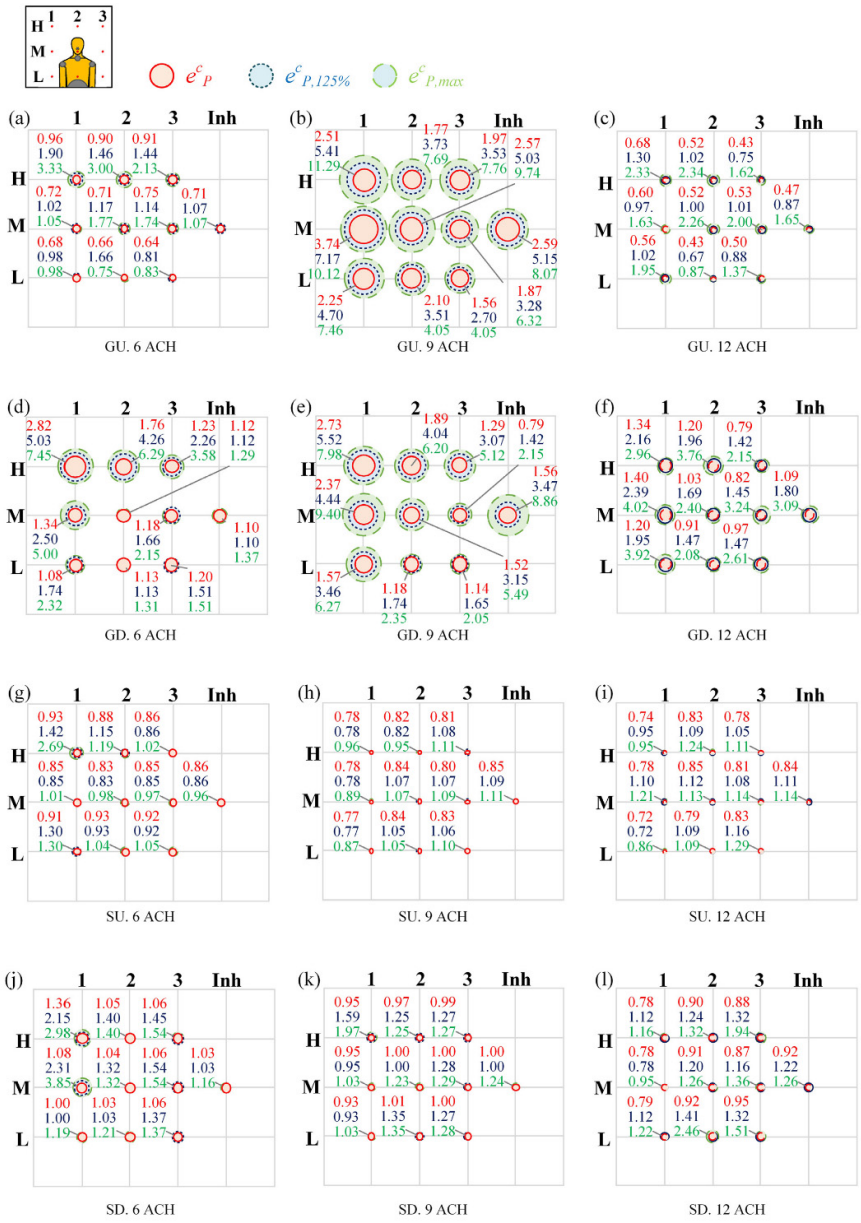


**Fig. 9.** Local relative contaminant exposure coefficient ($e^c_P$), local relative average peaks concentration exposure coefficient ($e^c_{P,125\%}$) and maximum peak exposition coefficient ($e^c_{P,max}$) for the tests carried out. (a) GU 6 ACH; (b) GU 9 ACH; (c) GU 12 ACH; (d) GD 6 ACH; (e) GD 9 ACH; (f) GD 12 ACH; (g) SU 6 ACH; (h) SU 9 ACH; (i) SU 12 ACH; (j) SD 6 ACH; (k) SD 9 ACH; (l) SD 12 ACH.


**Fig. 10.** Video frame captures showing throw development of the GU tests. (a) GU 6 ACH; (b) GU 9 ACH; (c) GU 12 ACH.

maintain homogeneous $e_P^c$ values in all the points, and in most of them the value is the same that $e_{P,125\%}^c$ and very close to 1. The values of $e_{P,max}^c$ show values not far from $e_P^c$ in all cases, revealing a high homogeneity over time for contaminant concentration. It can be noted that exposure indices show lower values for SU in comparison with SD.

In contrast, G supply exposure values behaves in a very different way, showing in some cases high discrepancies between exposure values depending on the position, the *ACH* and the height of the exhaust. GU 9 ACH stands out as the case where the exposition is higher in all the points around the HW and in its inhalation. The explanation might be found in the ventilation flow distribution inside the chamber. The clean air from the grille diffusers is not able to remove the exhaled contaminants from the occupied zone maybe due to a short circuit produced between the grilles and the exhausts for that case. Fig. 10(b) shows a capture from the smoke test video showing the ventilation flow development for this case, reinforcing this theory. The flow reaches the upper part of the West wall where part of it leaves directly the room, being short circuited. This situation produce a stagnation of the contaminants around HW inhalation area. The results are compatible with the results obtained for $\varepsilon^c$ that suggested that part of the contaminants are stacked into the room. However, for the same GU ventilation configuration under 6 and 12 ACH, low values of exposition in all the points are obtained. For 6 ACH case, the clean airflow from the grilles moves downward to the exhalation area improving the mixing process of the exhaled contaminants and reducing the exposure indexes, as it can be seen in Fig. 10(a). When using 12 ACH, the volume of clean air increases and generates a strong upward flow in the occupied area situated between the inlets and the outlets of the room, as a result of its reaching of the West wall, Fig. 10(c). This airflow pattern conduces the exhaled contaminants quickly to the exhausts generating a low risk of exposure to HW.

Some points with high contaminants exposure values can also be found for GD ventilation configuration. These points are found for 6 and 9 ACH cases. For GD 6 ACH case, high exposure points distribute at H positions, situated at the height of HW head. In this case the clean airflow coming from inlets could be displacing contaminants to the West wall going upward to the area of the HW head. However this fact maintains the breathing area of HW clean of contaminants. For the case of GD 9 ACH the clean airflow from the grilles interacts with the upward convective flow from the manikins making difficult for the exhaled contaminants to find the exhaust and creating a stagnant area. This fact produces a direct influence of the patient exhalation in the contaminant inhalation of HW. The average values of exposure ($e_P^c$) and the maximum values of exposure ($e_{P,max}^c$) show a significant difference. This situation changes when 12 ACH is set due to the increase of air volume that penetrates into the exhalation area in despite of the ascending thermal plumes leading the contaminants directly to the exhaust. Previous research on exposure to contaminants released by respi-

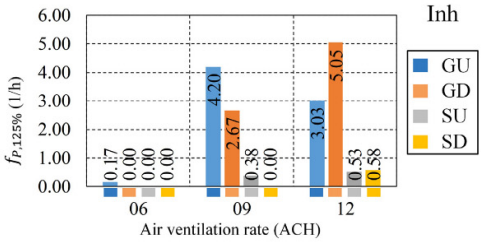


**Fig. 11.** Frequency of maximum exposure coefficients ($e_{P,\,max}$) inside the airways of HW.

ratory events reinforces the idea that an increase of ACH doesn't necessary leads to a better contaminants exposure indices due to the changes that it produces in airflow patterns inside the indoor space [50–52].

In general for G supply cases, the points where a high exposure value is obtained show a high discrepancy between $e_P^c$, $e_{P,125\%}^c$ and $e_{P,max}^c$. That reveals that the high contaminants exposure registered is not constant in time but it reveals a transient nature. High contaminant concentration exposure peaks $e_{P,125\%}^c$ arise without any evident periodicity. This situation could be related with the fact that contaminants are not released constantly but they are seeded into CP exhalation flows. That means that the peaks are not homogeneous, being possible high values of $e_{P,max}^c$ with low values of $e_P^c$. In the inhalation area for GD and 9 ACH the $e_{P,max}^c$ is more than 5 times the $e_P^c$.These two facts reinforce the idea that despite the conditions of the problem are stationary, the exposure to the contaminants reveals a transient nature.

The frequency of the peaks ($f_{P,\,125\%}$) registered inside the airways of HW (*Inh*) is shown in Fig. 11.

The swirl diffusers used for SU, SD cases avoid the tracer gas peak concentration in the inhalation due to an effective dilution of the contaminants emitted by CP. This way the direct influence of the exhalation on the breathing area of the HW is avoided, maintaining low $f_{P,\,125\%}$ values. For G supply, it exists a dependency between the air ventilation rate and the $f_{P,\,125\%}$ value. Very low values of $f_{P,\,125\%}$ are found when 6 ACH ventilation rate is performed showing a dilution process of the contaminants exhaled. On the contrary, $f_{P,\,125\%}$ increases for 9 and 12 ACH. This fact shows that the mixing process in the occupied area is not being complete and therefore there is an influence of *P* exhalation on the breathing area of HW. The high values of $f_{P,\,125\%}$ combined with the high values of $e_{P,125\%}^c$ indicates a high risk of exposure. However, for GU and GD under 12 ACH the high values of $f_{P,\,125\%}$ are not related with high values of exposure since the values of $e_{P,125\%}^c$ are low. That means that also there is an influence of CP exhalation on the

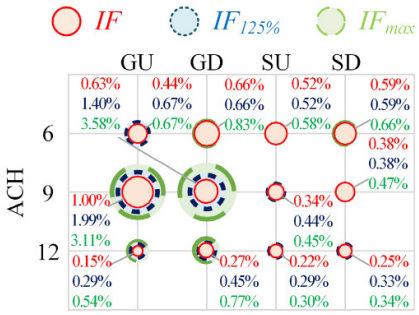


**Fig. 12.** Intake Fraction.

breathing area of HW when the occupied zone is maintained clean of contaminants.

The value of *IF* index is obtained to evaluate the amount of contaminants that are inhaled by HW respect to the amount exhaled by CP. Results are shown in Fig. 12.

Results show that the ventilation configurations tested present, in general, a similar decreasing *IF* tendency with the increasing of the air ventilation rate. The more volume of clean air entering the room, the less percentage of inhaled contaminants relative to the exhaled contaminants. The case of GU 9 ACH presents the only exception for this tendency due to a direct influence of the contaminants released by CP in the inhalation area of HW. The airflow pattern generated during this test maintains the exhaled contaminants released by CP in the breathing area of HW, making it difficult for the contaminants to evacuate the room through the exhausts. This phenomenon disappears when air ventilation rate is increased to 12 ACH, decreasing considerably the value of *IF*. When GD configuration is used, the values of *IF* are also high for 6 and 9 ACH. It has been observed for these tests that it is difficult for the exhaled contaminants to find the way to the exhaust. This fact may be due to the interaction between the upward flow of the manikiń s thermal plumes and the downward flow generated by this ventilation strategy. The values of *IF* and $IF_{125\%}$ show discrepancies which reveals that the high exposure is due to punctual peak concentrations episodes. The value of $IF_{max}$ is also quite higher than $IF_{125\%}$, so it can be stated that the peaks reach different values over the time. $IF_{max}$ can even reach values five times higher than *IF* ones such in the case of GU 9 ACH. The cases where S supply is used, *IF* values present a constant decreasing tendency, being in most cases the values of $IF_{P,\ 125\%}$ and $IF_{max}$ very close to *IF*. This shows that the dilution of the CP exhaled contaminant maintain a low and homogeneous tracer gas concentration in HW inhalation. It has been also noted that the *IF* values are somewhat lower for SU tests.

## 4. Discussion

This work examines the effectiveness of different mixing ventilation strategies in the removal of contaminants in an IHR analyzing different indexes.

The mixing ventilation study has been performed using the same experimental setup, thermal gains disposition and experimental equipment and methods than a previous study based on displacement ventilation (DV) [37]. Three different air changes per hour are performed for each ventilation strategy, which consider two different inlet diffusers: wall grilles (G) and swirl diffusers (S), and two different exhausts positions: in the lower part of the wall (D) and in the upper part of the wall (U). That leads to a total of 12 experimental cases studied. The results obtained are of significant relevance in order to understand which ventilation strategy will lead to a less risk of exposure to exhaled contaminants in a IHR. The risk of exposure is obtained for a health worker (HW) placed close to the patient (CP) which is considered the source of exhaled contaminants. Fig. 13 shows a comparison of the exposure indices for the different ventilation strategies, GD, GU, SD, SU and DV, in an IHR for *Inh* point placed inside the inhalation airway of HW.

Firstly, it is possible to see that the displacement ventilation strategy (DV) shows the best index value with very low exposure of HW for all the exposure indices analyzed. This result is in agreement with previous studies of displacement ventilation [28,53] where it is possible to find low values of the risk of infection with that strategy. In this particular case, the position of the source of contaminants (exhalation of the patient) in a lower position respect to the HW breathing area improve the results. The thermal stratification of the displacement ventilation system maintains the exhaled contaminants in a layer below the breathing area of the HW. Different relative position of the manikins may lead to completely different results.

Secondly, if we observe the results obtained for SD and SU, for the three ACH performed, both strategies show values typical of a complete mixing process, close to 1. The mixing process is complete and independent of the number of ACH. Nevertheless, a slight dependence of the exhaust positions is observed, SU performs slightly better than SD in contaminant removal and HW exposure indices. The values of $\varepsilon^c$ together with $e_P^c$ and *IF* exposure values suggest that part the tracer gas concentration inside the chamber remains higher in SD cases due the exhaust position.

Finally, high exposure values depending on the number of ACH and the position of the exhausts has been found in GD and GU cases. Considering GD and GU 9 ACH cases, the exhaled contaminants remain close to the breathing area of HW, increasing its exposure to contaminants. However, when 12 ACH in GD and GU cases, the increase of airflow decreases its exposure. This result points out that a specific study of a particular case, taking into account: position of the thermal loads, position of the inlets and exhausts, distance between the manikins, and relative positions between all these relevant parts of the room, may play the crucial role in understanding the risk of airborne exposure of people in a room.

### 4.1. Limitations of the work

It is important to bear in mind that the results obtained and discussed in this work are obtained under specific experimental conditions. The relative position of the source of contaminants, the different positions of the inlets and exhausts or different distances between the manikins may change the conclusions obtained. In the same way, the height at which the contaminants are exhaled plays a crucial role in the exposure to contaminants of the HW, especially for the DV system.

The experimental set up has not been carried out in a real hospital and the problem only treats tracer gas as a strategy to simulate small droplet nuclei, not real biological contaminants. The experimental results are not showing a complete real situation since the manikins are also steady. However, all the results analyzed could be helpful in the design of IHRs in order to create environments where the exposure to exhaled contaminants may be reduced in most of the situations.

The tracer gas measurement sample rate is lower than the periodic breathing process time. This situation implies that the possible fluctuations of tracer gas concentration in the considered locations, as the tracer gas concentration peaks occurence, are not

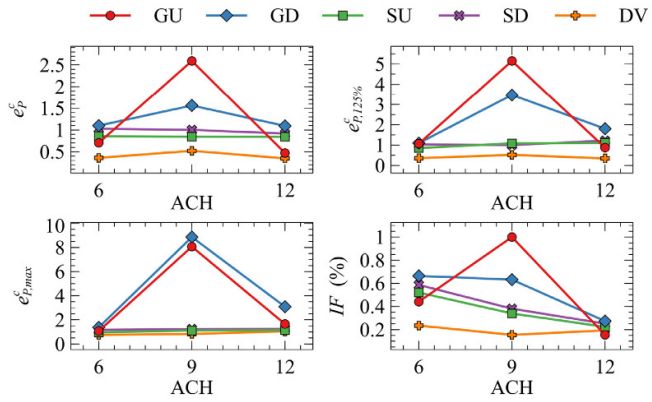


**Fig. 13.** Comparison between exposure indices at Inh point. (a) Local relative contaminant exposition index ($e_P^c$); (b) Average of peaks relative exposition index ($e_{P,125\%}^c$); (c) Maximum peak exposition index ($e_{max}^c$); (d) Intake fraction (*IF*).

completely registered. Experimental time periods are adjusted to assess this situation following the criterion included as Supplementary Information, however a higher frequency tracer gas concentration probes could enrich the gathered information about the recurrent perturbation registered in tracer gas concentration. The use of a equipment that allows performing a higher measurement frequency could lead to a better understanding of the peaks occurrence.

## 5. Conclusions

Experimental tests have been carried out to determine ventilation performance and contaminant exposure in a representative case of study of a typical individual hospital room configuration using two different mixing ventilation systems and three air ventilation rates and connected with previous DV studies. In view of the results of each test and the comparisons between them, the following conclusions can be stated:

- Airflow patterns generated by G and S ventilation configurations influence ventilation efficiency ($\varepsilon^a$, $\varepsilon_P^c$ and $\varepsilon_P^a$) and contaminant exposure ($e_P^c$ and *IF*) of HW. Swirl diffusers (S) generate a better mixing ventilation situation, leading to a better performance and exposure indices. So S supply could be considered as a more reliable strategy in hospital rooms. It has also been noted that HW exposure results are better if S supply is combined with D exhaust.
- Air renovation (ACH) has a very low influence in the HW exposure for S supply cases. However, the change of ACH for G supply cases determine completely different behavior of the dispersion of exhaled contaminants. For GU a short circuit between the inlet and the exhaust is generated for 9 ACH producing the highest exposure values in the inhalation of HW. For GD using 6 and 9 ACH the lack of a perfect mixing of the air in the room generates high peak values of exposure in the inhalation of HW.
- Being the human exhalation a transient process, the exposure to exhaled contaminants is also observed as a transient process. This fact leads to average ($e_P^c$) and peak ($e_{P,125\%}^c$ and $e_{P,max}^c$) different exposure values depending on the experimental case. Low average exposure ($e_P^c$) cases may present punctual high peak exposure ($e_{P,max}^c$) values. The peak frequency ($f_{P,\ 125\%}$), which is lower for S cases, can increase with the air ventilation rate.
- The exposure to contaminants of HW is lower when displacement ventilation strategy is used instead of mixing ventilation strategy. A similar exposure to contaminants is obtained in DV and MV systems when 12 ACH is used.

Considering all the results, it has been found that using a mixing ventilation strategy if a perfect mixing is not reached the ACH and the relative positions between supply and exhaust locations determine the HW exposure. The transient nature observed of the dispersion of the exhaled contaminants makes the authors think of the necessity of study the exposure using high frequency contaminant sensors. A deeper study considering different relative positions between the people occupying the room and the supply/exhaust positions will add knowledge about contaminants exposure in indoor environments.

## Acknowledgments

The authors acknowledge the financial support received from the Ministerio de Economia y Competitividad, Secretaría de Estado de Investigación, Desarrollo e Innovación, Spain, to the National R&D project TRACER with reference DPI2014-55357-C2-2-R, entitled "Ventilation system influence on airborne transmission of human exhaled bioaerosols. Cross infection risk evaluation". This project is cofinanced by the European Regional Development Fund (ERDF).

## Supplementary materials

Supplementary material associated with this article can be found, in the online version, at doi:10.1016/j.enbuild.2018.07.053.

## References

[1] C.B. Beggs, L.D. Knibbs, G.R. Johnson, L. Morawska, Environmental contamination and hospital-acquired infection: factors that are easily overlooked, Indoor Air 25 (2015) 462–474, doi:10.1111/ina.12170.
[2] M.P. Atkinson, L.M. Wein, Quantifying the routes of transmission for pandemic influenza, Bull. Math. Biol. 70 (2008) 820–867, doi:10.1007/s11538-007-9281-2.
[3] J.W. Tang, Investigating the airborne transmission pathway - different approaches with the same objectives, Indoor Air 25 (2015) 119–124, doi:10.1111/ina.12175.
[4] I. Eames, J.W. Tang, Y. Li, P. Wilson, Airborne transmission of disease in hospitals, J. R. Soc. Interface 6 (Suppl 6) (2009) S697–S702, doi:10.1098/rsif.2009.0407.focus.

[5] Centers for Disease Control and Prevention, Guidelines for preventing the transmission of Mycobacterium tuberculosis in health-care facilities, MMWR Morb. Mortal. Wkly. Rep. 43 (1994) 1–132, doi:10.2307/42000931.

[6] F.A. Berlanga, I. Olmedo, M. Ruiz de Adana, Experimental analysis of the air velocity and contaminant dispersion of human exhalation flows, Indoor Air (2016) 1–13, doi:10.1111/ina.12357.

[7] J.W. Tang, A. Nicolle, C. Klettner, J. Pantelic, L. Wang, A. Suhaimi, et al., Airflow dynamics of human jets: sneezing and breathing - potential sources of infectious aerosols, PLoS One 8 (2013) e59970, doi:10.1371/journal.pone.0059970.

[8] J.K. Gupta, C.H. Lin, Q. Chen, Flow dynamics and characterization of a cough, Indoor Air 19 (2009) 517–525, doi:10.1111/j.1600-0668.2009.00619.x.

[9] C.Y.H. Chao, M.P. Wan, L. Morawska, G.R. Johnson, Z.D. Ristovski, M. Hargreaves, et al., Characterization of expiration air jets and droplet size distributions immediately at the mouth opening, J. Aerosol Sci. 40 (2009) 122–133, doi:10.1016/j.jaerosci.2008.10.003.

[10] X. Xie, Y. Li, A.T.Y. Chwang, P.L. Ho, W.H. Seto, How far droplets can move in indoor environments - revisiting the Wells evaporation-falling curve, Indoor Air 17 (2007) 211–225, doi:10.1111/j.1600-0668.2007.00469.x.

[11] W.F. Wells, On air-borne infection. II. Droplets and droplet nuclei, Am. J. Hyg. 20 (1934) 611–618.

[12] A. Jurelionis, L. Gagytė, T. Prasauskas, D. Čiužas, E. Krugly, L. Šeduikytė, et al., The impact of the air distribution method in ventilated rooms on the aerosol particle dispersion and removal: The experimental approach, Energy Build. 86 (2015) 305–313, doi:10.1016/j.enbuild.2014.10.014.

[13] L. Liu, Y. Li, P.V. Nielsen, J. Wei, R.L. Jensen, Short-range airborne transmission of expiratory droplets between two people, Indoor Air (2016) 1–11, doi:10.1111/ina.12314.

[14] M. Bivolarova, W. Kierat, E. Zavrl, Z. Popiolek, A. Melikov, Effect of airflow interaction in the breathing zone on exposure to bio-effluents, Build. Environ. 125 (2017) 216–226, doi:10.1016/j.buildenv.2017.08.043.

[15] A. Jurelionis, L. Gagyte, L. Seduikyte, T. Prasauskas, D. Ciuzas, D. Martuzevičius, Combined air heating and ventilation increases risk of personal exposure to airborne pollutants released at the floor level, Energy Build. 116 (2016) 263–273, doi:10.1016/j.enbuild.2016.01.011.

[16] Y. Lv, H. Wang, S. Wei, The transmission characteristics of indoor particles under two ventilation modes, Energy Build. 163 (2018) 1–9, doi:10.1016/j.enbuild.2017.12.028.

[17] A.K. Melikov, Z.D. Bolashikov, E. Georgiev, Novel ventilation strategy for reducing the risk of airborne cross infection in hospital rooms, (2011) 1–6.

[18] N.J. Adams, D.L. Johnson, R. a. Lynch, The effect of pressure differential and care provider movement on airborne infectious isolation room containment effectiveness, Am. J. Infect. Control 39 (2011) 91–97, doi:10.1016/j.ajic.2010.05.025.

[19] J.D. Siegel, E. Rhinehart, M. Jackson, L. Chiarello, 2007 Guideline for isolation precautions: preventing transmission of infectious agents in health care settings, Am. J. Infect. Control 35 (2007), doi:10.1016/j.ajic.2007.10.007.

[20] E. Lingaas, J.P. Rydock, Best practice in design and testing of isolation rooms in Nordic hospitals, Round Table Ser. - R. Soc. Med. (2007) 87–107.

[21] Victorian Advisory Committee on Infection Control, Guidelines For the Classification and Design of Isolation Rooms in Health Care Facilities, 1st ed., Victorian Government, Melbourne, 2007.

[22] L. Sehulster, R.Y.W. Chinn, Guidelines for environmental infection control in health-care facilities, Morb. Mortal. Wkly. Rep. 52 (2003) 1–42.

[23] F. Memarzadeh, W. Xu, Role of air changes per hour (ACH) in possible transmission of airborne infections, Build. Simul. 5 (2012) 15–28, doi:10.1007/s12273-011-0053-4.

[24] P. Kalliomäki, P. Saarinen, J.W. Tang, H. Koskela, Airflow patterns through single hinged and sliding doors in hospital isolation rooms - Effect of ventilation, flow differential and passage, Build. Environ. 107 (2016) 154–168, doi:10.1016/j.buildenv.2016.07.009.

[25] P. Kumar, C. Martani, L. Morawska, L. Norford, R. Choudhary, M. Bell, et al., Indoor air quality and energy management through real-time sensing in commercial buildings, Energy Build. 111 (2016) 145–153, doi:10.1016/j.enbuild.2015.11.037.

[26] W. Yu, B. Li, H. Jia, M. Zhang, D. Wang, Application of multi-objective genetic algorithm to optimize energy efficiency and thermal comfort in building design, Energy Build. 88 (2015) 135–143, doi:10.1016/j.enbuild.2014.11.063.

[27] A. Kabanshi, H. Wigö, M. Sandberg, Experimental evaluation of an intermittent air supply system - Part 1: Thermal comfort and ventilation efficiency measurements, Build. Environ. 95 (2016) 240–250, doi:10.1016/j.buildenv.2015.09.025.

[28] H. Qian, Y. Li, P.V. Nielsen, C.E. Hyldgaard, T.W. Wong, aT.Y. Chwang, Dispersion of exhaled droplet nuclei in a two-bed hospital ward with three different ventilation systems, Indoor Air 16 (2006) 111–128, doi:10.1111/j.1600-0668.2005.00407.x.

[29] Y. Yin, W. Xu, J.K. Gupta, A. Guity, P. Marmion, A. Manning, et al., Experimental study on displacement and mixing ventilation systems for a patient ward, HVAC&R Res. 15 (2009) 1175–1191, doi:10.1080/10789669.2009.10390885.

[30] P.V. Nielsen, C.E. Hyldgaard, A.K. Melikov, H. Andersen, M. Soennichsen, Personal exposure between people in a room ventilated by textile terminals–with and without personalized ventilation, HVAC R Res. 13 (2007) 635–643, doi:10.1080/10789669.2007.10390976.

[31] J.W. Tang, C.J. Noakes, P.V. Nielsen, I. Eames, A. Nicolle, Y. Li, et al., Observing and quantifying airflows in the infection control of aerosol- and airborne-transmitted diseases: an overview of approaches, J. Hosp. Infect. 77 (2011) 213–222, doi:10.1016/j.jhin.2010.09.037.

[32] M. Bivolarova, A.K. Melikov, C. Mizutani, K. Kajiwara, Z.D. Bolashikov, Bed-integrated local exhaust ventilation system combined with local air cleaning for improved IAQ in hospital patient rooms, Build. Environ. 100 (2016) 10–18, doi:10.1016/j.buildenv.2016.02.006.

[33] M. Hyttinen, A. Rautio, P. Pasanen, T. Reponen, G.S. Earnest, A. Streifel, et al., Airborne infection isolation rooms - a review of experimental studies, Indoor Built Environ. 20 (2011) 584–594, doi:10.1177/1420326X11409452.

[34] G. Cao, H. Awbi, R. Yao, Y. Fan, K. Sirén, R. Kosonen, et al., A review of the performance of different ventilation and airflow distribution systems in buildings, Build. Environ. 73 (2014) 171–186, doi:10.1016/j.buildenv.2013.12.009.

[35] Y.C. Tung, S.C. Hu, T.I. Tsai, I.L. Chang, An experimental study on ventilation efficiency of isolation room, Build. Environ. 44 (2009) 271–279, doi:10.1016/j.buildenv.2008.03.003.

[36] J.M. Villafruela, F. Castro, J.F. San Jose, J. Saint-Martin, Comparison of air change efficiency, contaminant removal effectiveness and infection risk as IAQ indices in isolation rooms, Energy Build. 57 (2013) 210–219, doi:10.1016/j.enbuild.2012.10.053.

[37] F.A. Berlanga, M.R. de Adana, I. Olmedo, J.M. Villafruela, J.F. San José, F. Castro, et al., Experimental evaluation of thermal comfort, ventilation performance indices and exposure to airborne contaminant in an airborne infection isolation room equipped with a displacement air distribution system, Energy Build. (2017), doi:10.1016/J.ENBUILD.2017.09.100.

[38] H. Qian, Y. Li, P.V. Nielsen, C.E. Hyldgaard, Dispersion of exhalation pollutants in a two-bed hospital ward with a downward ventilation system, Build. Environ. 43 (2008) 344–354, doi:10.1016/j.buildenv.2006.03.025.

[39] M.P. Wan, C.Y.H. Chao, Y.D. Ng, G.N. Sze To, W.C. Yu, Dispersion of expiratory droplets in a general hospital ward with ceiling mixing type mechanical ventilation system, Aerosol Sci. Technol. 41 (2007) 244–258, doi:10.1080/02786820601146985.

[40] E. Mundt, H.M. Mathisen, P.V. Nielsen, A. Moser, Ventilation Effectiveness, 2004.

[41] J.W. Tang, Y. Li, I. Eames, P.K.S. Chan, G.L. Ridgway, Factors involved in the aerosol transmission of infection and control of ventilation in healthcare premises, J. Hosp. Infect. 64 (2006) 100–114, doi:10.1016/j.jhin.2006.05.022.

[42] F.A. Berlanga, M. Ruiz de Adana, I. Olmedo, Diseño y construcción de maniquíes térmicos para la realización de ensayos experimentales de sistemas de climatización, in: Proc. IX Congr. Nac. Ing. Termodinámica, Cartagena, 2015, pp. 1–8. doi:978-84-606-8931-7.

[43] Technical Comitee for Ergonomics of the physical environment, ISO 7726 Ergonomics of the Thermal Envinonment - Instruments for Measuring Physical Quantities, 2nd ed., ISO, 1998.

[44] R. Tomasi, M. Krajčík, A. Simone, B.W. Olesen, Experimental evaluation of air distribution in mechanically ventilated residential rooms: Thermal comfort and ventilation effectiveness, Energy Build. 60 (2013) 28–37, doi:10.1016/j.enbuild.2013.01.003.

[45] M. Krajčík, A. Simone, B.W. Olesen, Air distribution and ventilation effectiveness in an occupied room heated by warm air, Energy Build. 55 (2012) 94–101, doi:10.1016/j.enbuild.2012.08.015.

[46] ISO - AEN/CTN 81, ISO 7730, Ergonomics of the Thermal Environment—Analytical Determination and Interpretation of Thermal Comfort Using Calculation of the PMV and PPD Indices and Local Thermal Comfort Criteria, ISO, Geneva, 2005.

[47] ASHRAE, F09 SI: Thermal Comfort, ASHRAE Handbook Fundamentals, 2009 9.1–9.30.

[48] J. Laverge, M. Spilak, A. Novoselac, Experimental assessment of the inhalation zone of standing, sitting and sleeping persons, Build. Environ. 82 (2014) 258–266, doi:10.1016/j.buildenv.2014.08.014.

[49] M. De Carli, B.W. Olesen, in: Field measurements of operative temperatures in buildings heated or cooled by embedded water-based radiant systems, ASHRAE Transactions, 2002, pp. 714–725.

[50] Z.D. Bolashikov, A.K. Melikov, W. Kierat, Z. Popioek, M. Brand, Exposure of health care workers and occupants to coughed airborne pathogens in a double-bed hospital patient room with overhead mixing ventilation, HVAC R Res. (2012) 602–615, doi:10.1080/10789669.2012.682692.

[51] J. Pantelic, K.W. Tham, Adequacy of air change rate as the sole indicator of an air distribution system's effectiveness to mitigate airborne infectious disease transmission caused by a cough release in the room with overhead mixing ventilation: A case study, HVAC R Res. 19 (2013) 947–961, doi:10.1080/10789669.2013.842447.

[52] A.K. Melikov, Z.D. Bolashikov, W. Kierat, Z. Popiolek, Does increased ventilation help reduce cross-infection in isolation hospital wards? in: Proc. CLIMA 2010, Antalya, 2010.

[53] I. Olmedo, P.V. Nielsen, M. Ruiz de Adana, R.L. Jensen, P. Grzelecki, Distribution of exhaled contaminants and personal exposure in a room using three different air distribution strategies, Indoor Air 22 (2012) 64–76, doi:10.1111/j.1600-0668.2011.00736.x.

# Discussion

In order to solve the main question stated in the hypothesis and objectives section, it is important to evaluate the exposure to the contaminants in qualitative terms. The variable used for this purpose is the intake fraction ($IF$) since it represents the amount of contaminants that effectively are inhaled by the health worker. It is considered in the three forms presented in this study and defined in Paper IX, its mean value ($IF$), the average of the registered peaks ($IF_{125\%}$), and the maximum peak registered value $IF_{max}$. Additionally, the frequency of the peaks ($f_{P,125\%}$) is used to determine the occurrence of high contaminant concentrations in health worker airways.

The exposure to contaminants is weighted considering the minimum and the maximum index values registered. This way three categories are delimited that permit seize the influence of the tested parameters evaluated in each case. The mathematical expression used to classify the parameters listed above is detailed in the following expression considering $var$ as the variable used to evaluate the exposure to contaminants of HW in each case:

$$\begin{gathered} if\ (var_i) < \frac{1}{3}\cdot(\max(var_i) - \min(var_i))\ then\ LOW\ RISK \\ if\ \frac{1}{3}\cdot(\max(var_i) - \min(var_i)) < (var_i) < \frac{2}{3}\cdot(\max(var_i) - \min(var_i))\ then\ MEDIUM\ RISK \\ if\ (var_i) > \frac{2}{3}\cdot(\max(var_i) - \min(var_i))\ then\ HIGH\ RISK \end{gathered} \quad (1)$$

The influence of the ventilation strategies and the air ventilation rates tested on the exposure to contaminants is evaluated quantitatively. The results obtained in the cases studied in the Papers VIII and IX are used for this evaluation. The results of the analysis are shown in Figure 2.

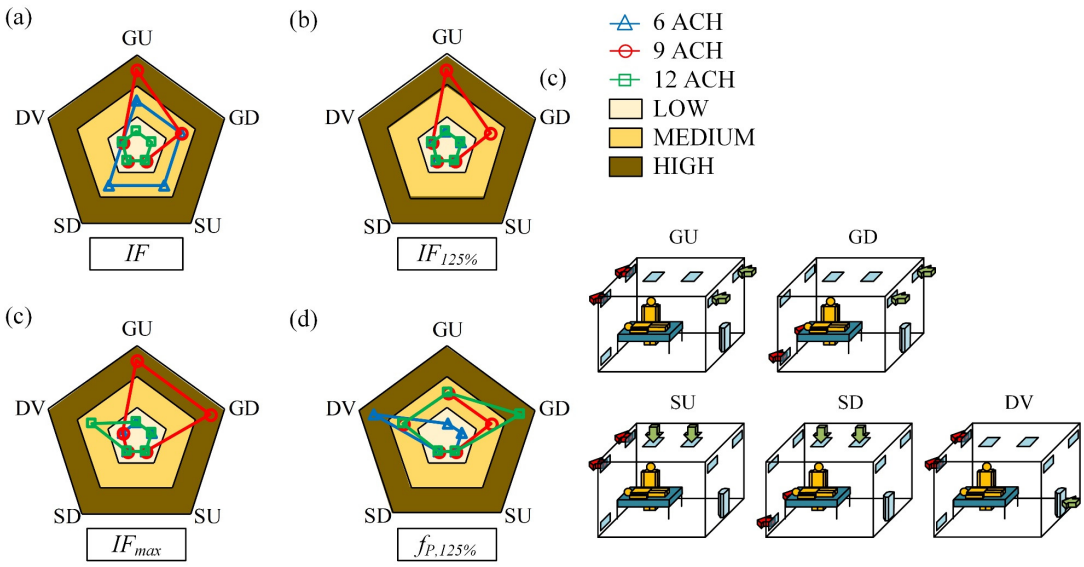


Figure 2. Qualitative analysis of the exposure risk of all the cases tested. (a) $IF$, Intake fraction; (b) $IF_{max}$, Maximum concentration intake fraction; (c) $IF_{125\%}$, Peak average intake fraction; (d) $f_{P,125\%}$, Contaminant concentration peak frequency.

Results show that the exposure risk depends on the experimental configuration used. Depending on the exposure index selected to evaluate the exposure $IF$, $IF_{125\%}$, $f_{P,125\%}$ or $IF_{max}$ the qualitative risk can also be different.

The analysis based on the average exposure values ($IF$) shows that the increase of the air ventilation rate has in general a positive impact on the exposure risk, registering a low risk when the ventilation rate is increased to 12 ACH in all cases. The improvement is evident when the swirl (S) diffusers are used to supply ventilation air to the experimental chamber, when the exposure risk registers a constant improvement. The tendency is not as clear when wall grille (G) supply grilles are used, where an increment of the exposure risk is registered for 9 ACH ventilation rate. The situation highlights that the air distribution inside the experimental chamber has an impact on HW exposure under this configuration, as it was analysed in Paper IX, and it could be a reason to discourage its use. Displacement ventilation (DV) shows low exposure risk values for all the air ventilation rates tested, so it arises as an interesting option to consider in hospital rooms.

The influence of the concentration peaks is evaluated by using the variables $IF_{125\%}$, $f_{P,125\%}$ and $IF_{max}$. The increase of the air ventilation rate generally decreases the scale of the peaks as it is shown by the decrease of the exposure risk obtained when the values of $IF_{125\%}$. The only exception to this tendency arises when G supply is used. Again, the dependency on the configuration of the flow distribution inside the indoor space makes the exposure risk increase for the intermediate air ventilation rate tested. The magnitude of the maximum exposure risk is evaluated by $IF_{max}$ index. In this case the tendencies are very similar to the obtained for $IF_{125\%}$. Nevertheless, it can be observed an increase of the exposure risk for DV configuration. For this strategy, the increase of the air ventilation rate weakens HW thermal plume, increasing the exposure risk. It has to be considered when selecting the air ventilation for this configuration.

The exposure risk based on the contaminant concentration peak frequency ($f_{P,125\%}$) shows that, there is not a direct relation between the magnitude of the peaks and its frequency. An increase of the ventilation rate increases the exposure risk for G supply cases, while the risk remains low for S supply in all cases. For DV, the exposure risk decreases with the increase of air ventilation rate but in any case decreases from medium value. Therefore, based on the peak frequency, mixing ventilation S supply cases assure a low risk regardless the air ventilation rate used and hence its use is recommended in these terms.

The influence of the exhalation mode and the breathing function performed are evaluated qualitatively using the results obtained in Paper VIII. The ventilation configuration chosen for this study is GU, supplying air through the upper part of the East wall and performing the exhaust through the grilles placed in the lower part of the West wall. Results are shown in Figure 3.

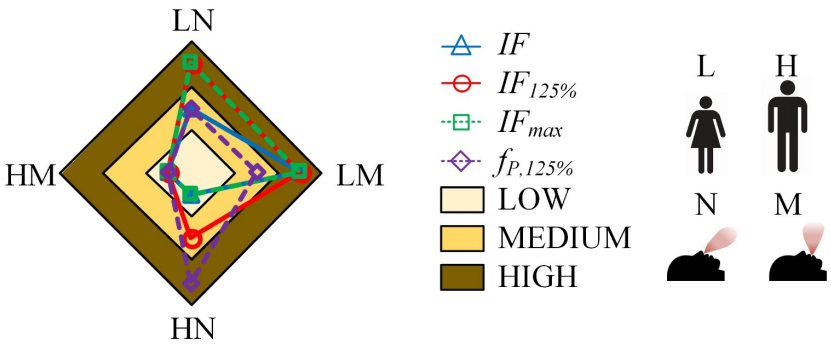


Figure 3. Influence of the breathing mode, breathing function and exhalation airway on HW contaminants exposure.

The analysis of the exposure risk based on the value of $IF$ shows a high exposure risk for LM case and a medium value for LN, while the risk is low for H breathing function cases. This situation highlights that L exhalation derives in a higher exposure risk. The analysis based on the $IF_{125\%}$ index delivers the same results obtained for $IF$. Again, the higher risk is located for L exhalation, being the only exception from previous analysis that, in this case, the exposure risk for HN case is medium. This fact highlights the influence of the nose exhalation airway in projecting contaminants to the inhalation area of HW. The magnitude of the maximum peak registered in this case ($IF_{max}$) reinforces the idea of the increase of the exposure risk when L exhalation is performed. The exposure risk based on the peak frequency ($f_{P,125\%}$) shows that the cases when L exhalation is performed maintain a medium frequency risk, being the higher risk located for HN case. The compound of all the variables considered to evaluate the exposure risk stands out that the L exhalation, shorter and with la lower momentum promotes higher exposure risk. The influence of the exhalation airway is not as clear, N exhaust reveals a higher peak frequency while the higher magnitude of the exposure values are found at LM case.

# Limitations of the work

All the research performed in this thesis has been is carried out in a laboratory under controlled conditions using static breathing thermal manikins instead of real people and using a single specific setup. This has been done in order to systematically analyse the problems stated and all the different variables tested in this study. Nevertheless, this limits the scope of the conclusions of this thesis. The main limitations are listed below:

- *The study has been performed in a controlled laboratory instead in a real hospital room, which undermines the realism of the study*. Nevertheless, the maintenance over time of a controlled conditions necessary to perform the experimental research would be a challenge in a real hospital room. In addition, the test of the different parameters evaluated in this thesis such as different ventilation configurations and air ventilation rates would be impossible.
- *The study uses breathing thermal manikins instead real people, which simplifies and homogenise the influence of the occupants*. However, the use of real people instead of thermal manikins require the specimens to maintain the same position for long periods of time, until 10 hours, for a high number of periods, until 80, which is psychologically harmful for real persons. Furthermore, it is known that each person can develop specific breathing tendencies depending of its specific conditions that could modify the obtained results depending of the day.
- *The occupants are maintained still during all the experimental time considered, which is not realistic, hence is well known that the displacement of the people inside an indoor space would affect the way they are exposed to the present contaminants*. Even through, this situation could be addressed by the use of dynamic manikins instead of considering a static position, the inclusion of this extra parameter would have been increased the

experimental complexity and perhaps constitutes an specific research item out of the scope of this thesis.

- *The study uses tracer gases to surrogate the exhaled contaminants that may be gases or particles*. The use of different substances to surrogate contaminants is always controversial but their use is widespread [26,29,42,80]. This study uses two different tracer gases, $CO_2$ and R134A, which have very different densities, being former quite lighter. While $CO_2$ is emitted in the same amount of a real exhalation and can be found in the atmosphere in a variable concentration, the R134A is emitted at a fixed rate and it is impossible to find it in natural environments. In the context of the experiments carried out, $CO_2$ is used in the short range measurements respect to the source because its background presence in normal environments hamper the obtaining relative values due to the small differences between the measurements in different points. For long range measurements R134A is used in order to detect all the contaminants emitted by the source.
- *A high exposure to an infected patient exhaled contaminants do not necessarily lead to a health worker infection.* It is true that the problem is more complex and requires the use of cross infection risk models such as the Wells-Riley model [2] to determine the probability of infection. Nevertheless, this model requires deal with the quantum generation rate, which is the amount of germs produced for each infection source per unit of time necessary to cause infection, that are difficult to estimate in experimental research. Thus, these methods are mainly focused for the use in simulations using computational fluid mechanics.

These decisions made in order to increase the repeatability of the experiments, could undermine the realism of the study. This situation make the conclusions stated in this study applicable only to the set up chosen. A further inference of the conclusions stated in this study general individual hospital rooms require a deeper field research in different real hospitals and is deferred to future works. Likewise, the number of cases studied could have been multiplied by using computational fluid dynamics once the case of study is validated. This technique properly validated could reduce required experimental research data and

help to achieve wider conclusions from the data collected, so it also is postponed to future works.

# Conclusions

This thesis intends to evaluate the influence of the ventilation configuration on the exposure of a health worker to the confined patient's exhaled contaminants in a hospital room. The exhalation of a lying patient confined inside this space is the source of contaminants considered. As a source of contaminants, the patient's exhalation flow has been studied in detail in order to better understand the factors governing the distribution of the exhaled contaminants. In the pursuit of determining which ventilation configuration is the most effective in reducing health worker contaminants exposure, different ventilation configurations are tested. The analysis has been performed taking into account the different parameters that are important to consider in the design of a ventilation facility such as the ventilation effectiveness indices and the thermal comfort of the occupants.

The patient exhalation flow as the source of contaminants plays an important role in their diffusion in the short and in the long range. The main conclusions that are obtained from its study are the following:

- The breathing function performed, which ultimately depends on the characteristic of the patient, determines the exhaled air flow rate over time. This has a direct impact on the broadening of the exhalation jet angle over the time and on the penetration of the flow. A lower maximum flow rate breathing function, would lead to wider jet angles and shorter penetration lengths. On the contrary, higher maximum flow rates lead to a narrower jet angles with a higher penetration lengths. Flow development determines the distribution of the emitted contaminants. A higher penetration jet would transport contaminants to a more distant position from the source, where the ventilation flows can then drive the contaminants to the exhaust. In contrast, considering the manikins

position and posture tested in this thesis, wider patient's exhalation jet angles permit the contaminants to reach the position of the health worker standing close to it.

- It exist also an influence of the breathing modes on the contaminants dispersion. This influence derives from the different area and orientation of the exit points. The opening of the mouth is bigger than the nostrils and it stands in a less oblique angle. Results show that the maximum health worker exposure arises when exhalation is released through the mouth of the patient using a low maximum flow rate breathing function due to the major influence of the breathing function.

The ventilation strategy play a crucial role in removing exhaled contaminants. The main conclusions that can be stated form the study of the different configuration tested are the following:

- Two different mixing ventilation supply configurations are tested, presenting different tendencies when the air ventilation rate increases. When the swirl supplies are used, S cases, the increase of the air ventilation rate is accompanied by a progressive reduction of the exposure values. However, when the wall grilles supplies, G cases, are used the exposure behaves erratically even when the air ventilation rate is increased. This is due to the different air distribution patterns created inside the room in this case.
- The use of exhaust grilles placed in the lower part of the wall results in slight higher health worker contaminants exposure values in comparison with the results obtained when the air removal is done through the same grilles placed in the upper part of the wall. This is perhaps due to the difficulty found by the contaminants released upwards to reach the exhaust when the exhaust is done at a low height.
- The use of a displacement ventilation configuration (DV) results in reduced health worker exposure values for lower ventilation rates. The use of this strategy allow the reduction of the air ventilation rate obtaining results comparable to the obtained using mixing ventilation at higher ventilation rates.
- The increase of the air ventilation rate does not necessarily leads to lower exposure values for the health worker in all cases. While the exposure decreases with air ventilation rate for swirl (S) diffusers mixing cases, this reduction is no effective in wall grille mounted diffusers (G) and displacement ventilation cases (DV). The reduction of

the health worker exposure is more related with a proper air distribution of the ventilation flows that achieve in maintaining the contaminants far from health worker inhalation.

According with the results obtained and the conclusions stated it is possible to select a ventilation configuration in order to reduce health worker exposure to the contaminants exhaled by the confined patient. Results show that the use of mixing ventilation strategy using swirl diffusers permit achieve a lower health worker exposure to contaminants. For this configuration, the exposure decrease with the increase of the air ventilation rate, thus 12 ACH, which is the air ventilation rate recommended for these spaces [5], is chosen. In order to enhance the evacuation of the contaminants the exhaust must be performed though the grilles placed the upper part of the wall. Considering this configuration, the exposure of the health worker to the exhaled contaminants by the confined manikin is minimized for the considered scenario. As an alternative, it is worth stressing that the use of the displacement ventilation configuration tested in this experimental scenario maintains the health worker exposure in low values for low air ventilation rates. This solution permits the reduction of the ventilation air flow which could lead to collateral beneficial situations such as the reduction of draft local thermal discomfort or the decrease of the cost of the ventilation facility, reducing the size of the fans the costs of operation.

# Future Works

This thesis lays the foundations for widening the scope of the stated conclusions through additional research. The future research to be done can be divided in different lines:

- *A pursuit of more realistic airway models for thermal manikins that lead to realistic exhalation flows*. The use of thermal manikins instead of real people assumes a series of compromises. Between the more important ones, it can be noted the simplification of the manikins airways. The use of simplified airways affect the way the exhalation flows development, compromising the realism of the experiments performed. An investigation about the way to obtain a model that balances the complexity of real airflows and the possibility to be installed in thermal manikins must be carried out.
- *Perform field studies to validate the conclusions obtained in the laboratory*. This thesis states a series of conclusions that needs to be checked in real individual hospital rooms. Thus a field study considering different typologies of individual hospital rooms must be carried out to determine if the conclusions are still valid.
- *Carry out computational fluid dynamics studies that permit the study of different variables out of the scope of this thesis.* Different parameters, such as the movement of the manikins, the relative position of the health worker and the thermal manikin respect of the ventilation elements or a different disposition of the heat gains that can affect the exposure of the health worker to the contaminants exhaled by the confined patient are not tested in this study. The use of computational fluid mechanics can help to obtain conclusions for these variables once the cases are validated using the experimental research carried out in this thesis. In the same way, it would be interesting to numerically evaluate the health worker cross infection risk considering methods such as the Wells-Riley model [2].

All these possible future research lines would help to gain knowledge on the topic and this way help to improve the conditions of patients and health workers in hospital rooms.

# References


[1] W.G. Lindsley, F.M. Blachere, D.H. Beezhold, R.E. Thewlis, B. Noorbakhsh, S. Othumpangat, W.T. Goldsmith, C.M. McMillen, M.E. Andrew, C.N. Burrell, J.D. Noti, Viable influenza A virus in airborne particles expelled during coughs versus exhalations, Influenza Other Respi. Viruses. 10 (2016) 404–413. doi:10.1111/irv.12390.

[2] R.L. Riley, Indoor airborne infection, Environ. Int. 8 (1982) 317–320. doi:10.1016/0160-4120(82)90043-5.

[3] K. Lyngby, T.H. Kuehn, H.E.B. Burroughs, C.O. Muller, D. Tompkins, W.J. Fisk, J.A. Siegel, M.C. Jackson, ASHRAE Position Document on Airborne Infectious Diseases, 2015.

[4] CDC, Guidelines for preventing the transmission of Mycobacterium tuberculosis in health-care facilities., Centers for Disease Control & Prevention (CDC), 1994. doi:10.2307/42000931.

[5] CDC, Guidelines for environmental infection control in health-care facilities, Atlanta, GA, 2003.

[6] S. Stelzer-Braid, B.G. Oliver, A.J. Blazey, A. Elizabeth, T.P. Newsome, W.D. Rawlinson, E.R. Tovey, Exhalation of respiratory viruses by breathing, coughing, and talking, J. Med. Virol. 81 (2009) 1674–1679. doi:10.1002/jmv.

[7] P. Fabian, J.J. McDevitt, W.H. DeHaan, R.O.P. Fung, B.J. Cowling, K.H. Chan, G.M. Leung, D.K. Milton, Influenza virus in human exhaled breath: an observational study, PLoS One. 3 (2008) e2691. doi:10.1371/journal.pone.0002691.

[8] D.K. Milton, M.P. Fabian, B.J. Cowling, M.L. Grantham, J.J. McDevitt, Influenza virus

aerosols in human exhaled breath: particle size, culturability, and effect of surgical masks, PLoS Pathog. 9 (2013) e1003205. doi:10.1371/journal.ppat.1003205.

[9] C.I. Fairchild, J.F. Stampfer, Particle Concentration in Exhaled Breath - Summary Report, Am. Ind. Hyg. Assoc. J. 48 (1987) 948–949. doi:10.1080/15298668791385868.

[10] R.S. Papineni, F.S. Rosenthal, The size distribution of droplets in the exhaled breath of healthy human subjects., J. Aerosol Med. 10 (1997) 105–116. doi:10.1089/jam.1997.10.105.

[11] L. Morawska, G.R. Johnson, Z.D. Ristovski, M. Hargreaves, K. Mengersen, S. Corbett, C.Y.H. Chao, Y. Li, D. Katoshevski, Size distribution and sites of origin of droplets expelled from the human respiratory tract during expiratory activities, J. Aerosol Sci. 40 (2009) 256–269. doi:10.1016/j.jaerosci.2008.11.002.

[12] H. Qian, Y. Li, P. V. Nielsen, C.E. Hyldgaard, T.W. Wong, a T.Y. Chwang, Dispersion of exhaled droplet nuclei in a two-bed hospital ward with three different ventilation systems, Indoor Air. 16 (2006) 111–28. doi:10.1111/j.1600-0668.2005.00407.x.

[13] L. Liu, Y. Li, P. V. Nielsen, J. Wei, R.L. Jensen, Short-range airborne transmission of expiratory droplets between two people, Indoor Air. (2016) 1–11. doi:10.1111/ina.12314.

[14] A. Jurelionis, L. Gagytė, T. Prasauskas, D. Čiužas, E. Krugly, L. Šeduikytė, D. Martuzevičius, The impact of the air distribution method in ventilated rooms on the aerosol particle dispersion and removal: The experimental approach, Energy Build. 86 (2015) 305–313. doi:http://dx.doi.org/10.1016/j.enbuild.2014.10.014.

[15] B. Chenari, J. Dias Carrilho, M. Gameiro Da Silva, Towards sustainable, energy-efficient and healthy ventilation strategies in buildings: A review, Renew. Sustain. Energy Rev. (2016). doi:10.1016/j.rser.2016.01.074.

[16] G. Cao, H. Awbi, R. Yao, Y. Fan, K. Sirén, R. Kosonen, J. (Jensen) Zhang, A review of the performance of different ventilation and airflow distribution systems in buildings, Build. Environ. (2014). doi:10.1016/j.buildenv.2013.12.009.

[17] E. Mundt, H.M. Mathisen, P. V. Nielsen, A. Moser, Ventilation Effectiveness, 2004.

[18] P. V. Nielsen, C.E. Hyldgaard, A. Melikov, H. Andersen, M. Soennichsen, Personal exposure between people in a room ventilated by textile terminals—with and without personalized ventilation, HVAC R Res. 13 (2007) 635–643. doi:10.1080/10789669.2007.10390976.

[19] M. Bivolarova, A. Krikor, Z. Dimitrov, D. Version, Control of Indoor Airflows for Reduction of Human Exposure to Aerosol Contaminants, Tecnical University of Denmark, 2017.

[20] J. Pantelic, K.W. Tham, D. Licina, Effectiveness of a personalized ventilation system in reducing personal exposure against directly released simulated cough droplets, Indoor Air. 25 (2015) 683–693. doi:10.1111/ina.12187.

[21] D. Licina, Y. Tian, W.W. Nazaroff, Inhalation intake fraction of particulate matter from localized indoor emissions, Build. Environ. 123 (2017). doi:10.1016/j.buildenv.2017.06.037.

[22] D.H. Bennett, T.E. McKone, J.S. Evans, M.D. Margini, K.R. Smith, Defining Intake Fraction, Environ. Sci. Technol. (2002). doi:10.1021/es0222770.

[23] W.W. Nazaroff, Inhalation intake fraction of particulate matter from localized indoor emissions, Build. Environ. 123 (2017) 14–22. doi:10.1016/j.buildenv.2017.06.037.

[24] M. Krajčík, A. Simone, B.W. Olesen, Air distribution and ventilation effectiveness in an occupied room heated by warm air, Energy Build. 55 (2012) 94–101. doi:10.1016/j.enbuild.2012.08.015.

[25] A. Novoselac, J. Srebric, Comparison of air exchange efficiency and contaminant removal effectiveness as IAQ indices, ASHRAE Trans. 109 PART 2 (2003) 339–349. doi:citeulike-article-id:9277731.

[26] R. Tomasi, M. Krajčík, A. Simone, B.W. Olesen, Experimental evaluation of air distribution in mechanically ventilated residential rooms: Thermal comfort and ventilation effectiveness, Energy Build. 60 (2013) 28–37. doi:10.1016/j.enbuild.2013.01.003.

[27] E. Lingaas, J.P. Rydock, Best practice in design and testing of isolation rooms in Nordic hospitals, Round Table Ser. - R. Soc. Med. (2007) 87–107.

[28] J.P. Rydock, A simple method for tracer containment testing of hospital isolation rooms., Appl. Occup. Environ. Hyg. 17 (2002) 486–90. doi:10.1080/10473220290035688.

[29] M. Bivolarova, J. Ondráček, A.K. Melikov, V. Ždímal, A comparison between tracer gas and aerosol particles distribution indoors: The impact of ventilation rate, interaction of airflows, and presence of objects, Indoor Air. 27 (2017) 1201–1212. doi:10.1111/ina.12388.

[30] D. Rim, A. Novoselac, Transport of particulate and gaseous pollutants in the vicinity of a human body, Build. Environ. 44 (2009) 1840–1849. doi:10.1016/j.buildenv.2008.12.009.

[31] C.J. Noakes, L.A. Fletcher, P.A. Sleigh, W.B. Booth, N. Beato-Arribas, B. Tomlinson, Comparison of tracer techniques for evaluating the behaviour of bioaerosols in hospital isolation rooms, in: Proc. Heal. Build. 2009, 2009: pp. 13–17.

[32] T.T. Chow, X.Y. Yang, Ventilation performance in operating theatres against airborne infection: Review of research activities and practical guidance, J. Hosp. Infect. 56 (2004) 85–92. doi:10.1016/j.jhin.2003.09.020.

[33] T.T. Chow, X.Y. Yang, Ventilation performance in the operating theatre against airborne infection: Numerical study on an ultra-clean system, J. Hosp. Infect. 59 (2005) 138–147. doi:10.1016/j.jhin.2004.09.006.

[34] R. Sommerstein, C. Rüegg, P. Kohler, G. Bloemberg, S.P. Kuster, H. Sax, Transmission of Mycobacterium chimaera from heater-cooler units during cardiac surgery despite an ultraclean air ventilation system, Emerg. Infect. Dis. 22 (2016) 1008–1013. doi:10.3201/eid2206.160045.

[35] A. Aganovic, G. Cao, L.I. Stenstad, J.G. Skogås, Impact of surgical lights on the velocity distribution and airborne contamination level in an operating room with laminar airflow system, Build. Environ. 126 (2017) 42–53. doi:10.1016/j.buildenv.2017.09.024.

[36] M.-F. King, C.J. Noakes, P. a Sleigh, Modeling environmental contamination in hospital single- and four-bed rooms., Indoor Air. (2015) 1–14. doi:10.1111/ina.12186.

[37] C.B. Beggs, K.G. Kerr, C.J. Noakes, E.A. Hathway, P.A. Sleigh, The ventilation of multiple-bed hospital wards: Review and analysis, Am. J. Infect. Control. 36 (2008) 250–259. doi:10.1016/j.ajic.2007.07.012.

[38] M.P. Wan, C.Y.H. Chao, Y.D. Ng, G.N. Sze To, W.C. Yu, Dispersion of expiratory droplets in a general hospital ward with ceiling mixing type mechanical ventilation system, Aerosol Sci. Technol. 41 (2007) 244–258. doi:10.1080/02786820601146985.

[39] H. Qian, Y. Li, P. V. Nielsen, X. Huang, Spatial distribution of infection risk of SARS transmission in a hospital ward, Build. Environ. 44 (2009) 1651–1658. doi:10.1016/j.buildenv.2008.11.002.

[40] H. Qian, Y. Li, P. V. Nielsen, C.E. Hyldgaard, Dispersion of exhalation pollutants in a two-bed hospital ward with a downward ventilation system, Build. Environ. 43 (2008) 344–354. doi:10.1016/j.buildenv.2006.03.025.

[41] Y. Yin, J.K. Gupta, X. Zhang, J. Liu, Q. Chen, Distributions of respiratory contaminants from a patient with different postures and exhaling modes in a single-bed inpatient room, Build. Environ. 46 (2011) 75–81. doi:10.1016/j.buildenv.2010.07.003.

[42] I. Olmedo, P. V. Nielsen, M. Ruiz de Adana, R.L. Jensen, P. Grzelecki, Distribution of exhaled contaminants and personal exposure in a room using three different air distribution strategies, Indoor Air. 22 (2012) 64–76. doi:10.1111/j.1600-0668.2011.00736.x.

[43] E. Bjørn, P. V. Nielsen, Dispersal of exhaled air and personal exposure in displacement ventilated rooms, Indoor Air. 12 (2002) 147–64.

[44] J. Richmond-Bryant, Transport of exhaled particulate matter in airborne infection isolation rooms, Build. Environ. 44 (2009) 44–55. doi:10.1016/j.buildenv.2008.01.009.

[45] J. Wang, T.T. Chow, Numerical investigation of influence of human walking on dispersion and deposition of expiratory droplets in airborne infection isolation room, Build. Environ. 46 (2011) 1993–2002. doi:10.1016/j.buildenv.2011.04.008.

[46] F. Memarzadeh, A. Manning, Thermal comfort, uniformity, and ventilation effectiveness in patient rooms: performance assessment using ventilation indices, ASHRAE Trans. 106 (2000).

[47] F. Memarzadeh, W. Xu, Role of air changes per hour (ACH) in possible transmission of airborne infections, Build. Simul. 5 (2012) 15–28. doi:10.1007/s12273-011-0053-4.

[48] J.M. Villafruela, F. Castro, J.F. San Jose, J. Saint-Martin, Comparison of air change efficiency, contaminant removal effectiveness and infection risk as IAQ indices in isolation rooms, Energy Build. 57 (2013) 210–219. doi:10.1016/j.enbuild.2012.10.053.

[49] Y.C. Tung, S.C. Hu, T.I. Tsai, I.L. Chang, An experimental study on ventilation efficiency of isolation room, Build. Environ. 44 (2009) 271–279. doi:10.1016/j.buildenv.2008.03.003.

[50] M. Bivolarova, A. Melikov, C. Mizutani, K. Kajiwara, Z.D. Bolashikov, Bed-integrated local exhaust ventilation system combined with local air cleaning for improved IAQ in hospital patient rooms, Build. Environ. 100 (2016) 10–18. doi:10.1016/j.buildenv.2016.02.006.

[51] A. Melikov, Z.D. Bolashikov, E. Georgiev, Novel ventilation strategy for reducing the risk of airborne cross infection in hospital rooms, (2011) 1–6.

[52] P. Kalliomäki, P. Saarinen, J.W. Tang, H. Koskela, Airflow patterns through single hinged and sliding doors in hospital isolation rooms - Effect of ventilation, flow differential and passage, Build. Environ. 107 (2016) 154–168. doi:10.1016/j.buildenv.2016.07.009.

[53] F.J. Offermann, A. Eagan, A.C. Offermann, S.S. Subhash, S.L. Miller, L.J. Radonovich, Potential airborne pathogen transmission in a hospital with and without surge control ventilation system modifications, Build. Environ. 106 (2016) 175–180. doi:10.1016/j.buildenv.2016.06.029.

[54] H. Nishimura, S. Sakata, A. Kaga, A new methodology for studying dynamics of aerosol particles in sneeze and cough using a digital high-vision, high-speed video system and

vector analyses, PLoS One. 8 (2013). doi:10.1371/journal.pone.0080244.

[55] A. Afshari, S. Azadi, T. Ebeling, A. Badeau, W.T. Goldsmith, K.C. Weber, D.G. Frazer, Evaluation of cough using digital particle image velocimetry, in: Proc. Second Jt. 24th Annu. Conf. Annu. Fall Meet. Biomed. Eng. Soc., 2002: pp. 975–976. doi:10.1109/IEMBS.2002.1106233.

[56] M. VanSciver, S. Miller, J. Hertzberg, Particle image velocimetry of human cough, Aerosol Sci. Technol. 45 (2011) 415–422. doi:10.1080/02786826.2010.542785.

[57] S. Zhu, S. Kato, J.-H. Yang, Study on transport characteristics of saliva droplets produced by coughing in a calm indoor environment, Build. Environ. 41 (2006) 1691–1702. doi:10.1016/j.buildenv.2005.06.024.

[58] L. Feng, S. Yao, H. Sun, N. Jiang, J. Liu, TR-PIV measurement of exhaled flow using a breathing thermal manikin, Build. Environ. 94 (2015) 683–693. doi:10.1016/j.buildenv.2015.11.001.

[59] C.Y.H. Chao, M.P. Wan, L. Morawska, G.R. Johnson, Z.D. Ristovski, M. Hargreaves, K. Mengersen, S. Corbett, Y. Li, X. Xie, D. Katoshevski, Characterization of expiration air jets and droplet size distributions immediately at the mouth opening, J. Aerosol Sci. 40 (2009) 122–133. doi:10.1016/j.jaerosci.2008.10.003.

[60] L. Bourouiba, E. Dehandschoewercker, J.W.M. Bush, Violent expiratory events: On coughing and sneezing, J. Fluid Mech. (2014). doi:10.1017/jfm.2014.88.

[61] C.H. Habchi, K. Ghali, N. Ghaddar, Transient model for particle dispersion generated by high momentum respiratory activities in spaces ventilated by displacement ventilation system, in: IMECE (Ed.), Proc. ASME 2015 Int. Mech. Eng. Congr. Expo., ASME, Houston, 2015: pp. 1–10.

[62] J.W. Tang, A. Nicolle, C. Klettner, J. Pantelic, L. Wang, A. Suhaimi, A. Tan, G. Ong, R. Su, C. Sekhar, D. Cheong, K.W. Tham, Airflow dynamics of human jets: sneezing and breathing - potential sources of infectious aerosols, PLoS One. 8 (2013) e59970. doi:10.1371/journal.pone.0059970.

[63] S.-B. Kwon, J. Park, J. Jang, Y. Cho, D.-S. Park, C. Kim, G.-N. Bae, A. Jang, Study on

the initial velocity distribution of exhaled air from coughing and speaking, Chemosphere. 87 (2012) 1260–4. doi:10.1016/j.chemosphere.2012.01.032.

[64] D. Licina, A. Melikov, J. Pantelic, C. Sekhar, K.W. Tham, Personal exposure to cough released droplets in quiescent environment and ventilated spaces, in: Roomvent (Ed.), 13th SCANVEC Int. Conf. Air Distrib. Rooms, Sao Paulo, 2014: pp. 174–181.

[65] W.G. Lindsley, W.P. King, R.E. Thewlis, J.S. Reynolds, K. Panday, G. Cao, J. V Szalajda, Dispersion and exposure to a cough-generated aerosol in a simulated medical examination room., J. Occup. Environ. Hyg. 9 (2012) 681–90. doi:10.1080/15459624.2012.725986.

[66] D.R. Marr, T. Khan, M. Glauser, H. Higuchi, J.S. Zhang, On Particle Image Velocimetry (PIV) Measurements in the Breathing Zone of a Thermal Breathing Manikin, ASHRAE Trans. 111 (2005) 299–305.

[67] F.A. Berlanga, I. Olmedo, M. Ruiz de Adana, Experimental analysis of the air velocity and contaminant dispersion of human exhalation flows, Indoor Air. (2016) 1–13. doi:10.1111/ina.12357.

[68] J.K. Gupta, C.-H. Lin, Q. Chen, Characterizing exhaled airflow from breathing and talking, Indoor Air. 20 (2010) 31–9. doi:10.1111/j.1600-0668.2009.00623.x.

[69] C. Xu, P. V. Nielsen, G. Gong, R.L. Jensen, L. Liu, Influence of air stability and metabolic rate on exhaled flow, Indoor Air. 25 (2015) 198–209. doi:10.1111/ina.12135.

[70] C. Xu, P. V. Nielsen, G. Gong, L. Liu, R.L. Jensen, Measuring the exhaled breath of a manikin and human subjects, Indoor Air. 25 (2015) 188–197. doi:10.1111/ina.12129.

[71] C. Xu, P. V. Nielsen, L. Liu, R.L. Jensen, G. Gong, Human exhalation characterization with the aid of schlieren imaging technique, Build. Environ. 112 (2017) 190–199. doi:10.1016/j.buildenv.2016.11.032.

[72] ASHRAE, F20 SI : Space Air Diffusion, in: ASHRAE Handb. Fundam., 2013: p. 20.1-20.9.

[73] J. Khodakarami, N. Nasrollahi, Thermal comfort in hospitals - A literature review, Renew. Sustain. Energy Rev. 16 (2012) 4071–4077. doi:10.1016/j.rser.2012.03.054.

[74] R. Van Gaever, V.A. Jacobs, M. Diltoer, L. Peeters, S. Vanlanduit, Thermal comfort of the surgical staff in the operating room, Build. Environ. 81 (2014) 37–41. doi:10.1016/j.buildenv.2014.05.036.

[75] J. Verheyen, N. Theys, L. Allonsius, F. Descamps, Thermal comfort of patients: Objective and subjective measurements in patient rooms of a Belgian healthcare facility, Build. Environ. 46 (2011) 1195–1204. doi:10.1016/j.buildenv.2010.12.014.

[76] L. Lan, K. Tsuzuki, Y.F. Liu, Z.W. Lian, Thermal environment and sleep quality : A review, Energy Build. 149 (2017) 101–113. doi:10.1016/j.enbuild.2017.05.043.

[77] S. Zhu, W. Cai, J.D. Spengler, Control of sleep environment of an infant by wide-cover type personalized ventilation, Energy Build. 129 (2016) 69–80. doi:10.1016/j.enbuild.2016.07.064.

[78] S. Del Ferraro, S. Iavicoli, S. Russo, V. Molinaro, A field study on thermal comfort in an Italian hospital considering differences in gender and age, Appl. Ergon. 50 (2015) 177–184. doi:10.1016/j.apergo.2015.03.014.

[79] ISO - AEN/CTN 81, ISO 7730. Ergonomics of the thermal environment—Analytical determination and interpretation of thermal comfort using calculation of the PMV and PPD indices and local thermal comfort criteria, ISO, Geneva, 2005.

[80] M.-F. King, M. Camargo-Valero, A. Matamoros-Veloza, P. Sleigh, C. Noakes, An Effective Surrogate Tracer Technique for S. aureus Bioaerosols in a Mechanically Ventilated Hospital Room Replica Using Dilute Aqueous Lithium Chloride, Atmosphere (Basel). 8 (2017) 238. doi:10.3390/atmos8120238.